INDSWG-25

EANDC-33 "U"

INDC(EAN)002

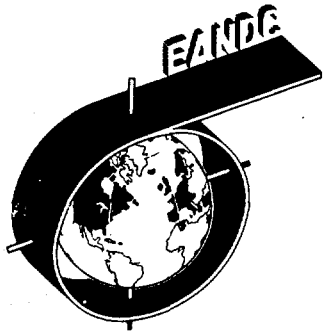

SYMPOSIUM ON THE ABSOLUTE DETERMINATION OF NEUTRON FLUX IN THE ENERGY RANGE 1-100 keV

10th-13th September, 1963

St-John's College, Oxford, U.K.

Organised by

A.W.R.E., Aldermaston,
Berks., United Kingdom

EUROPEAN-AMERICAN NUCLEAR DATA COMMITTEE

SYMPOSIUM ON THE ABSOLUTE DETERMINATION OF NEUTRON FLUX IN THE ENERGY RANGE 1-100 keV

10th - 13th September, 1963
St. John's College, Oxford,
United Kingdom

Organised by
A.W.R.E., Aldermaston
Berks, United Kingdom

EUROPEAN AMERICAN NUCLEAR DATA COMMITTEE
Central Secretariat
O.E.C.D. European Nuclear Energy Agency
38, Bd. Suchet, Paris, 16e

A.44918

TABLE OF CONTENTS

2. PROGRAMME OF THE SYMPOSIUM

Monday, 9th September, 1963 — Visit to the Atomic Energy Research Establishment, Harwell.

Monday, 9th September, 1963 — Arrival of delegates at St. John's College, Oxford, for dinner.

Tuesday, 10th September, 1963

9.30 — Welcome to delegates

Session 1 Chairman. W.W. Havens (Columbia)

Neutron cross section measurements in the energy range 1-100 keV with particular emphasis on the determination of neutron flux.

(a) Capture cross section measurements
L.W. Weston (Oak Ridge)

(b) Fission cross section measurements
B.C. Diven (Los Alamos)

14.00 — Session 2(a) Chairman. Prof. M.H. Barshall (Wisconsin)

Standard cross sections for absolute neutron flux measurements

Choice of standard. Preliminary remarks by R. Batchelor, (Aldermaston). Techniques for measuring standard cross-sections.

(i) Sphere transmission method
P.H. White (Aldermaston)

(ii) Other methods /e.g. the subtraction of σ (elastic) from σ(total)/
E. Rae (Harwell)

Wednesday, 11th September, 1963

9.30 — Session 2(b) Chairman. Dr. A.B. Smith (Argonne)

Further flux measuring techniques

(iii) Tank methods including

(a) The large scintillator. N. Starfelt (Res. Inst. Defence, Sweden).

Wednesday,
11th September, 1963
(continued)

(b) The $MnSO_4$ bath and graphite pile
R.L. Macklin (Oak Ridge)

(iv) Absolute flux measurements by the detection of associated particles or activities in neutron producing reactions.
R.G. Johnson, (Lockheed, California).

14.00

Session 3 Chairman. E. Paul (Manchester)

Neutron sources of 1-100 keV for cross section measurements

(a) General review of sources with mono-kinetic and continuous spectra
H.W. Newson (Duke)

(b) Comments on the slowing down spectrometer
K.H. Beckurts (Karlsruhe).

Thursday,
12th September, 1963
9.00

Visit to the Nuclear Research Division, AWRE, Aldermaston.

Friday,
13th September, 1963
9.30

Session 4 Chairman. K.H. Beckurts (Karlsruhe)

Flux measuring instruments based on standard cross sections

(a) Proton recoil devices
J.W. Weale (Aldermaston)

(b) Instruments based on $He^3(n,p)$ $Li^6(n,\alpha)$ $B^{10}(n,\alpha$, etc. reactions
A.T.G. Ferguson (Harwell)

14.00

Session 5

Recapitulation of the symposium with possible proposals for future action.
R. Batchelor (Aldermaston).

2. EDITED SUMMARY OF THE SYMPOSIUM BY R. BATCHELOR, ALDERMASTON UNITED KINGDOM

You have probably noticed that the speaker for this session was not announced until the beginning of the Conference. The reason for this was that all along we had hoped that Dick Taschek would be with us and would sum up the proceedings. It is unfortunate for us all and particularly unfortunate for me, that he has not been able to come, because this task of recapitulating on this rather difficult problem now rests on my shoulders.

Before I sum it up, I think it is worth stating again what we are here for.

The Conference was brought about as a result of a suggestion at the last EANDC Meeting in Chalk River. I need hardly remind you that the major tasks of this Committee are to review the nuclear data requests of the member countries and to keep an eye on the various measurements and programmes which are going on to meet these requests. Now this problem of how to measure flux which we have discussed here, bears very heavily on a lot of these requests, and unless we solve it, we are going to have a very uneasy conscience about the numbers which our reactor physicists put into their calculations. As has been said before, the particular energy region which we have been interested in is particularly important for the design of fast reactors. These seem to be increasing in importance as time goes on so it is important that we get to grips with the problem now.

The question of accuracy requirement was brought up by John Weale this morning but in order to get our perspective right, I am going to put up a couple of requests pertinent to our discussion, which I have taken out of the latest EANDC request list.

U^{235} $\sigma(n,f)$ 1 keV to 5 MeV accuracy required $\pm$ 2%

U^{238} $\sigma(n,\gamma)$ 1 keV to 1 MeV " " $\pm$ 2%

Now that is how they stand at the moment, but the accuracies could very well be tightened up in the future.

With these and other similar ones in mind I think I would have to come to the conclusion that we have not seen an

immediate solution to the problem of measurement at this Conference. I do not want to get involved in the pros and cons of these requests. This is a matter for the reactor physicists to sort out. I take the view, however, that we should regard the accuracy requirement as a goal and we should assemble our best available techniques, within our resources and do as good a job as we can. We should not be unduly pessimistic if we can't quite achieve the desired accuracy. Provided we are not too far off our endeavours will have been worthwhile. It is in this spirit which I am going to leave this Conference in a fairly optimistic mood.

We started off, and indeed we came back to it many times, by showing off our problem. We heard of the present large discrepancies in the capture cross-sections, and particularly that of gold. In the case of the fission cross-sections there does not appear to be large discrepancies, but maybe the reason for this is that there is much less data available than for capture cross-sections. I do not propose to dwell too much on the gold capture cross-section now. No one here has been able to offer a reasonable explanation of the discrepancies and I have nothing further to add here, except this. I think it would be foolish for anyone to go back to their laboratory and immediately launch into another measurement of this cross-section using one of the previously used methods. New methods, yes, and we heard of two or three new techniques which might help. These are the Los Alamos idea of using a large sodium iodide detector and the two German ideas, one employing the manganese sulphate bath and the other utilising the measurement of neutron decay time in a block of material. As I see it we are presently overloaded with Au(n,γ) data and I would like to see someone sit down and have another good look at what has been done. I know that people have already done this, but maybe these people have themselves been intimately involved in one or other of the experiments. Maybe it is worth a neutral person having a go this time. For what it is worth, I will therefore put up my first recommendation - "Study gold capture data".

This Symposium has surely brought out the fact that we really need to consolidate our position with regard to standard cross-sections on which we base our flux measurements. We have heard of very fine measurements of capture and fission cross-sections being made on linacs but many of them referred to a cross-section on which we have no direct reliable measurements. In retrospect this sounds completely illogical and we ought to rectify the situation as soon as possible. Fortunately we have heard about several diverse schemes for measuring standards. It is therefore relatively straightforward for me to write down a programme of work on these standards which ought to yield reliable data provided we can get consistency in the results.

I have already given my views on what standard I like, of the $B^{10}(n,\alpha)$ $Li^{6}(n,\alpha)$ and $He^{3}(n,p)$ reactions, but I am going to be the first to accept that, at this stage, we should not decide on one only. I think we should accept each other's likes and dislikes and make the best measurements we possibly can on all three.

If we accept this, then it seems obvious that we need some more measurements on the ratios of these cross-sections.

There appears to be only one measurement of these ratios; I refer to the Russian measurements using the slowing down spectrometer. I think we need another measurement, using a more straightforward technique. A possible way to do it is to calibrate helium, lithium and boron detectors at 2200 m/sec and then measure the relative count rates as a function of energy with a Linac.

So my second recommendation is "Measure ratios of $B^{10}(n,\alpha)$, $Li^{6}(n,\alpha)$ and $He^{3}(n,p)$ cross-sections".

The next job to list is a relatively simple one - the measurements of the ratio $\sigma B^{10}(n,\alpha_0)/\sigma B^{10}(n,\alpha_1)$. We presently assume that this branching ratio is constant in our energy range, but this point needs checking. No measurement of flux is required in this experiment.

We have heard of several methods of measuring the absorption cross-sections of He^3, Li^6 and B^{10}, and I will refer to them soon. Since, in the case of B^{10}, there could be significant contributions of $B^{10}(n,p)$ and $B^{10}(n,t)$ to the absorption cross-section, it would be nice to have some data on these reactions. We suspect that their contributions are small - a few per cent - so the measurements need not be very accurate.

Coming now to absolute measurements on the standards we have first the sphere transmission method for Li^6 and B^{10}. The complications of this method have been outlined, but it was pointed out that the corrections required are not excessively large since the capture in these nuclei is a large fraction of the total cross-section. I can add that my group at AWRE is now firmly committed to this measurement and we shall press on with it.

Second, we have heard of various suggestions for measuring the absorption and scattering in single experiments. I will mention two here. The work started by Starfelt and co-workers, using a giant scintillator, is very interesting and I hope this symposium will give them encouragement to carry on. Schmitt's suggestion, which we heard about this morning, also shows promise. (The proposition was to place a small Li^6 sample in the forward cone of $Li^7(p,n)$ at threshhold and surround target and sample with the ORNL graphite sphere. The transmitted and scattered neutron intensity is thereby measured. If the sample is now moved out of the beam, the incident flux is measured). The difficulty of keeping the neutron cone angle sufficiently constant was mentioned and this point needs further thought.

We also need, what might be referred to as "conventional" data on scattering by the three nuclei under consideration, i.e., we need some angular distributions within our energy range. Apart from yeilding the absorption cross-section by subtraction of $\sigma_{elastic}$ from σ_{total} - the accuracy would admittedly not be very high - the information would also be useful for multiple scattering corrections in, e.g., the sphere transmission method. Either a linac or pulsed Van de Graaff using a "white source" could be considered for these measurements.

Finally, I hope that Professor Newson will follow up his suggestions for obtaining data on the $He^3(n,p)$. We all acknowledge his beautiful work on thin sources and he is better equipped than anyone to measure accurate data on the T(p,n) source and hence get $He^3(n,p)$ by detailed balance. His suggestion to irradiate a proportional counter containing both He^3 and H is also very interesting. As we heard this morning, there are difficulties in running the counter at low energies but one $He^3(n,p)$ point in terms of the hydrogen cross-section would be very valuable

This sums up our ideas for measurements on standard cross-sections. The methods proposed are quite diverse and if we can get consistency in the results, then we should have reliable information on which to base our flux measurements. This programme is one which the EANDC should follow closely and, as a member of the Committee, I will urge that it does so.

So much for the standard cross-section. It would be wrong, however, to take this question of the standard cross-section out of the context of the general problem of measuring cross sections. At this meeting, we have seen that there are other methods of approach and surely these will play an important function in the overall progress.

Technically, I believe that we are confronted with two problems, that of source intensity and that of detection.

Regarding sources, I have not heard the Linac physicists forcibly express the need for greater intensities but I suspect they would like to have them available. With Van de Graaffs our efforts in the region below 100 keV are very often hampered by insufficient intensity and I would urge all those who try to improve the quality of these machines to go on doing so, because the more neutrons we have then the happier we will be. We also have to make our neutron producing targets compatible with high currents and this problem needs looking into.

Ben Diven expounded on the virtues of the bomb method. He told us quite clearly that these devices are perhaps the only ones which at the present time offer the possibility of obtaining data on the highly radio-active isotopes.

We discussed the detection problem this morning. Scintillation and semiconductor counter advance has been quite dramatic in the last few years but these and other devices still leave us with plenty of headaches for our particular problem. An accurate standard is not going to be much good unless we can use it to measure a cross-section, and it was brought out today that we have no obvious method in view. We must continue to work hard on detectors and solve the messy problems of multiple scattering and assaying the amount of sensitive material in the counter. Concerning the latter it is fortunate that there are people at Dr. Spaepen's laboratory who are devoting their time to the problem of assay and I think their efforts should be borne very carefully in mind.

We have also heard about interesting developments in direct methods of measuring a cross-section not requiring the use of a standard cross-section. Measurement of the strength of a radio-active product from a neutron producing reaction and also monitoring the He^3 particle from the T(p,n) reaction have been discussed. My own feeling is that these techniques are difficult and limited in scope but will be very useful for some applications. The French idea to use the monitored T(p,n) reaction to calibrate a detector might prove to be extremely valuable.

I would like to conclude with one firm recommendation for a measurement of the U^{235} fission cross-section. Over the years many people have spent a long time learning how to calibrate natural sources with very high precision and a lot of experience has been accumulated. There must surely be a way of applying this experience to our problem and I suggest we do it in the following way. We first calibrate an antimony beryllium source of sufficient intensity to carry out a direct measurement of the U^{235} fission cross-section. It has been stated here that a 1% accuracy on source strength could probably be achieved. For the measurement of fission events induced by this source it is probably best to use an accurately calibrated foil in a fission chamber, although a method based upon the observation of fission neutrons is worth consideration since we are now getting very

precise information in $\bar{\nu}$. Such an experiment might well be considered as a collaborative venture between laboratories having source calibration, foil manufacture and assay and fission detector experience.

3. PAPERS AND NOTES WRITTEN FOR THE SYMPOSIUM

a) THE FISSION CROSS SECTION OF Pu^{239} FROM 1 keV TO 160 keV

G.D. James
Atomic Energy Research Establishment,
Harwell, United Kingdom

Abstract

The fission cross section of Pu^{239} from 1 keV to 160 keV has been measured by time-of-flight experiment using 40 mg Pu^{239} and a 15 m flight path. The experimental method is described and the accuracy of the results is discussed.

1. Introduction

The fission cross section of Pu^{239} in the energy range 1 keV to 160 keV is important in the design of both thermal and fast reactors. Measurements around 30 keV are interesting also because they overlap with the range of measurements possible on a Van de Graaff generator. The fission cross section of Pu^{239} has been measured from 3 eV to 160 keV using one of the Harwell neutron project time-of-flight spectrometers. The experimental method used is described in Section 2. In Section 3 the accuracy of the results is discussed and some ways of improving the data are given in Section 4.

2. Experimental Method

A measurement of fission cross section by time-of-flight experiment requires the determination of the fission yield, the neutron spectrum and the background for these two quantities, as a function of neutron time-of-flight. In the present experiment the neutron booster[1] was used as a pulsed source of neutrons and the flight path length was 15 m. The booster was excited by 0.2 μsec electron pulses and the neutron time-of-flight was analysed into 4096, 0.25 μsec timing channels and recorded on magnetic tape[2]. The neutrons from the target were moderated in a 1 cm thick slab of water and traversed 2.5 cm aluminium

(beam port and beam tube windows) before reaching the detector. The neutron beam was collimated to 5 in diameter at the detector.

A cylindrical gas scintillator, 4.5 in diameter and 6 in long was used as the fission detector. This held a foil, containing 40 mg Pu^{239} at a superficial density of 0.5 mg/cm^2 on a 0.005 in platinum backing, in a plane at 74° to its axis. The detector was placed in the neutron beam such that the foil was at 78° to the neutron beam direction. This arrangement gave a better fission pulse height spectrum than would be obtained by viewing the foil end-on and enabled the 56 AVP photomultiplier, attached to the gas scintillator, to be kept out of the neutron beam but, at a cost of introducing a flight path uncertainty of 2.5 cm. Pulses from the photomultiplier were sent to a fast discriminator which converted all pulses greater than 100 mV into 6 V pulses. These were used to stop the time-of-flight analyser. A gas mixture consisting of 99.7% helium and 0.3% nitrogen, which acts as a wavelength shifter was flowed continuously through the detector at a rate of 100 cc/min. The photomultiplier voltage was chosen so that the alpha pile-up count rate was about 0.2 per minute.

To measure the neutron spectrum, an enriched BF_3 counter (96% B^{10}) 1.3 cm diameter and 5 cm long was used. The counter voltage was held down to 1.5 kV to keep the pulse due to X-rays from the accelerator at a level where it would not saturate the amplifier. An experiment is in progress to confirm that the base line is not disturbed for more than a few microsecs after this pulse.

For both the fission and BF_3 counters the background was determined as a function of time-of-flight (t) by placing a layer of resonant scattering material in the neutron beam between the source and the detector. The resonances used were:- Al, 35.2 keV; Na, 2.85 keV; Mn, 335 eV; W, 18.8 eV; Ta, 4.28 eV and In, 1.457 eV. Backgrounds measured in this way are depressed because the transmission of the resonant scattering material to the background neutrons is not unity. A correction was made for this effect after determining the transmission by introducing a second layer of material into the beam. Three fission monitors

in the booster target cell were used to normalise the background runs to the fission and BF_3 runs. It was found that the background for both the fission and BF_3 counters may be expressed as:

$$B = B_0 t^n \qquad (1)$$

where B is the number of background counts per timing channel, n is a constant and B_0 is a normalising constant. The value of n was found to be the same for both detectors.

The fission cross section as a function of neutron time-of-flight was deduced as follows. The magnetic tape recordings were analysed on a computer to deduce the number of fission, spectrum or background counts per channel. This number was corrected, using the Mercury computer, for the fact that the time analyser could record only one event per neutron burst. A quantity (S) proportional to the fission cross section was then found for each timing channel from the equation:

$$S = \frac{\sigma f}{K} = \frac{(A-B)}{(C-D)} = t \qquad (2)$$

Here A is the number of fission counts per channel and C is the number of spectrum counts per channel. B and D are expressions (1) for the background. The constant K was found by normalising the cross section to the data of Bollinger et al.(3). The area under the 7.83 eV resonance in a curve of S against energy was made equal to $\pi/2 \times 108.2$ barns -eV.

The number of spectrum counts per channel (C-D), can be expressed as:

$$(C-D) = Rf(t)t^{\lambda} \qquad (3)$$

where R and λ are constants and f(t) is the function of neutron time-of-flight shown in fig.1. Below 0.1 keV, f(t) is unity and apart from dips due to resonances in aluminium and manganese, gradually increases with increasing energy. To deduce f(t) the value used for λ was -1.455, a mean of the values found by several experimenters on the neutron booster. The function shown in fig.1. is similar to that given for the neutron booster by Moxon and Rae (4).

3. Discussion of results

The data fall into two regions, those below 35.2 keV for which the background has been measured and is given by equation (1) and those above 35.2 keV for which no background measurements were possible. In deducing the fission cross section above 35.2 keV, it has been assumed that the background is given by equation (1). In the region below 20 keV where the neutron spectrum does not show pronounced fine structure, the fission cross section is determined for each timing channel by equation (2). However, in the region of fine structure in the neutron spectrum, equation (2) is valid for each timing channel only if the time resolution of the fission and spectrum detectors are equal. In the present experiment the resolutions of these two detectors are not equal and only average values of the fission cross section over wide energy bands can be deduced above 20 keV. Furthermore, the neutrons reaching the Pu^{239} traverse 0.15 in more aluminium (the chamber wall thickness) than those reaching the BF_3 counter. A correction has been made for the mean transmission of 0.15 in aluminium whenever the aluminium cross section differs from 1.4 barns, the value allowed for by the normalisation. A correction has also been made for the deviation of the $B^{10}(n,\alpha)$ cross section from 1/V above 50 keV. The $B^{10}(n,\alpha)$ cross section used was taken from BNL-325 (8).

Fig.2 shows the Pu^{239} fission cross section as a function of neutron energy up to 20 keV as determined for each timing channel by equation (2). Only one set of data has been taken and the timing channels have been widened to 1 μsec to improve the statistics over this energy range. Below 10 keV the data show the same fluctuations as those of Bollinger et al (5); maxima at 1.2 keV and 1.8 keV and minima at 1.6 keV and 2 keV. Table 1 gives the mean fission cross section over four energy ranges above 10 keV and also the mean fission cross section found from BNL-325(6) and from the data of Allen and Ferguson(7). The short energy range 55 keV - 75 keV was chosen because the aluminium cross section remains below 2 barns and therefore no fine structure is expected in the neutron spectrum,

over this range. The three sets of data in Table 1 are in fair agreement except over the energy range 10 keV to 15 keV where the agreement is poor.

Table 1

Average values of the Pu^{239} fission cross section above 10 keV

Energy range (keV)	σ_f (barns)		
	Present data	BNL-325[6]	Allen and Ferguson
10 - 15	1.8 ± 0.1	2.35	-
15 - 50	1.92 ± 0.1	2.06	-
55 - 75	2.05 ± 0.1	1.82	1.95 ± 0.05
50 - 160	1.8 ± 0.1	1.78	1.69 ± 0.05

4. Conclusion

The present measurements of the Pu^{239} fission cross section are in good agreement with the data of Bollinger et al.[7] between 1 keV and 10 keV and show the same fluctuations. Above 20 keV the data are capable of giving the average cross sections over wide energy bands only. The data are fair agreement with other measurements above 15 keV and in particular with the Van de Graaff measurements of Allen and Ferguson. Between 10 keV and 15 keV however, the agreement is poor. The measurements could be improved above 20 keV by reducing the amount of aluminium in the neutron beam and by using a spectrum detector with a time resolution equal to that of the fission detector. Measurements with better resolution on a longer flight path would enable the background above 35.2 keV to be measured.

Acknowledgements

Thanks are due to Dr. M.J. Poole and Dr. E.R. Rae for their advice and encouragement and to Mr. D.A.J. Endacott for assistance with the experiment.

References

1. Poole, M.J. and Wiblin, E.R., Proc. Int. Conf. on Peaceful Uses of Atomic Energy, Geneva, 1958, 14, 226.
2. Waters, J.R. and Bird, J.R., Nucleonics, 19, 70, (1961).
3. Bollinger, L.M., Coté, R.E. and Thomas, G.E., Proc. Int. Conf. on Peaceful Uses of Atomic Energy, Geneva, 1958, 15, 127.
4. Moxon, M.C. and Rae, E.R., A.E.R.E. - NP/GEN/30.
5. Hughes, D.J. and Schwarz, R.B., BNL-325 (2nd Ed.), 350, (1958)
6. Hughes, D.J. and Schwarz, R.B., BNL-325 (Suppl. No.1) 115, (1957).
7. Allen, W.D. and Ferguson, A.T.G., A.E.R.E. NP/GEN/3.
8. Hughes, D.J. and Schwarz, R.B., BNL-325 (2nd Ed.), 94, (1958).

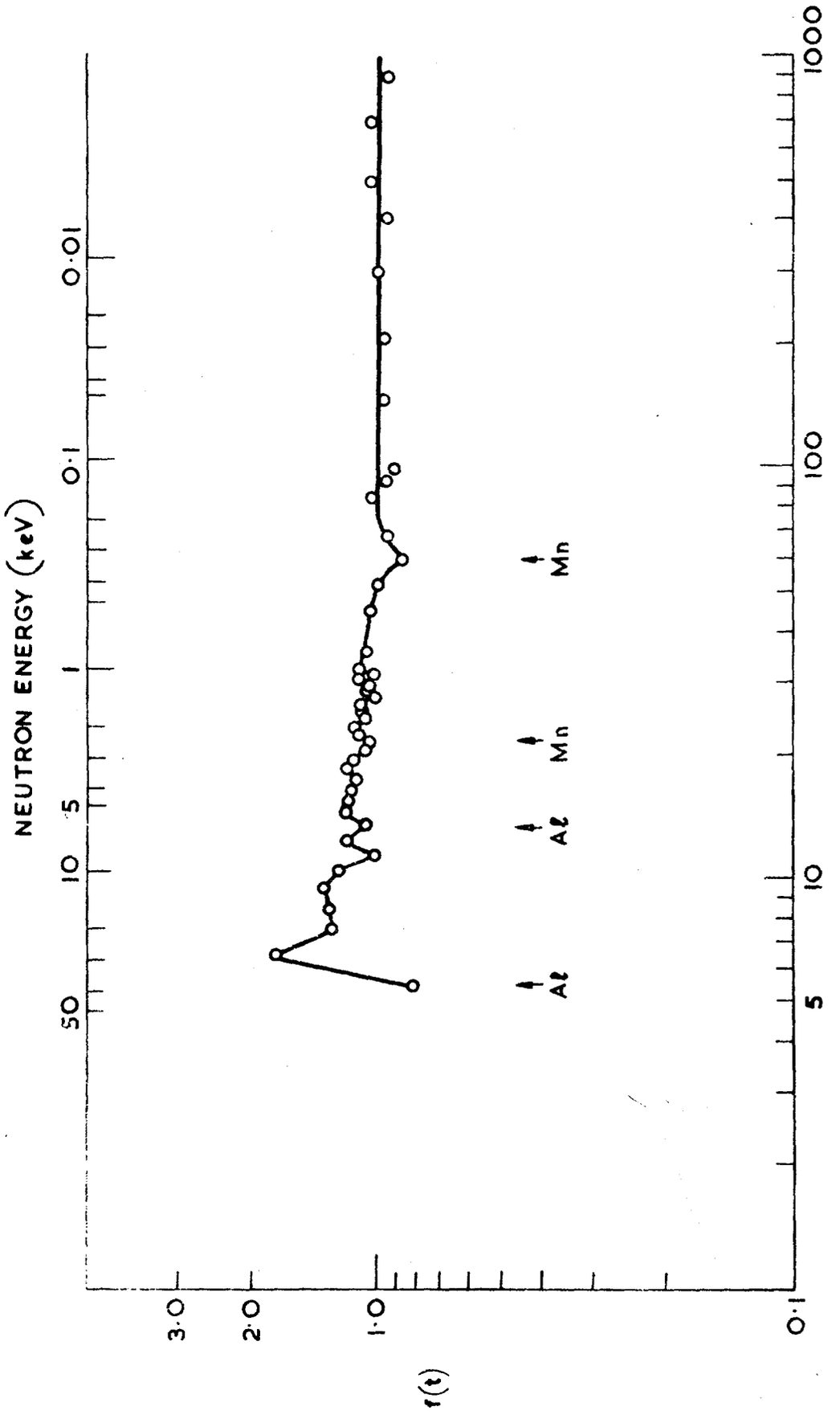

FIG. 1. THE SPECTRUM FUNCTION r(t)

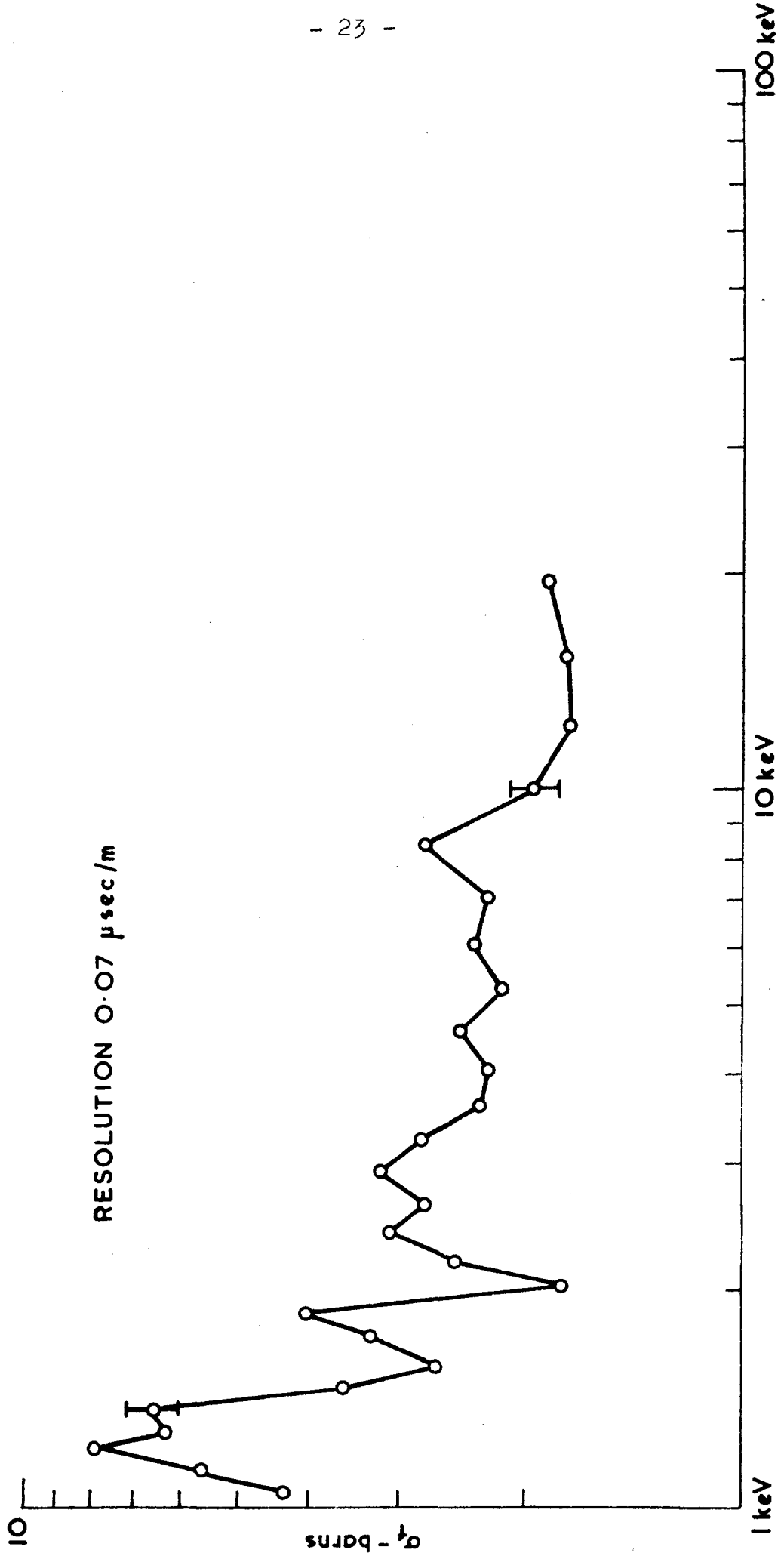

FIG. 2. Pu^{239} FISSION CROSS SECTION. 1 – 35 keV.

b) THE HYDROGEN GAS RECOIL COUNTER FOR NEUTRON FLUX MEASUREMENTS BELOW 100 keV

P.H. White
Atomic Weapons Research Establishment,
Aldermaston, United Kingdom

INTRODUCTION

The proton recoil gas counter has been used extensively for the measurement of neutron flux up to several MeV[1]. Accurate methods of estimating the wall and end effects have been developed [2], [3] and above 100 keV good agreement between the calculated and observed shape of the proton recoil spectra have been obtained. As a result the neutron flux can be measured to an accuracy of about 2%.

As the energy is reduced below 100 keV accurate measurements become progressively more difficult due to 1) the rounding off of the high energy end of the proton recoil spectrum (P.R.S.) due to factors affecting the resolution of the instrument and 2) the enhanced effect of background.

This paper considers these factors in some detail and shows that after proper allowance for them, accuracies of 3 - 5% in flux measurement can be obtained down to 40 keV and probably down to 20 keV.

Description of the counter will be limited to the use as a proportional counter since the noise level in even the best present day equipment precludes the detection of such low energy particles in an ion chamber.

1. RESOLUTION EFFECTS

Five factors need to be considered here. They are:

(1a) Target thickness
(1b) Beam energy spread
(1c) Finite counter size
(1d) Statistics of ion production
(1e) Electronic Noise

Other effects such as anode wire non-uniformity and end effects are certainly present but in this energy region are small compared to those mentioned above.

To compare these processes the extrapolated end width of the recoil spectrum ΔE in Fig. 1 will be taken as a measure of the uncertainty*. All spectra will be referred to as if plotted on a recoil proton energy scale.

(1a) Target thickness

Neutrons at 135° from the $Li^7(p,n)$ reaction were used as a neutron source. For this angle the spread in neutron energy, and hence ΔE_t is approximately 0.5 t where t is the energy lost in the target by the incident proton beam. t may be calculated from the known rate of energy loss of protons.

(dE/dx) = 0.13 keV $cm^2/\mu g$ in LiF at 2 MeV proton energy
= 0.15 keV $cm^2/\mu g$ in Li_3N at 2 MeV proton energy

Targets of Li_3N were used in preference to those of LiF since for the same energy spread the neutron yield is over twice that of LiF. Li_3N is stable in dry air and is therefore easier to handle that metallic Li targets. The target thickness measured using the threshold method [(1), p.161] gave target thicknesses always greater than expected. The difference was attributed to an energy spread in the incident proton beam.

(1b) Beam energy spread

As in the case of target thickness the contribution E_b to ΔE in the PRS will be 0.5 x the beam energy spread. The value of this spread for the analysing magnet used was calculated to be 4 keV, giving a value of 2 keV for ΔE_b and was confirmed by the measurement of target thickness using the threshold method (see 1a).

---

*If the distribution of proton recoils is given approximately by the integral error function then it is easy to show that $\Delta E/E_o$ is given by $3\sigma / \mu (2.93\ \sigma/\mu)$.

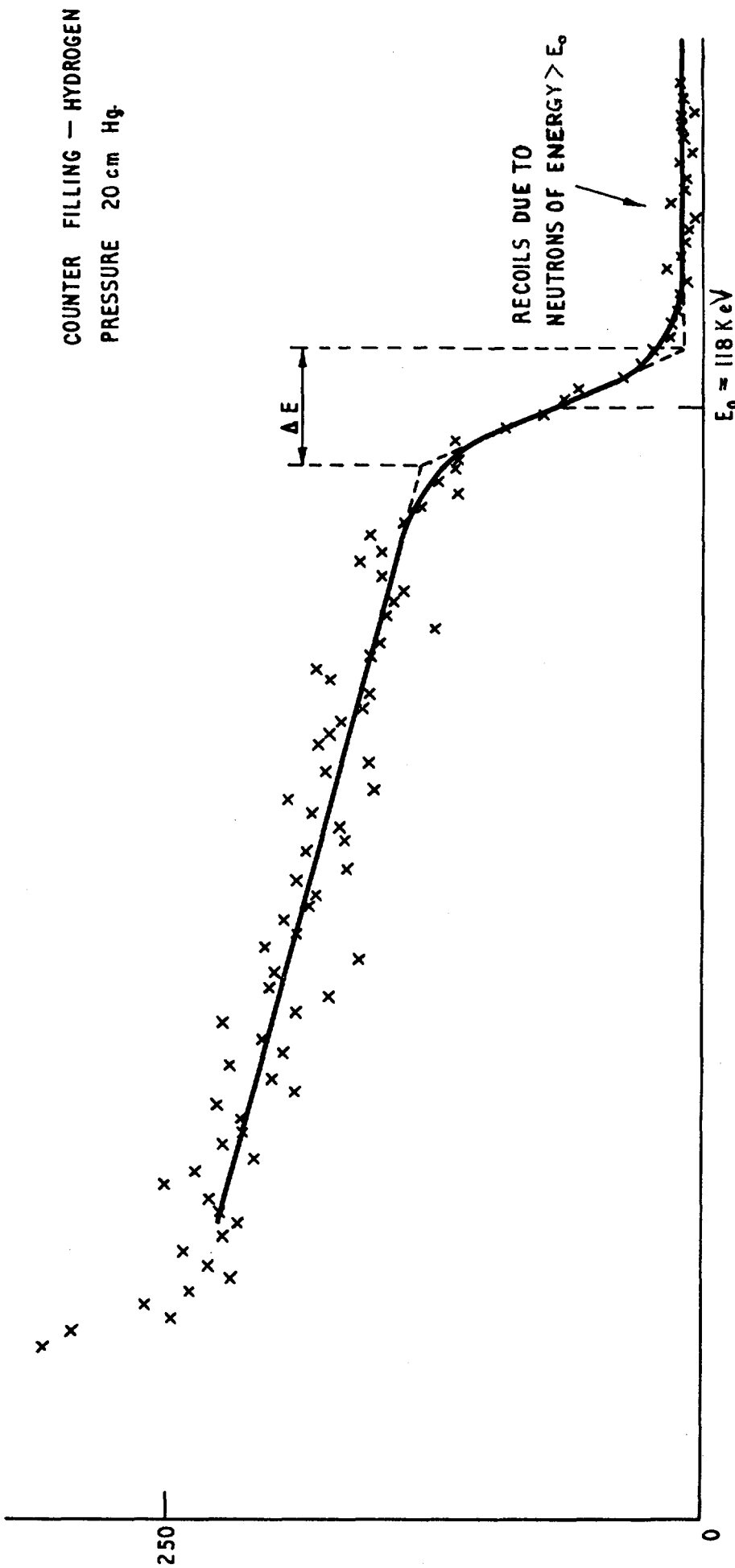

FIGURE 1 PROTON RECOIL SPECTRUM AT 118 KeV NEUTRON ENERGY

(1c) Finite counter size

Recoil counters are usually used at distances between 0.5 metres and 3 metres from the neutron source and therefore subtend an angle of several degrees at the source. The energy spread of the neutrons passing through the counter can be calculated from the reaction dynamics[1]. For this work the counter was 5 cm diameter a and 78 cm mean distance from the target and gave an energy spread of 3.5 keV, 2.5 keV, and 1.8 keV at 118 keV, 67 keV and 40 keV respectively.

(1d) Statistics of ion production

The fluctuation in the number of ion pairs produced leads to a spread ΔE_s in the peak height. This fluctuation is not entirely random and the details of the statistical process have been discussed [4], [5]. Quantitative measurements have been made for electrons in argon and electrons in xenon.

Quoting the results given by West if V_o is the variance in the number of ion pairs produced (m_o) then for ionising electrons $V_o \simeq m_o/3$. However the low energy protons detected in the recoil counter have velocities comparable with the orbital velocity of the electrons in hydrogen. In these circumstances (Fano[6] sub note 6) it is believed that $V_o \simeq m_o$ and will give a variance v' on the pulse from a proportional counter of $v' = 1.68\ m_o$, a result different from that for electrons. Table 1 summarises the expected value of ΔE_s for different neutron energies.

TABLE 1

End width ΔE_s due to the statistics on ion production

Neutron Energy (keV)	10	20	30	40	50	60	70	80	100
ΔE_s (keV)	2.2	3.3	4.0	4.7	5.3	5.7	6.1	6.6	7.4

(1e) Electronic Noise

The shot noise and grid current noise in the pulse amplifier will also contribute to ΔE. The RMS noise voltage v_n at the amplifier input is given by

$$v_n = \sqrt{4\ kT\ R_{eq}\ (1/\tau)}$$

where k is the Boltzman constant (1.38×10^{-16} erg/^oC)

T the ambient temperature (300^oK)

R_{eq} the equivalent noise resistance of the input value ($300\ \Omega$)

τ the electronic time constants (0.3×10^{-6} sec)

The recoil proton pulse amplitude v is given by

$$v = \frac{f\ E_o\ A}{I\ C}$$

where A is the gas multiplication (20)

I the mean ionisation potential (36 ev)

C the amplifier input capacity (60 pF)

f the reduction of the pulse height due to differentiation (0.5) [see ref. 47]

The quantity ΔE as defined is then given by

$$\Delta E_n = 3.I.C.\sqrt{4kT\ R_{eq}\ (1/\tau)}\ .\ (1/A)\ (1/f)$$

Substituting reasonable values as given in the brackets $\Delta E \sim 3$ keV. Since ΔE_n is inversely proportional to A, a recoil counter should be operated with as high a value of gas multiplication as is consistent with stable operation.

(1f) Summary

Measurements of ΔE were made at mean neutron energies of 118 keV, 67 keV and 40 keV, figures 1 - 3. In all cases ΔE could be accounted by adding (vectorially) the constituent parts as discussed in 1 a to 1 e. For example at 40 keV the observed value of ΔE was 6.6 ± 0.3 keV. The value calculated was

		20 μg target	5 μg target
Statistical	ΔE_s	4.7 keV	4.7 keV
Beam energy spread	ΔE_b	2.0	2.0
Target thickness	ΔE_t	3.0	0.8
Finite Counter size	ΔE_p	1.8	1.8
Electronic noise	ΔE_n	3.0	3.0
		6.8 keV	6.2 keV

Changes were made in the target thickness 5 μg - 20 μg of both LiF and Li_3N. As would be expected from the above figures, no significant change in ΔE from target to target was observed.

No attempt was made to reduce the proton beam energy spread to less than 4 keV although this would be desirable at energies below 40 keV.

In one measurement in which the counter EHT was reduced and hence the gas multiplication A, an increase in ΔE was observed as indicated in le and confirms the need for a high value of gas multiplication.

The recoil counter was operated with two values of hydrogen pressure; 40 cm Hg and 20 cm Hg: no significant difference in performance was noted between these two pressures. Therefore the higher pressure is to be preferred as it gives the higher rate of recoil events.

A pentode input amplifying system was used for these measurements. Triode connection of the input valve would reduce the noise level to a value not significant at energies greater than 10 keV.

The recoil proton pulse height corresponding to E_o was found to be proportional to the neutron energy down to 20 keV neutron energy and any energy defect if present is less than 3 keV.

2. THE COUNTER BACKGROUND

The background for the recoil counter can be subdivided into

(2a) High energy neutrons
(2b) Cosmic ray background
(2c) Electronic Noise
(2d) Neutron induced background
(2e) γ-ray induced background

Practically all measurements made using a recoil counter necessitate the use of a shadow bar in order to subtract the background of wall scattered neutrons. This technique will also subtract off accurately the background due to 2b, 2c and that part of 2e due to terrestrial radio activity. Provided of course that these backgrounds are not too large.

(2a) High energy neutrons

These are present when the recoil counter is used at background angles, with the $Li^7(p,n)$ neutron source and are due to neutrons backscattered by the target backing. The backing should therefore be made as thin as possible. Subtraction of the background may present some difficulty since the PRS for neutron energies much greater than E_o will, due to wall effects, give a spectrum departing markedly from the ideal spectrum. To give a reliable subtraction we should measure the neutron spectrum at the position of the counter using perhaps time of lfight methods. However since the background is small, usually 5 - 10% a reasonable estimate of the initial scattered neutron spectrum and hence the PRS, may be calculated using the known scattering cross sections for neutrons in the target backing. This may be checked against that part of the spectrum at energies greater than E_o as indicated in Fig. 1.

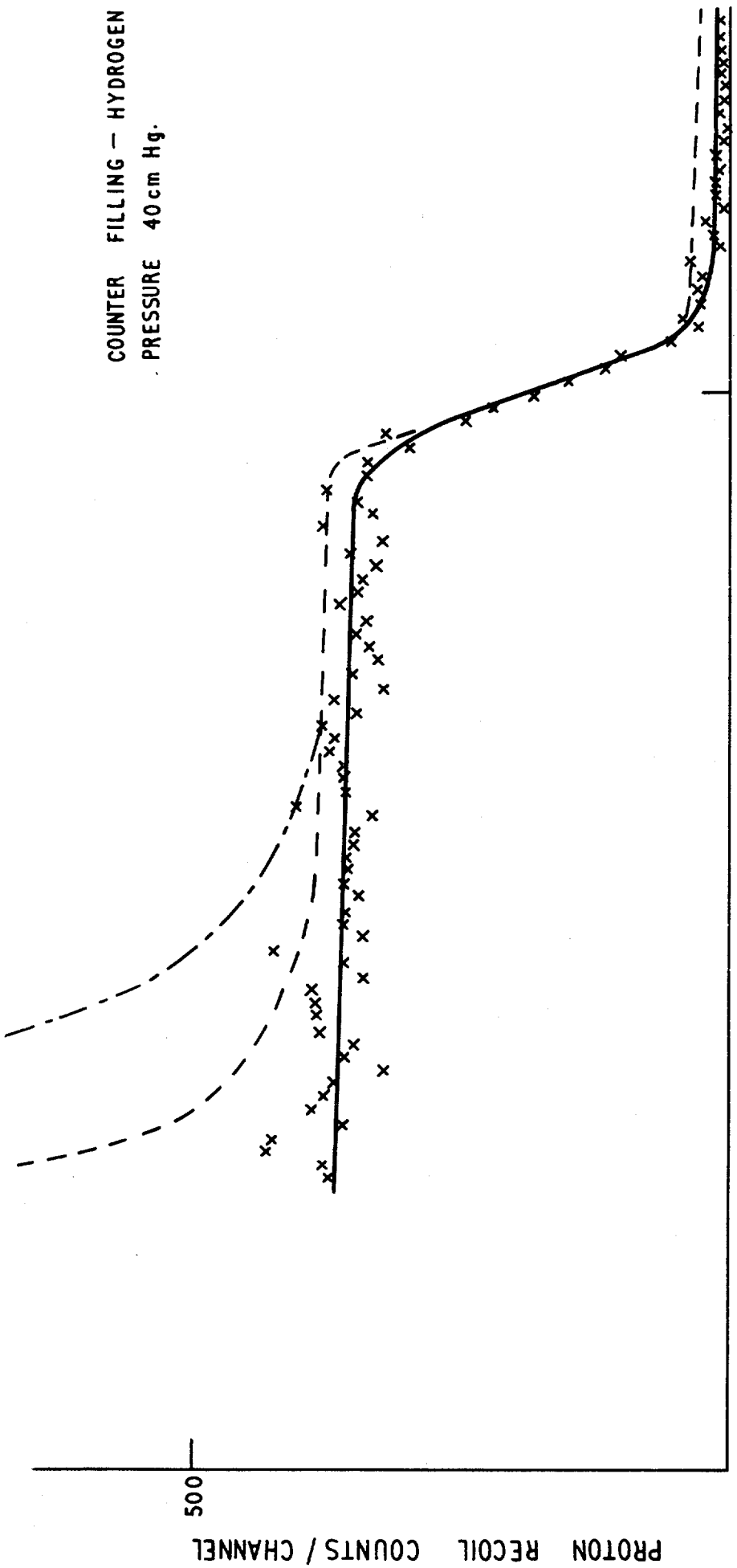

FIGURE 2 PROTON RECOIL SPECTRUM AT 67 KeV NEUTRON ENERGY

---- RECOIL SPECTRUM BEFORE BACKGROUND SUBTRACTION

—·— RECOIL SPECTRUM BEFORE BACKGROUND SUBTRACTION WITHOUT SCREENING & WITHOUT OPTIMAL CHOICE OF PARAMETERS

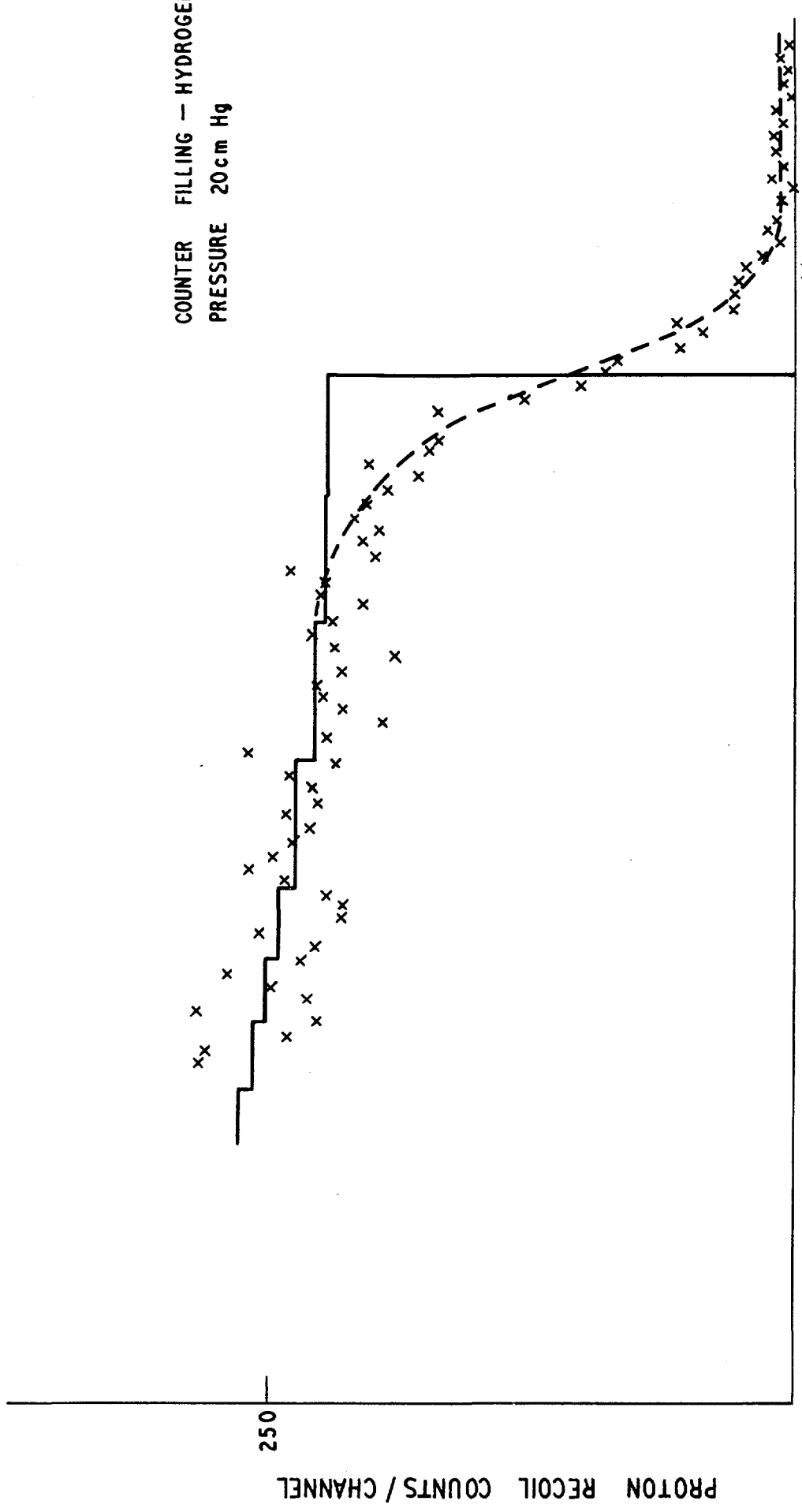

FIGURE 3 PROTON RECOIL SPECTRUM AT 40 KeV NEUTRON ENERGY

—— COMPUTED HISTOGRAM

(2b) Cosmic ray background

Particles of charge 1 at minimum ionisation produce approximately 8 ion pairs/cm H_2 at NTP. In a typical recoil counter with length 19 cm and H_2 pressure 40 cm there will be 80 ion pairs produced in a counter length. This is the same number of ion pairs that would be produced by a 2.2 keV proton. This background will therefore be small for all recoil proton energies greater than say 5 keV and to obtain a reliable estimate of the recoil spectrum down to $E_o/3$ the neutron energy E_o should be greater than 15 keV.

(2c) Electronic noise

The relative importance of this background is determined by the absolute rate at which the neutrons are detected. However, it is likely that the noise level will make measurement impossible for energies less than a few times (5 say) the RMS noise level. Using the figures in 1e, measurement would be impossible below 5 keV. As in 2b the neutron energy should be greater than 15 keV.

(2d) Neutron induced background

Inelastic scattering of neutrons and subsequent conversion of the γ-rays to electrons is not important below 90 keV neutron energy for most of the commom materials used in counter construction (Al, Mg, Zr, Cu, Zn, Au, Ag). The one exception is iron where inelastic scattering can occur from the 14 keV metastable state in Fe^{57}. The use of iron as a cathode material is therefore undesirable.

(2e) γ-ray induced background

This background will include γ-rays from the high energy accelerator, from (n,γ) reactions in the target room and from the decay of terrestrial radioactivity. The γ-rays are probably converted in the walls of the counter to electrons which are then detected in the counter gas.

The specific ionisation for 30 keV electrons in hydrogen is roughly 100 ion pairs/cm NTP[7], which is sufficient to stop the electron in the counter length (19 cm at 40 cm Hg pressure). This is then roughly the maximum energy which can be dissipated in the counter by an electron.

A large part of this background will be due to events in which the ionisation has a large radial extent in the counter. Such pulses are expected to be slow rising compared to the recoil proton pulses[4] and the background can be reduced considerably by the appropriate choice of differentiating time constants.

A further reduction could be expected by the appropriate choice of γ-screening material for the counter.

(2f) Summary

A substantial reduction in the background (40%) was obtained by interposing a 5 cm thick lead wall in the line of sight between the counter and the high voltage accelerator. This combined with experiments in which the proton beam was stopped at various positions in the drift tube indicated that the major part of the observed background was due to γ-rays from the accelerator and that very little if any of the background originated in the target.

No observable difference in γ-ray background was observed between LiF and Li_3N targets and no significant difference was observed in a change of recoil counter gas pressure from 40 cm Hg to 20 cm Hg.

The optimal differentiation time constants were found to be 0.7 μsec for 67 keV neutrons and 0.4 μsec for 40 keV neutrons and is roughly that given by calculating from the electron mobilities in hydrogen the longest rise time for a proton recoil pulse, i.e., the collection time for the ions produced by the proton recoil track with the greatest radial extent. Increasing the time constant by a factor 2 increased the background relatively by $\sim$ 100%, reducing the time constant did not reduce the background much and may well distort the recoil spectrum.

Well fitting screens on the cylindrical wall of the recoil counter were used to reduce the γ-background. Al, Cu,

Ag, Pb and combinations of these were tried. A screen of 0.150 cm Cu + 0.025 cm Pb gave a reduction in background of 50%. Although not actually tried a screen of 0.075 cm Cu + 0.025 cm Ag + 0.025 cm Pb is expected to give slightly improved screening due to the better coverage of the photon energy range over which photoelectric absorption can take place and at the same time give a slightly reduced thickness of absorber.

The use of a screen of 5 cm thick lead gave rather surprisingly a background reduction of only a further 10%. It was however not a good fit to the recoil counter.

The γ-screens suggested will introduce extra inscattering of neutrons into the recoil counter. However a calculation of this effect gives 3% inscattering for a copper screen 0.15 cm thick (verified experimentally at 150 keV neutron energy) and any error in the inscattering should amount to less than 1%.

With these conditions the spectra given in figures 2 and 3 were obtained. The background at recoil proton energies as low as 0.3 E_o is still comparatively small (< 20%) and its subtraction should introduce no error greater than 2%.

CONCLUSION

Recoil proton spectra have been obtained at 67 keV and 40 keV neutron energy. The spectra can be observed down to proton energies of approximately 15 keV and quantitative measurements to an accuracy of 3 - 5% should certainly be possible.

Methods of shielding from γ-rays and the choice of parameters are discussed and compared with the measurements. Light shielding of Cu + Pb + Ag together with optimal choice of counter multiplication, electronic time constants and target thickness are the parameters which give the greatest improvement.

Extrapolation of the results to lower energies indicate that the present design of recoil counter is unlikely to be useful at energies below 10 keV or for quantitative measurements below 20 keV.

REFERENCES

(1) J.B. Marion and J.L. Fowler; Fast Neutron Physics, Part I. Techniques. Interscience Publishers Inc. New York and London (1960).

(2) T.H.R. Skyrme, P.R. Tunnicliffe and A.G. Ward; Rev. Sci. Instr. 23 204 (1962).

(3) J.B. Parker, P.H. White and R.J. Webster; Nucl. Instr. and Methods, 23 61 (1963).

(4) D.H. Wilkinson; Ionisation Chambers and Counters, Cambridge University Press (1950).

(5) D. West; Progress in Nuclear Physics, 3 18 (1953).

(6) U. Fano, Phys. Rev. 72 26 (1947).

(7) K. Siegbahn; Beta and Gamma Ray Spectroscopy, Ch. I. North Holland Publishing Co., Amsterdam, (1955).

c) REMARKS ON ABSOLUTE HEAVY-ELEMENT NEUTRON CAPTURE CROSS SECTIONS DETERMINED BY THE SPHERE TRANSMISSION METHOD

H. W. Schmitt
Oak Ridge National Laboratory
Oak Ridge, Tennessee, U.S.A.

Neutron absorption cross sections determined by the sphere transmission method are, for kilovolt energies and heavy elements, essentially equivalent to capture cross sections. The method, because it does not require absolute determination of neutron fluxes, allows, in principle, very accurate determinations of absolute neutron capture cross sections. There are two effects, however, which prevent arbitrarily small, statistically-determined uncertainties. These effects concern (a) the dependence of σ_a values obtained by this method on σ_t, the total cross section, and (b) resonance self protection. In this paper, we shall bring up to date our previously measured 24-keV capture cross sections,[1] taking advantage of recent total cross section data.[2] We shall discuss briefly the resonance self protection problem and the final uncertainties in absorption cross sections.

Recent total cross section measurements[2] have been used to improve the accuracy of some of the absorption cross sections reported in Ref. 1. Results of the measurements of total cross sections for neutrons of 24 keV energy are as follows: Ag, 7.85 $\pm$ 0.23 barns; In, 6.11 $\pm$ 0.18 barns; Sb, 5.99 $\pm$ 0.14 barns; I, 6.69 $\pm$ 0.36 barns; and Au, 13.67 $\pm$ 0.28 barns.

The effects of changes and uncertainties in total cross section are discussed in Ref. 1; performing the necessary analyses, we obtain the following revised absorption cross sections for 24 keV neutrons:

Element	Absorption Cross Section
Ag	1127 ± 80 mb
In	854 ± 60 mb
Sb	578 ± 45 mb
I	768 ± 90 mb
Au	532 ± 60 mb

In spite of the improved accuracy of the new total cross sections, the uncertainties in absorption cross sections have not been changed from those given in Ref. 1; uncertainties in the resonance self-protection corrections are sufficiently large that no change seemed justified.

The problem of resonance self protection for spherical shells has remained unsolved. Dresner[3] and Macklin[4] have recently discussed the problem for disc samples. In a proper analysis of the problem for either geometry, the multiple scattering and resonance self protection effects must be combined, as indeed is done in these papers for disc samples. The problem for the case of spherical shells is a formidable one. Dresner[5] has discussed the problem of resonance absorption by a convex body in a sea of neutrons; this treatment has been adapted to the case of spherical shells.[6,1] Approximation methods for evaluation of the integrals were developed, Doppler-broadening of resonances was included, and a means of averaging over the Porter-Thomas distribution of level widths was developed. It has been pointed out by Dresner[6] that the resonance self protection effects would appear much larger indeed if Doppler-broadening and the Porter-Thomas distribution of widths were not taken into account. The elements listed above are the most favourable of those included in Ref. 1; the resonance self protection correction is 15 percent or less in all cases. Uncertainties conservatively assigned to the correction factor range from 30 to 100 percent of the correction. The absolute

absorption cross sections tabulated above, therefore, are to date the best we have available for heavy elements in the keV energy range, as obtained from sphere transmission measurements.

References

(1) H. W. Schmitt and C. W. Cook, Nuclear Physics 20, 202 (1960).
(2) K. K. Seth, Private Communication, 1963.
(3) L. Dresner, Nuclear Instruments and Methods 16, 176 (1962).
(4) R. L. Macklin, Nuclear Instruments and Methods (to be published, 1963).
(5) L. Dresner, CRNL-2659 (1959).
(6) L. Dresner, Private Communication.

d) THE ACCURATE MEASUREMENT OF NEUTRON FLUX BY THE BORON PILE

D. W. Colvin and M. G. Sowerby,
Atomic Energy Research Establishment,
Harwell, United Kingdom.

1. Introduction

The accurate measurement of neutron flux has always proved difficult. Standard neutron sources have been used but only in recent years have these been calibrated to approximately one percent and usually they have a neutron energy spectrum markedly different from the neutrons being used in an experiment. The Boron Pile experiment was designed to measure accurately the average number of neutrons emitted per fission ($\bar{\nu}$). In the course of this experiment, the neutron detector, the Boron Pile, was accurately calibrated as a function of neutron energy. In this paper the calibration and its errors are discussed. In the final section possible uses of the pile which would help to improve the accuracy of flux measurement in the neutron energy region of 30 to 100 keV are described.

The Boron Pile has previously been described in detail [1,2] and therefore only a brief description will be given.

2. Experimental Method

The Boron Pile consists of a graphite stack with cubic core of side 220 cms in which there is a 11 x 11 lattice of holes. In each of these holes except the central one there are two 5 cm diameter $^{10}BF_3$ counters. Round this core there is a 35 cm thick graphite reflector and a neutron shield consisting of 0.4 mm of Cd. inside 61 cms. of concrete. The central hole is key-hole shaped with the circular part 10.1 cms in diameter. This assembly has a counting efficiency of approximately 63% for a neutron source placed at the centre and when the pile was designed it was anticipated that the efficiency would vary by approximately 2% over the fission neutron spectrum.

In order to measure the efficiency of the pile use has been made of a reaction in which one neutron of known energy is emitted, namely the photo-disintegration of the deuteron. Deuterium in the form of tetra-deutero-methane is contained in a gridded ionisation chamber which is placed at the centre of the pile. Using the photo-proton pulses to trigger a gating system the efficiency of the pile can be determined as a function of neutron energy using γ-rays of different energies. Table 1 shows the γ-rays that have been used. The proton beam required for the (pγ) reactions was obtained from

Table 1
Calibration γ-rays

γ ray	γ ray Energy (MeV)	Approximate neutron Energy (Mev)
Th C^{11}	2.618	0.190
^{24}Na	2.757	0.265
^{19}F (p$\alpha\gamma$)	6.14, 6.92, 7.12	1.96
^{27}Al (pγ)	11.135, 12.915	4.9

the Harwell 5 MeV Van de Graaff. It was necessary to carry the proton beam to the centre of the pile so that the γ-rays were produced close to the ion chamber.

The gating system consists of two gates of the same length, the "prompt" and the "background" gates separated by a delay. The "prompt" gate is opened by the photoproton pulse and the "background" gate is usually opened 15 milliseconds later. The difference between the average neutron counts through the two gates gives the number of neutrons detected per photoproton pulse ($\bar{R}$)for the gate length used. The choice of gate length depends upon the experiment being performed; for a typical value of

4 milliseconds approximately 4% of the neutrons are captured after the prompt gate and the cosmic ray background is 0.2 neutrons per gate. A feature of this system which is essential for precise measurements is that the background is sampled close to each photoproton event.

3. Corrections to Experimental Data

Only a brief description of these corrections will be given as they will be discussed in detail in a future paper. There are five corrections which will be described:

(a) The count rate effect.
(b) The overlap correction.
(c) The effect of the ion chamber and beam tube on pile efficiency.
(d) The correction for neutrons captured after the "prompt" gate.
(e) The variation of efficiency with position in the central channel.

The count rate correction exists because the gating system has a dead time circuit which does not allow the prompt gate to open until after the background gate has closed. Since the prompt gate is opened by the first photoproton pulse after the end of the dead time there is less background in the "prompt" gate due to photo-disintegrations occuring before the gate than there is in the "background" gate. The calculated magnitude of this correction, which has been verified experimentally, depends upon the neutron mean life and upon the photoproton count rate and is 2.5% for a count rate of 20 photoprotons per second. The correction can be rendered infinitesimal by duplicating the twin gates and triggering each "twin" in turn, thus using all photoprotons.

The overlap correction, which must be applied to the value of $\bar{R}$ to allow for the dead time of the scalers used to record the neutron counts through the gates, is small. Typically

a dead time of 5 microseconds is used (3.5 microseconds is the minimum set by the pulses from the $^{10}B\ F_3$ counters) and for this, a 4 millisecond gate and a neutron background of one per gate the correction is 0.25% of $\bar{R}$. This correction may be accurately calculated for the neutron probability distributions used and introduces no error.

The deuterium ion chamber and the beam tube reduce the efficiency of the pile. Care was taken to minimize this effect by using, as far as possible, materials with low thermal absorption cross sections but even so it is important because the maximum of the thermal neutron distribution occurs at the centre of the pile. The effect has been measured by observing the reduction in the counts of Radio Thorium, D_2O, ^{240}Pu (spontaneous fission) and Pu-Be neutron sources, placed at the centre of the pile, produced by the Ion Chamber and the beam tube. The results were normalised to the thermal neutron density distributions calculated by Age-diffusion theory assuming the pile had no reflector so that the effects could be predicted as a function of neutron energy. Table 2 gives the reduction in pile efficiency obtained. The errors in the quantities are $\pm$ 0.1%.

Table 2

Reduction in Pile Efficiency produced by the Ion Chamber and Beam Tube

Neutron Energy (MeV)	Ion Chamber	Ratio of Efficiency with and without Ion Chamber + Beam Tube
0.190 (Rd Th D_2O)	1.0200	
0.265 (^{24}Na)	1.0197	
2.0 (^{19}F (p,$\alpha\gamma$))	1.0141	1.0273
5.0 (^{27}Al (p,γ))	1.0102	1.0195

A small fraction of the neutrons are captured after the "prompt" gate has closed. It is found experimentally that for times greater than 2 milliseconds after the opening of the gate the rate of neutron capture is exponential in form with a characteristic mean life which is slightly dependent upon the absorption of the ion chamber and beam tube. The correction can be made in most runs to an accuracy of $\pm$ 0.1%.

There are two $^{10}B\ F_3$ counters in all the lattice holes in the pile core except the central one. Because of the counter construction all the neutrons captured in the B^{10} within 3 cms of the counter are not recorded. This causes a dip in pile efficiency at the centre which though small must be allowed for in all the runs. It is found for instance that the efficiency increases by 1.002 if a fission source is moved 3 inches away from the centre of the pile.

4. Experimental Difficulties and Possible Errors

Electrical interference caused much difficulty during the calibration of the pile even though many precautions were taken. The effect on the neutron counters was not serious but for the ion chamber much trouble was experienced particularly when ThC'' and ^{24}Na γ-rays were being used. The problem was reduced by only accepting pulses in anticoincidence with pulses from an aerial and by making frequent "no source" runs. This technique introduces a small correction because there is likely to be less pick up in the "prompt" gate than in the "background" gate.

During the experiment it was found that the Van de Graaff beam was modulated at 50 c/s because of the interaction of the beam with the magnetic field of the belt motors. Since the γ-rays produced by the beam give rise to neutrons this means that the neutrons recorded by the pile were also modulated. The photo-disintegration are most likely to occur in the peaks of current and if the "background" gate opens after 15 milliseconds delay an incorrect background is obtained. This error can easily be eliminated by using a 20 millisecond delay.

One of the most important effects that must be checked is the possible anisotropy in the Boron Pile Efficiency. It is possible to imagine that because of streaming down the lattice that neutrons starting out parallel to the lattice will be detected less efficiently than those starting perpendicular to the lattice. Experiments have been done with ^{24}Na γ-rays making use of the anisotropy of the photo-neutrons. No evidence for any anisotropy in efficiency was found within the experimental error of ± 0.4%. It is therefore believed that any anisotropy in efficiency cannot affect the calibration of an isotropic source by more than 0.1%.

5. Results of Calibration

Table 3 gives the list of errors that exist in the calibration of the Boron Pile neglecting the statistical errors. The statistical errors vary for the different calibration points, for Th C'' and Al γ-rays (i.e. 0.19 and 5 MeV neutrons) the statistical accuracies are ± 1% and 1.7% respectively. For ^{24}Na and ^{19}F (pαγ) γ-rays the statistical accuracy is negligible in comparison with the errors (± <0.5%) in the neutrons detected from the spontaneous fission of ^{240}Pu and ^{252}Cf which have been used as standards. It is found within experimental error that all the measured efficiencies are the same. The absolute efficiency is approximately 63% (the exact value depends upon experimental conditions) and it is known to an accuracy of ± 0.5% for a fission spectrum.

Table 3

Errors in Calibration

Error	% Error in Efficiency
Effect of Pick up	0.03
Van de Graaff beam modulation	0.05
Overlap correction	0.05
Efficiency change due to Ion Chamber and Beam Tube	0.1
Correction for Neutrons captured after "prompt" gate	0.1
Variation of Efficiency with position	0.05
Anisotropy in efficiency	0.1
Electronic Stability	0.07

6. Measurement of Neutron Flux in the energy range 1-100 keV

It has been seen in the previous section that the Boron Pile Efficiency is known to the order of ½% for neutrons of approximately 200 keV. It is not expected that the efficiency will be altered significantly for neutrons of 1 keV because neutron leakage is unimportant and the probability of capture during the slowing down from 200 to 1 keV is small. Therefore the Boron Pile is a detector whose efficiency is well known in the energy region of interest and it is worth considering what contributions it can make to the problem being discussed at this symposium. Rather than put forward a programme of work some idea of the problems that can be tackled will be given. After the symposium a decision can be made on the experiments, if any, that can be done, influenced by any comments you would like to make.

The Boron Pile can be used to measure the strength of sources. There are difficulties because many sources used as standard contain fissile material (e.g. The Harwell spontaneous fission source contains 179.93 grms of plutonium 90.6% of which is ^{239}Pu) and multiplication is caused by neutrons interacting with the source after thermalisation. A programme of source calibration is taking place in conjunction with N.P.L. and A.W.R.E.

The measurements made during the past year have included some measurements of $\bar{\nu}$ as a function of neutron energy. In order to do this a neutron shield and collimating system have been set up so that a collimated neutron beam, obtained at 0° from (p,n) reactions produced by the Harwell 5 MeV Van de Graaff, is passed through the central hole in the pile. The neutrons are not believed to be seriously contaminated by scattering from the collimator walls because the beam is only accepted over a solid angle of 10^{-4} radians. It is possible to measure the neutron beam intensity by placing a graphite scatterer at the centre of the pile. Therefore, it is possible in principle to measure the efficiency of a fast neutron detector. Such

measurements will probably be difficult because of the low intensity of the neutron beam but since high accuracy is obtainable they would appear to be desirable particularly if a standard detector is adopted.

References

(1) D. W. Colvin and M. G. Sowerby, Proc. Second Int. Conf. Peaceful Uses of Atomic Energy 1958, 16, 121.

(2) D. W. Colvin and M. G. Sowerby, EANDC/UK/3.

e) STANDARD CROSS-SECTION FOR NEUTRON FLUX MEASUREMENTS BETWEEN 10 keV AND 100 keV

R. Batchelor, and J. F. Barry
Atomic Weapons Research
Establishment, Aldermaston,
United Kingdom.

1. Introduction

The measurement of any partial cross-section for a reaction induced by neutrons requires the measurement of neutron flux.

There are basically three methods of measuring neutron flux:-

(1) Absolute methods including, e.g.,
   (a) Monitoring the associated α particles from the $T(d,n)He^4$ reaction in the case of 14 MeV neutrons.
   (b) Detection of protons produced by the $D(\gamma,n)p$ reaction; each proton corresponds to the emission of one neutron.

(2) Methods based upon an accurately measured cross-section, which in this report will be called a standard.

(3) Methods based upon the use of a previously calibrated detection system - a secondary detector, e.g., long counter, manganese sulphate bath.

In general absolute methods are very limited in application. Secondary detectors are either limited in application, cumbersome to use or are not capable of yielding high accuracy. Consequently Method (2) is that generally employed for reasonably accurate measurements over a wide energy range. Fortunately, the (n,p) scattering cross-section is accurately known and this serves as a very convenient standard for fast neutron flux measurements above about 100 keV. However, below 100 keV a severe practical difficulty arises since the recoil protons do

not have sufficient energy to be detected with precision. Consequently it is necessary to look for another standard applicable to this energy region. Such a standard should fulfil the following requirements:-

(1) The cross-section should be accurately known or should be capable of measurement - hopefully to about 1% - over the required energy range. This implies that the cross-section should vary smoothly with energy.

(2) The reaction should have a positive Q-value.

(3) A convenient detector based upon the standard can be constructed. This implies that the cross-section should be of the order of 1 barn.

These requirements limit the choice of standard to one of three reactions:-

$B^{10}(n, \alpha)$, $Li^{6}(n, \alpha)$ and $He^{3}(n,p)$.

2. Status of Cross-Section Measurements and Possible Future Improvements

The present status on measurements of these cross-sections can be seen in Figures 1, 2 and 3. We can summarise the information in the critical region 1 keV to 100 keV as follows:-

$B^{10}(n, \alpha)$:- Only one set of direct measurements exist (Bischel and Bonner 1957). These measurements are normalised to the $1/v$ -value at 20 keV. Bergman and Shapiro (1961) suggest that the constant term of the correction to the $1/v$ law is -0.40 ± 0.03 barn.

$Li^{6}(n, \alpha)$:- Several independent measurements exist with deviations up to 30%.

$He^{3}(n,p)$:- There are two indirect measurements:-

(a) By Bergman and Shapiro (1961) suggesting that the constant term correction to the 1/v law is -1.1 ± 0.2 barn.

(b) By Macklin and Gibbons (1958) who measured the inverse reaction T(p,n) to an accuracy of about 10%.

Obviously none of these cross-sections are as yet known with sufficient accuracy to be adopted as a standard so we must now enquire into possible methods of improving these accuracies.

A paper study at AWRE has shown that the total absorption cross-section for B^{10} could be measured to an accuracy of 2 or 3% using the sphere transmission technique. The $Li^{7}(p,n)$ reaction would be used as a source of neutrons and the detector would be a spherical (and hence isotropic), fission counter (either U^{235} or Pu^{239}) of the gas scintillation type as described by White (1962). Transmission measurements would be made with a spherical shell 10 cm internal diameter, 12 cm external diameter, surrounding the detector. To obtain a 2% accuracy on the absorption cross-section at 30 keV, it would be necessary to measure the transmission to about 1%.

Corrections will be required for multiple elastic collisions in the shell and their magnitude will be a function of the elastic scattering cross-section and elastic angular distribution for the nuclei in the shell and also the energy variation of the fission cross-section of the material used in the fission counter. Calculation has shown that a 14% error in $\sigma_{elastic}$ at 30 keV would lead to a 2% error in absorption cross-section. If the fission cross-section is known to 10% at 10 keV relative to the 30 keV value, then the uncertainty in σ_f will lead to an uncertainty in transmission of $<0.6\%$.

It appears therefore that this method is capable of yielding a 2 - 3% measurement of the absorption cross-section of

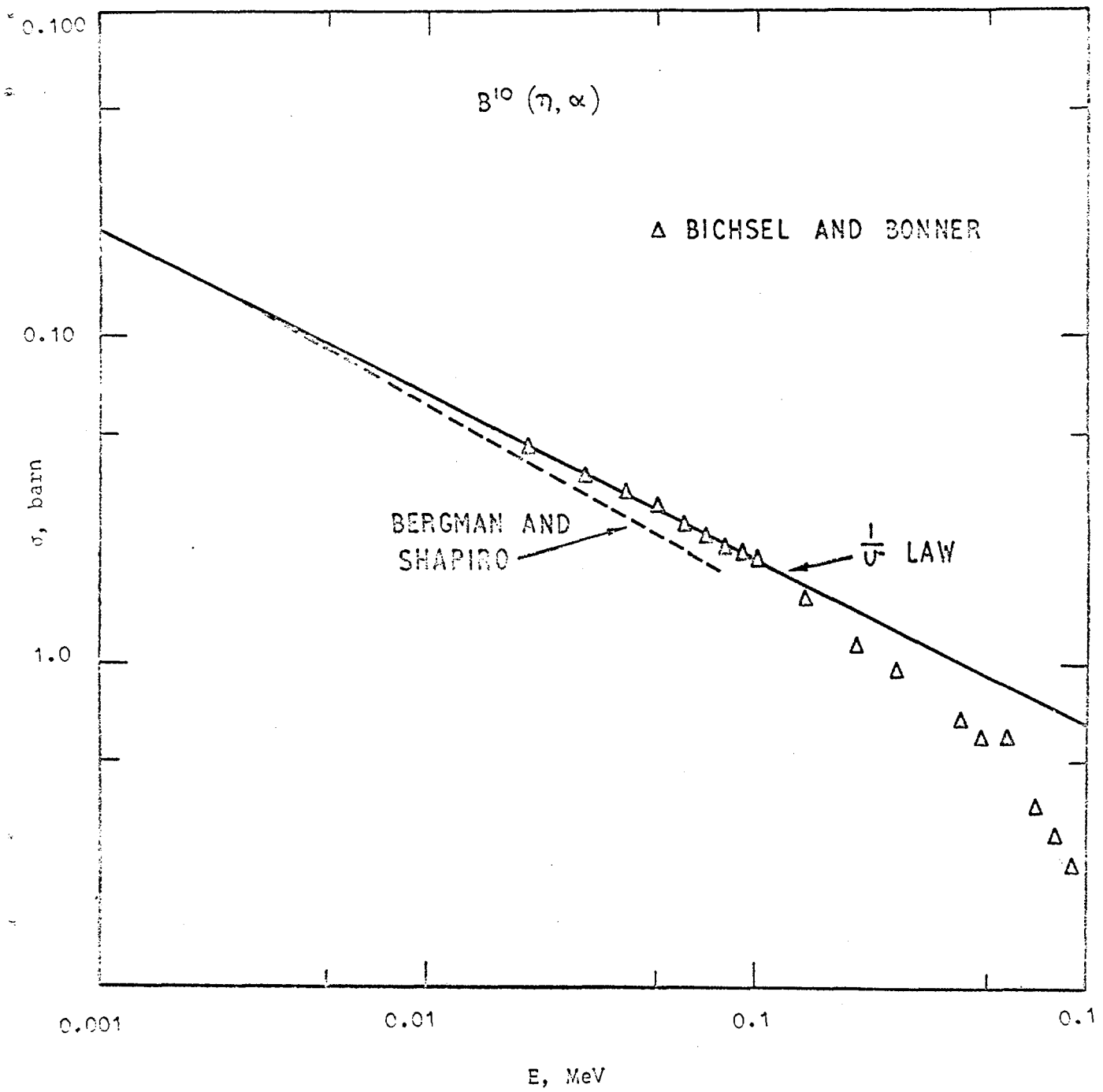
0.100
0.10
1.0
σ, barn
$B^{10}(n, \alpha)$
Δ BICHSEL AND BONNER
BERGMAN AND SHAPIRO
$\frac{1}{v}$ LAW
0.001
0.01
0.1
0.1
E, MeV

FIGURE 1

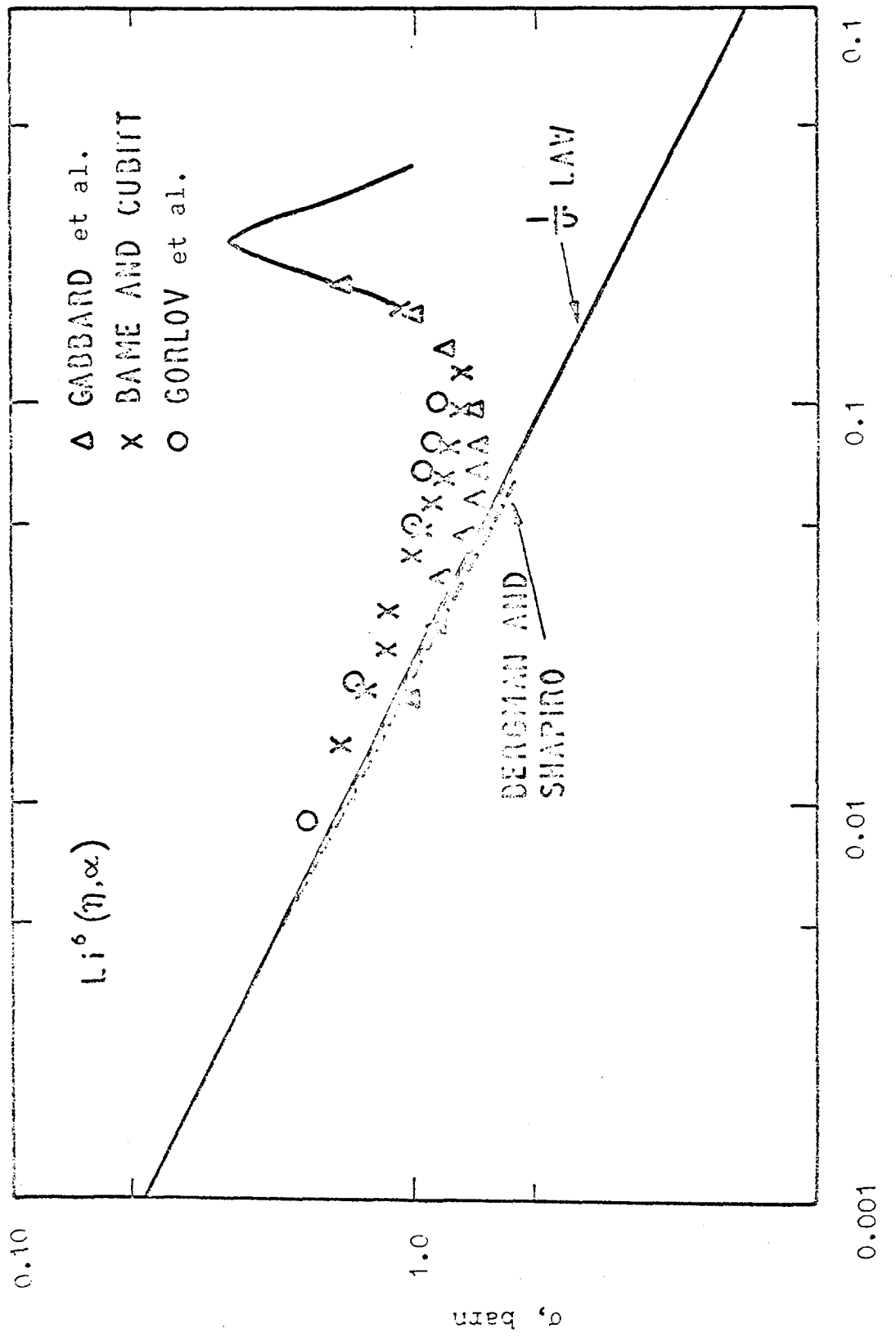
Li⁶ (η,α)
Δ GABBARD et al.
x BAME AND CUBITT
O GORLOV et al.
BERGMAN AND SHAPIRO
1/v LAW
σ, barn
0.10
1.0
0.001
0.01
0.1
0.1
E, MeV

FIGURE 2

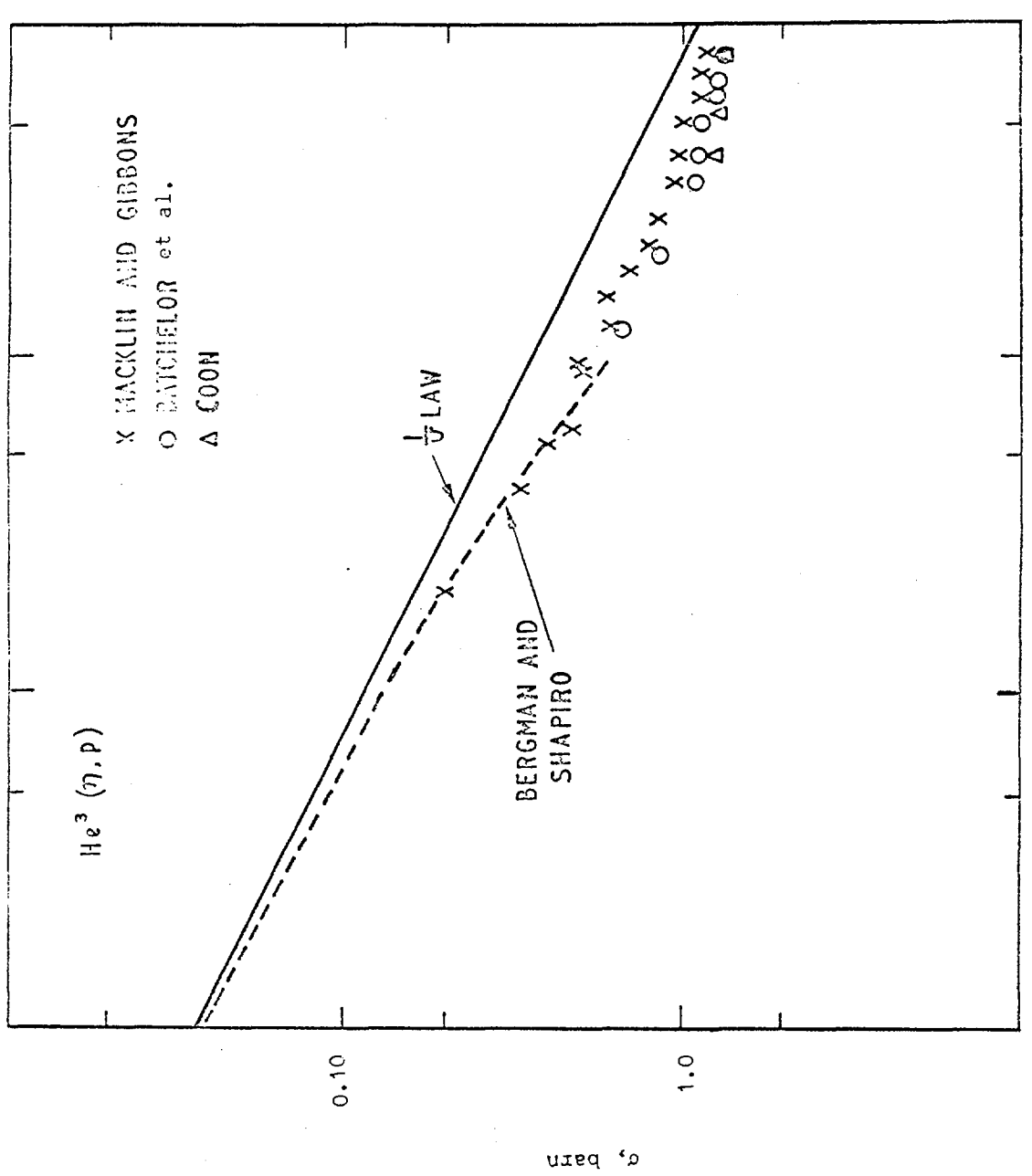
He^3 (n, p)
X MACKLIN AND GIBBONS
O BATCHELOR et al.
Δ COON
$\frac{1}{v}$ LAW
BERGMAN AND SHAPIRO
σ, barn
0.10
1.0
0.001
0.01
0.1
1.0
E, MeV

FIGURE 3

B^{10}. The method is also applicable to Li^6 and should lead to similar accuracy but is not practical for He^3 (if helium gas is considered a shell containing several hundred atmospheres pressure would be required).

It must be stressed that this experiment measures the total absorption cross-section. In the case of Li^6, this is equal to the $Li^6(n,\alpha)$ cross-section, apart from a negligible correction for the $Li^6(n,\gamma)$ reaction. However, this is not the case for B^{10}, since (n,p) and (n,t) reactions are energetically possible and may contribute to the extent of several per cent of the total absorption cross-section in the energy region under consideration. At the present time it is difficult to see how the (n,p) and (n,t) reaction cross-sections can be measured, even crudely.

Because the absorption cross-section of Li^6 is lower than that of B^{10}, the thickness of the Li shell would have to be about 5 cm. This would not introduce any difficulties, although considerable care would have to be taken in fabricating a lithium shell of high chemical purity.

3. Detector for Flux Measurements, based upon the Standard Cross-Section

The previous section has led us to the view that, of the three reactions under consideration, it is most likely that the $Li^6(n,\alpha)$ cross-section can be obtained most accurately.

It is desirable for any detector for flux measurements to have the following properties. (We are primarily considering the measurement of flux from the $Li(\hat{p},n)$ reaction, the protons being accelerated by a Van de Graaff; these considerations may differ slightly for LINAC experiments.):-

(1) Fast response ($\leq$10 ns).
(2) Reasonably high efficiency (about 10^{-4}).
(3) Low γ sensitivity.

(4) Reasonably small physical size.
(5) B^{10} or Li^6 content can be determined accurately.

The fast response is required so that time of flight selection can be employed to differentiate required flux from background flux. It must be borne in mind that to cover the required energy region it is necessary to use the $Li^7(p,n)$ reaction at backward angles. The direct flux is therefore low whereas the background flux might be relatively high and will be counted with high efficiency.

In considering the efficiency let us take a representative case for 20 keV neutrons; $Li^7(p,n)$ reaction, E_n = 1.97 MeV, $\theta = 120^o$. With a pulsed proton beam of pulse width 10^{-8}s, duty cycle 1 in 10, incident on a Li^7 target, 15 keV thick, the flux at a detector placed 20 cm away is $\sim 5 \times 10^3/cm^2$ s for 5 μA mean pulsed current. The corresponding energy resolution is 20% (sufficient for time of flight selection). If the detector is assumed to be 3 cm diameter, then to obtain a counting rate of 5 per second it is necessary to use an equivalent thickness of 1.4 mg/cm^2 and 0.7 mg/cm^2 for Li^6 and B^{10} respectively.

The restriction to a fast response allows only two types of detector, presently known. These are solid state detectors coated with thin films and loaded glass scintillators. Although the solid state detector is very attractive, it must be ruled out since the film thickness has to be restricted to ≤ 100 μg/cm^2 to avoid excessive loss of energy by the reaction products in the film. Glass scintillators, loaded with either Li^6 or B^{10} have high efficiency, but the problem of determining the number of active atoms in them is acute. Failing an accurate chemical analysis it should be possible to calibrate at, say, 0.025 eV with a chopper. Such a calibration must be made with a scintillator having relatively low absorption and this requirement conflicts with the need for high efficiency in the 10 keV - 100 keV region. However, a Li^6 glass is commercially available having a thickness of 3.2 mm and containing 2.5% natural lithium. This

transmits about 87% of thermal neutrons and corresponds to an equivalent thickness of 1.4 mg/cm^2 Li^6. Moreover, this scintillator, unlike a boron loaded scintillator, exhibits excellent discrimination against γ rays.

Calibration in a 0.025 eV beam would necessarily depend on a precise 0.025 eV (n,α) cross-section value. No direct precision measurements of $B^{10}(n,\alpha)$ and $Li^6(n,\alpha)$ exist although transmission data are available.

4. Recommendations

On the basis of the above reasoning we recommend that the $Li^6(n,\alpha)$ reaction be adopted as the primary standard for flux measurements between 10 keV and 100 keV. We have chosen this because

(a) A precise method of measurement of this cross-section is feasible.

(b) A simple and yet adequate, detector for measuring flux is available.

For these recommendations to be effective it seemshighly desirable that an accurate measurement of the 0.025 eV cross-section for $Li^6(n,\alpha)$ be made.

References

S. J. Bame and R. L. Cubitt, Phys. Rev., 114, 1580 (1959).
R. Batchelor, et al., Rev. Sci. Instr., 26, 1037 (1955).
A. A. Bergman and F. L. Shapiro, J.E.T.P., 13, 895 (1961).
H. Bischel and T. W. Bonner, Phys. Rev., 108, 1025 (1957).
J. H. Coon, Phys. Rev., 80, 488 (1950).
F. Gabbard et al., Phys. Rev., 114, 201 (1959).
Gorlov, et al., Soviet Physics, Dokladay, 1, 705 (1956).
R. L. Machlin and J. H. Gibbons, Phys. Rev., 109, 105 (1959).
P. H. White, Reactor Science and Technology, 16, 261 (1962).

f) NEUTRON CAPTURE IN U^{238} AND THE RATIO OF CAPTURE TO FISSION IN U^{235}

L. W. Weston, G. de Saussure, and R. Gwin
Oak Ridge National Laboratory*
Oak Ridge, Tennessee, U.S.A.

Abstract

Large liquid scintillator tanks have been applied to the measurement of the capture cross section of U^{238} at 30 and 64 keV and the measurement of the ratio of capture to fission in U^{235}. The ratio of capture to fission in U^{235} is being studied over a wide neutron energy range (4 eV to 700 keV) by two different methods.

I. INTRODUCTION

The ratio of capture to fission in U^{235} and the capture cross section of U^{238} are being studied in an effort to satisfy the requirements of reactor physics, as well as to better understand the processes involved. The U^{238} capture cross-section measurements are at keV neutron energies where the cross section is not well known because of the onset of p-wave and higher ℓ-wave reactions. This cross section is of particular interest because it appears to have an abnormally high p-wave contribution.(1) The ratio of capture to fission in U^{235} at neutron energies higher than thermal is of prime importance in the design of reactors with an appreciable fraction of neutrons at intermediate energies. This ratio has been measured in the neutron energy range from 10 to 700 keV, and measurements down to ~4 eV have been undertaken.

The neutron capture cross sections of U^{235} and U^{238} are measured relative to the fission cross section of U^{235}. Not only are these ratios of direct interest in reactor physics, but for U^{235} the ratio comes directly from the experiment since the capture cross section is obtained by discriminating capture events

---

* Operated by Union Carbide Corporation for the U.S. Atomic Energy Commission.

from fission events. The alternative standard cross section, $B^{10}(n, \alpha\gamma)$, is not used in this case because it would entail the use of a separate scintillation detector with resultant difficulties in comparison of detector efficiencies and time of flight. These difficulties, which arise because of the low gamma-ray energy from the $B^{10}(n, \alpha\gamma)$ reaction, can also be avoided by the use of $In(n, \gamma)$, and this reaction is in fact used here as a second standard.

II. NEUTRON CAPTURE IN U^{238} AT 30 AND 64 keV

Measurements of the U^{238} capture cross section at neutron energies of 30 and 64 keV were carried out by the technique described by Gibbons, Macklin, Miller, and Neiler.[2] Protons from the CRNL 3-MeV Van de Graaff which were just above the threshold of the Li(p,n) and T(p,n) reactions were incident on a target placed about 10 in. from a sample located at the centre of the ~1.2-meter-diam liquid scintillator tank shown in Fig.1. Kinematically collimated neutrons were thus produced in such a way that all neutrons penetrated the sample but did not strike the conical centre tube of the scintillator. The proton beam was pulsed with a width of ~10 ns at 8-μsec intervals so that the time-of-flight technique could be used to distinguish neutron absorption gamma rays from gamma rays produced by the (p, γ) reaction in the target. The time resolution of the liquid scintillator using a crossover-pickoff type discriminator[3,4] was ~24 ns under operating conditions.

Repetitive measurements were made with samples of U^{238}, U^{235}, and In to minimize the effect of changes in the neutron flux. Both time-of-flight spectra and pulse-height spectra were obtained so that backgrounds could be subtracted and the scintillation tank efficiency determined.

The uranium samples were in the form of pressed discs of U_3O_8, each 6 in. in diameter and containing 1 wt% paraffin as a binder. Each disc was encased in a steel container (0.001-in.-thick walls). The In sample was a metallic disc, also 6 in. in

diameter. Thicknesses of the U^{238}, U^{235}, and In samples were 0.00575, 0.00280, and 0.0121 atoms/barn, respectively. The U^{238} sample was chemically purified a few hours before irradiation to reduce the amount of radioactive contaminants which caused background in the scintillation tank.

The efficiency for detecting capture events in U^{238} and absorption events (capture or fission) in U^{235} above the 2.75-MeV bias was determined by the extrapolation of pulse-height spectra to zero. Major contributions to experimental errors were the uncertainty (5%) in the relative tank efficiency and the variation of the neutron flux (5%), the latter being quite sensitive to proton energy near threshold. The results were corrected for the ratio of the resonance self-protection[5,6] and average path length[7] in the samples.

Ratios of the U^{238} capture cross section to the U^{235} absorption cross section were found to be 0.150 $\pm$ 0.012 at 30 keV and 0.126 $\pm$ 0.010 at 64 keV. Using values of α for U^{235} reported in Section III, ratios of the U^{238} capture cross section to the U^{235} fission cross section were determined to be 0.206 $\pm$ 0.017 at 30 keV and 0.166 $\pm$ 0.014 at 64 keV. Assuming values for the U^{235} fission cross section from BNL-325[8] to be 2.58 $\pm$ 0.16 barns at 30 keV and 2.05 $\pm$ 0.12 barns at 64 keV, one obtains corresponding values for the U^{238} capture cross section of 0.531 $\pm$ 0.53 barn and 0.340 $\pm$ 0.034 barn, respectively. These results are compared with previous data in Fig.2. Agreement is good in most cases, and the agreement with previous ORNL measurements[2] is well within quoted errors.

Measurements with the In sample provided a secondary standard n, γ cross section as a check on the experiment. A comparison of the results is shown in Table I. The agreement is within errors, and it can be concluded that there should be no large systematic errors in the neutron monitor.

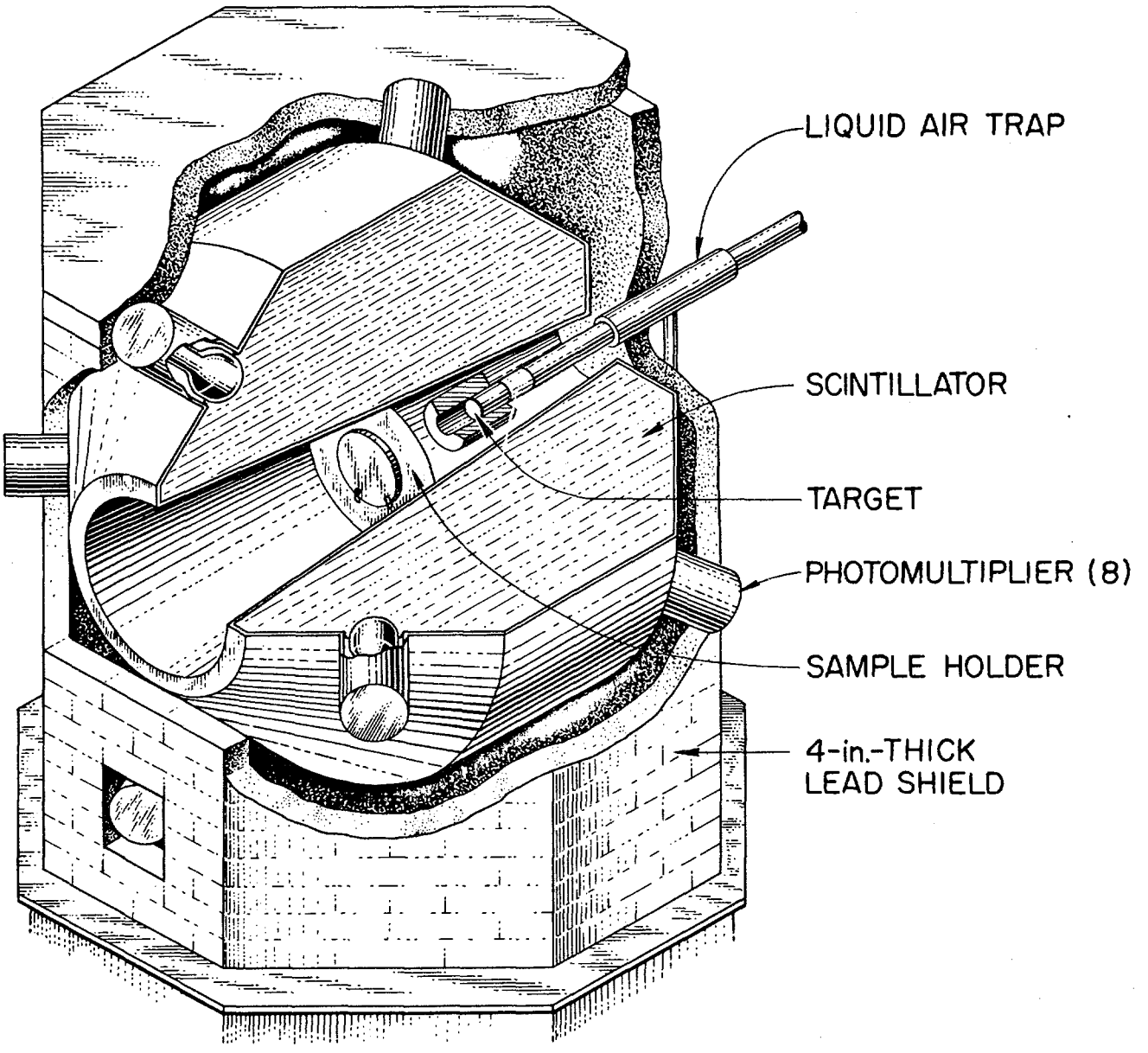

Fig. 1. Scintillator Tank

Table I. Values of $\sigma_{n\gamma}$ for U^{238} at 30 and 64 keV

	$\sigma_{n\gamma}$ (30 keV)	$\sigma_{n\gamma}$ (64 keV)
U^{235} Monitor	0.531 ± 0.053 b	0.340 ± 0.034 b
In Monitor	0.557 ± 0.056 b	0.281 ± 0.028 b

III. RATIO OF CAPTURE TO FISSION IN U^{235}

Preliminary measurements of α, the ratio of capture to fission, for U^{235} have been made from 10 to 700 keV. The large scintillator tank shown in Fig. 1 was again used to detect the capture or fission gamma rays which follow neutron absorption in all cases. Two basically different methods of discriminating between fission and capture events were used. In the first method the liquid scintillator was loaded with gadolinium so that the fission neutrons could be detected and in the second method the ~5-g U^{235} sample was in a fission chamber which was used to detect fission fragments.

It is fortunate that in the measurement of α no direct measurement of the neutron flux is necessary. The U^{235} fission cross section automatically becomes the standard cross section for the measurements, and, since both fissions and captures are observed simultaneously in the same sample, effects of resonance self-protection and multiple scattering cancel to a large extent.

Gadolinium-Loaded Scintillator Method

This method of measuring α was developed and discussed in detail by Diven et al.[10,11] The major difference between their experiments and the present experiment is the use of the time-of-flight technique to determine neutron energies below 100 keV. The method is usable since fission events can be distinguished from capture events by a liquid scintillator loaded with gadolinium (or cadmium). A capture event is characterized by a single fast cascade of gamma rays while a fission event is characterized by a pulse due to prompt fission

gamma rays followed by additional pulses a few μsec later due to gamma rays produced by the capture of fission neutrons in the gadolinium-loaded solution.

In this method for measuring α, the neutron-producing target (Li^7) was placed outside the scintillator tank 97 cm from the U^{235} sample, which was in the centre of the tank. The sample consisted of 20 discs, each 2-1/8 in. in diameter and 0.01 in. thick, spaced 0.1 in. apart. Each disc weighed 10 g. A collimator of Li^6-loaded paraffin shielded the scintillator material in the tank from direct neutrons from the target. Figure 3 shows a block diagrm of the experiment. The scintillator used in the tank was different from that previously used in that 16 g per litre of gadolinium 2-ethylhexoate was dissolved in the solution.

Above a neutron energy of 100 keV the time of flight of the neutrons was used to discriminate against background. Below 100 keV the time of flight was used to determine the neutron energies except at 30 keV at which energy approximately monoenergetic neutrons can be obtained with the Li(p,n) reaction.

Pulses from the scintillator tank corresponding to an absorbed gamma-ray energy of more than 2.75 MeV were accepted for analysis. Two microseconds after an event in the tank a 32-μsec-wide gate was opened to inspect for delayed pulses above 1.9 MeV due to the absorption of thermalized fission neutrons in the gadolinium. The efficiency for determining an event to be a fission was 87%. If an event was followed by a delayed pulse (and thus was most probably a fission event), the time-of-flight signal being taken in the analyzer was transferred to the second half of the analyzer memory.

From such data, the ratio of capture to fission (α) could be determined with the relation:

$$\alpha = \frac{(S.F.)_F}{(S.F.)_C} \quad \frac{\nu[I - C_o(1 - P_T)] - [C_o(1 - P_T)]}{(1 - P_T) - \nu P_T} ,$$

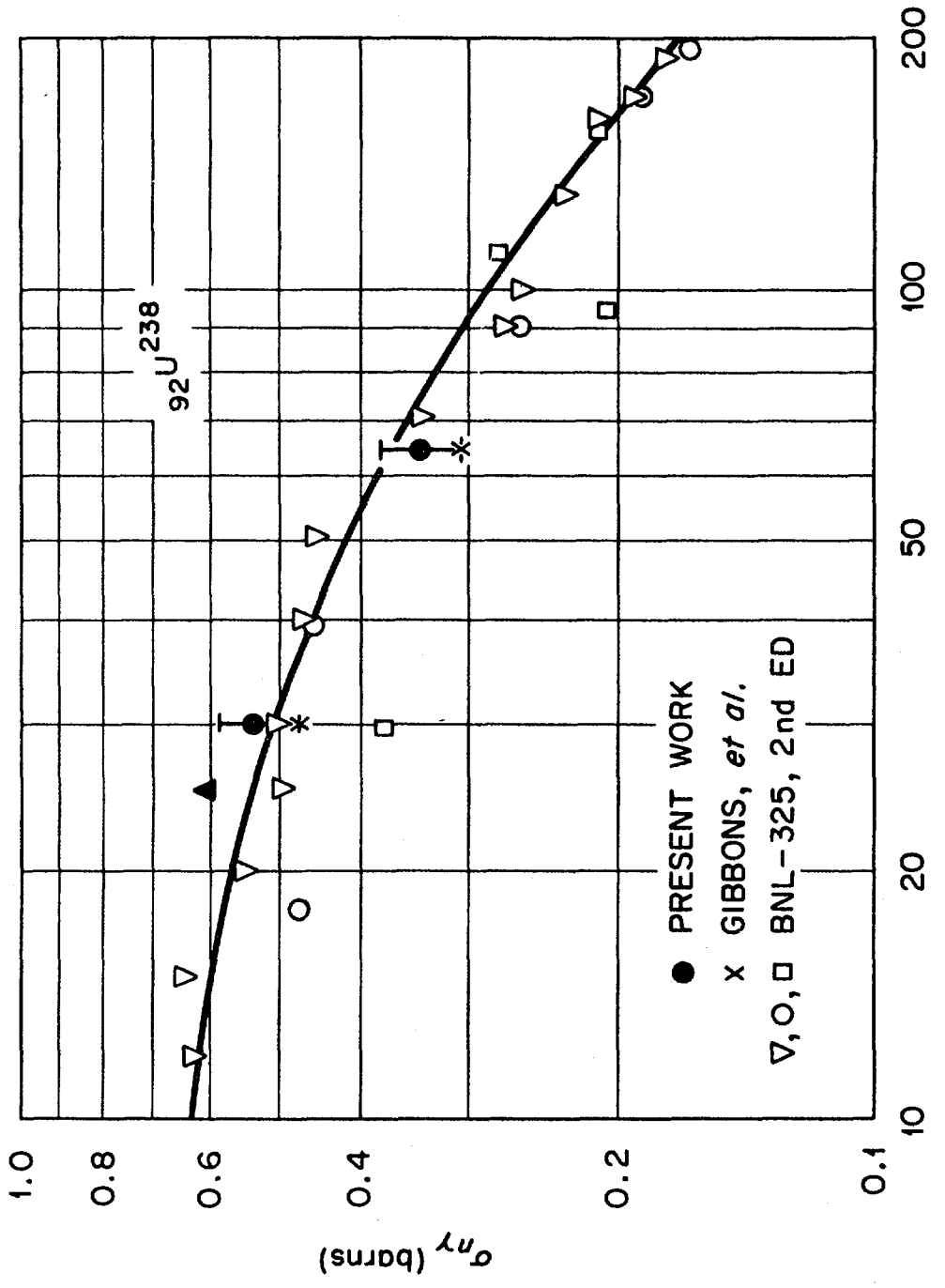

Fig. 2. Capture Cross Section of U^{238}. Results of other experimenters are also shown; (x) Ref. 7; (∇) Ref. 5; (O) Los Alamos, unpublished; (□) Harwell, unpublished; and (▲) Ref. 9.

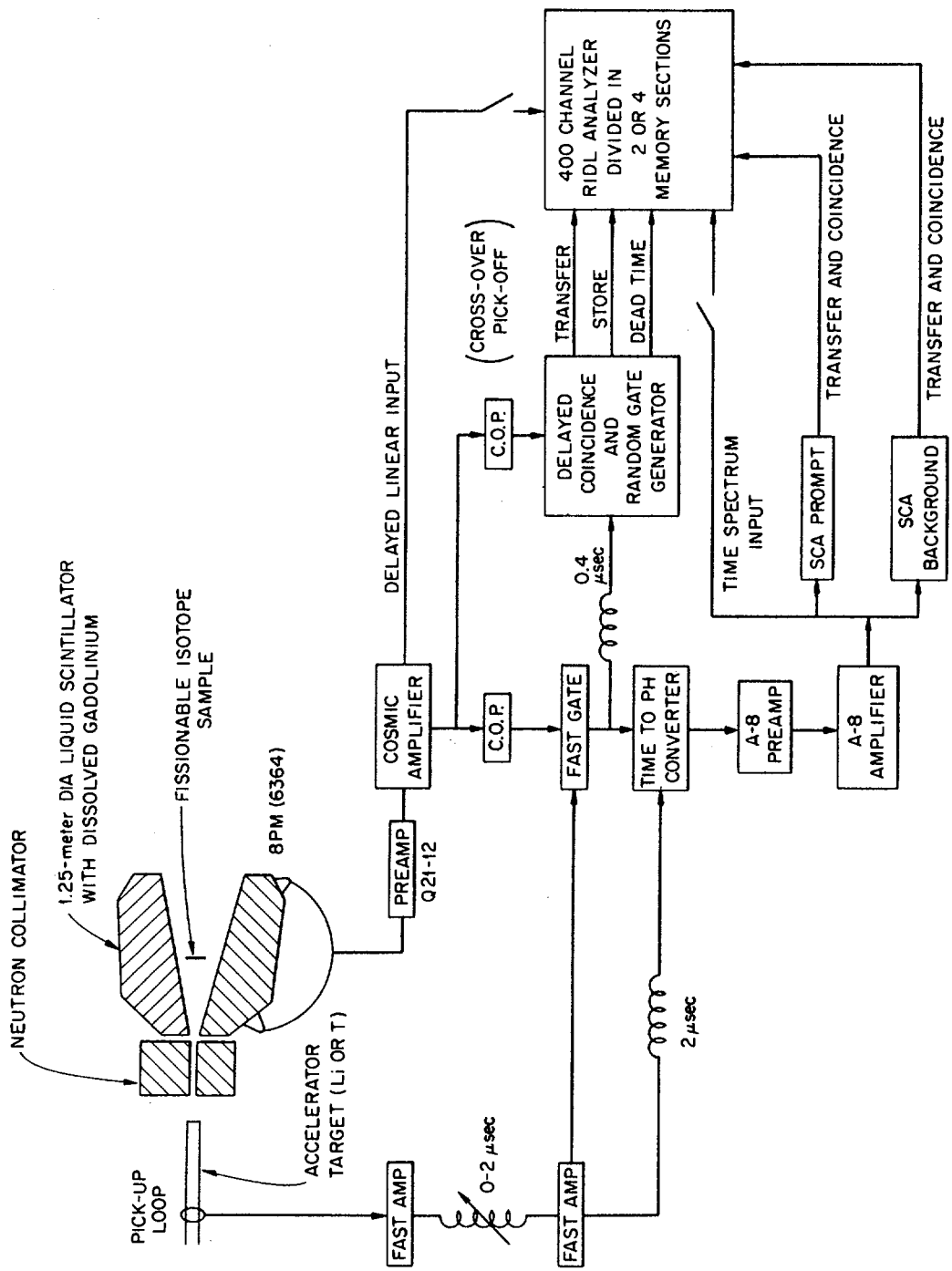

Fig. 3. Block Diagram of Electronics for Measuring α with a Gadolinium-Loaded Liquid Scintillator.

where

ν = ratio of events not followed by delayed pulses to events followed by delayed pulses,

C_o = probability that no delayed pulses would be detected following fission (0.125 ± 0.007),

P_T = probability that an event would be followed by an accidental background pulse (~5%),

$(S.F.)_F/(S.F.)_c$ = spectral fraction ratio, i.e. the ratio of the fraction of fission pulses detected above the electronic bias to the fraction of capture pulses detected above the bias (1.14 ± 0.08).

The ratio $(S.F.)_F/(S.F.)_c$ was determined by studying the pulse-height spectra of events at 30 and 600 keV. Figure 4 shows the pulse-height spectra resulting from capture and fission events. The fission gamma-raysspectrum was extended to zero bias with the use of a coincidence measurement between the scintillator tank and a fission chamber. The capture pulse-height spectrum was extrapolated to zero with the help of Monte Carlo calculations done by Macklin et al.(12)

The probability P_T was measured by observing whether a pulse occurred in a randomly generated gate identical to the one used for inspecting for fission neutron events. The probability C_o was measured with the use of a fission chamber containing ~5 g of U^{235}. Whenever a fission fragment was detected during the neutron burst, the same gate that was used for the thick sample experiment was applied to determine whether there was a detectable fission neutron pulse during the gate.

For monoenergetic neutron measurements, ν was taken to be the ratio of the area in the time-of-flight peak characterised by delayed events to the area of the peak characterized by delayed events. For time-of-flight runs, a channel-by-channel ratio or the sum-over-a-few channels ratio was used. A difficulty which was encountered in this procedure is that there appeared to be a slight shift in time (~4 ns) between capture and fission events. This is not completely understood but is

probably due in part to the energy imparted to the scintillator by the scattering of fission neutrons which occurs a few nanoseconds after the prompt fission gamma rays are emitted.

Preliminary results of the experiment are shown in Fig.5. Significant error reduction is expected as improvements in the experimental techniques are developed.

Fission Chamber Plus Large Liquid Scintillator Method

In this method of measuring α, both capture and fission events were detected by the liquid scintillator while fission alone was detected by means of a parallel-plate fission chamber. By taking coincidences and anticoincidences between the fission chamber and liquid scintillator, α could be determined. This method was applied at neutron energies of 30 and 64 keV in preparation for its use at lower neutron energies with an electron linear accelerator. It is limited to these two energies in Van de Graaff experiments because of neutron intensity requirements.

The technique was essentially the same as that used in the U^{238} measurement described in Section II except that a parallel-plate fission chamber containing ~5 g of U^{235} was the sample. The measurement consisted of gating a pulse-height analyzer over a "prompt interval" which covered the time neutrons passed through the fission chamber and at a "background interval" in order to measure the background simultaneously. Figure 6 is a time spectrum illustrating these intervals. The poor signal-to-background ratio made the simultaneous measurement of the background necessary. The pulse-height analyzer was thus routed into four sections according to time interval and whether there was a fission-chamber pulse in coincidence.

After backgrounds were subtracted from the pulse-height spectra, a fission pulse-height spectrum and an anticoincidence spectrum containing predominantly capture were obtained. The two spectra required correction for the fact that the fission chamber was only ~70% efficient in detecting fission fragments.

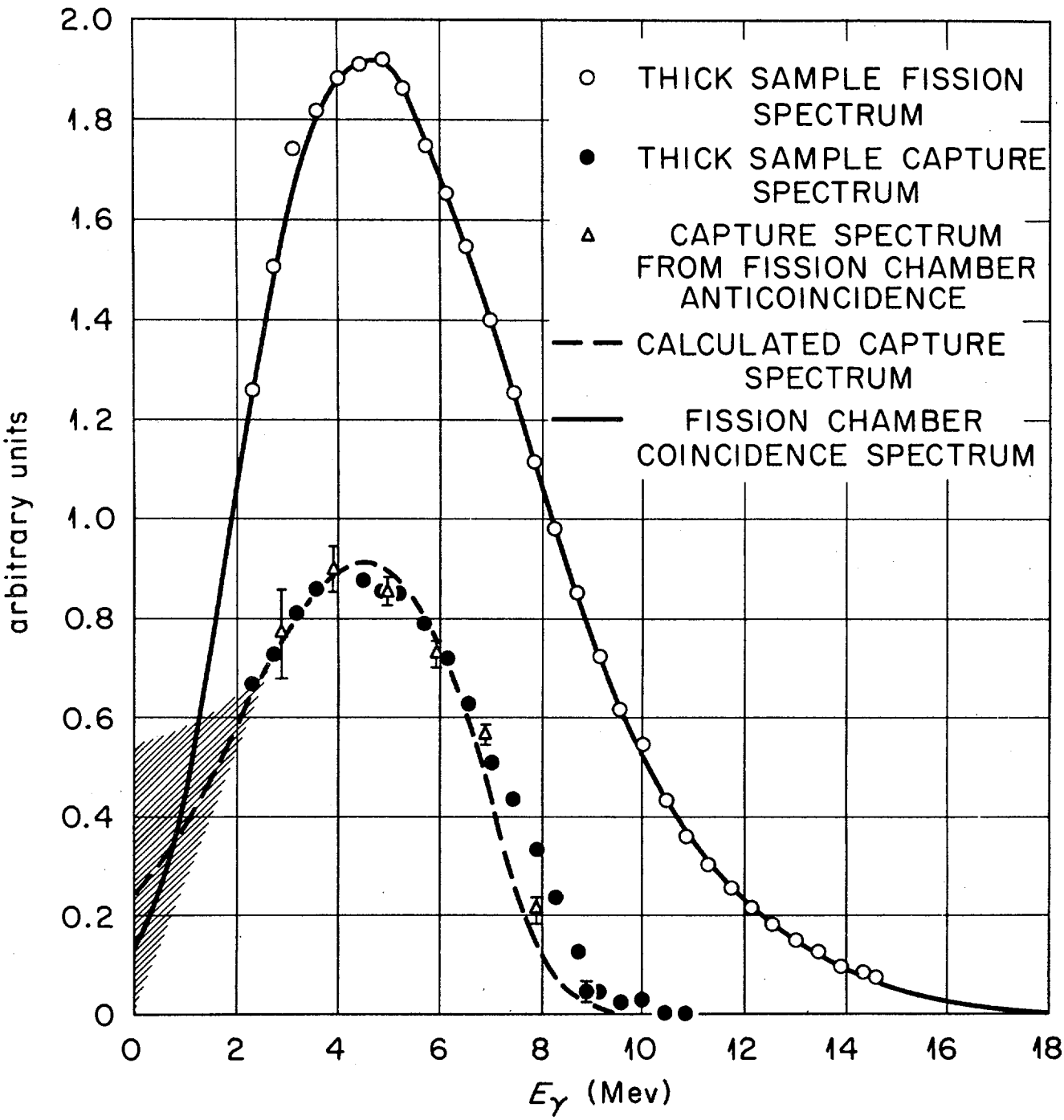

Fig. 4. Pulse-Height Spectra of Capture and Fission in U^{235}.

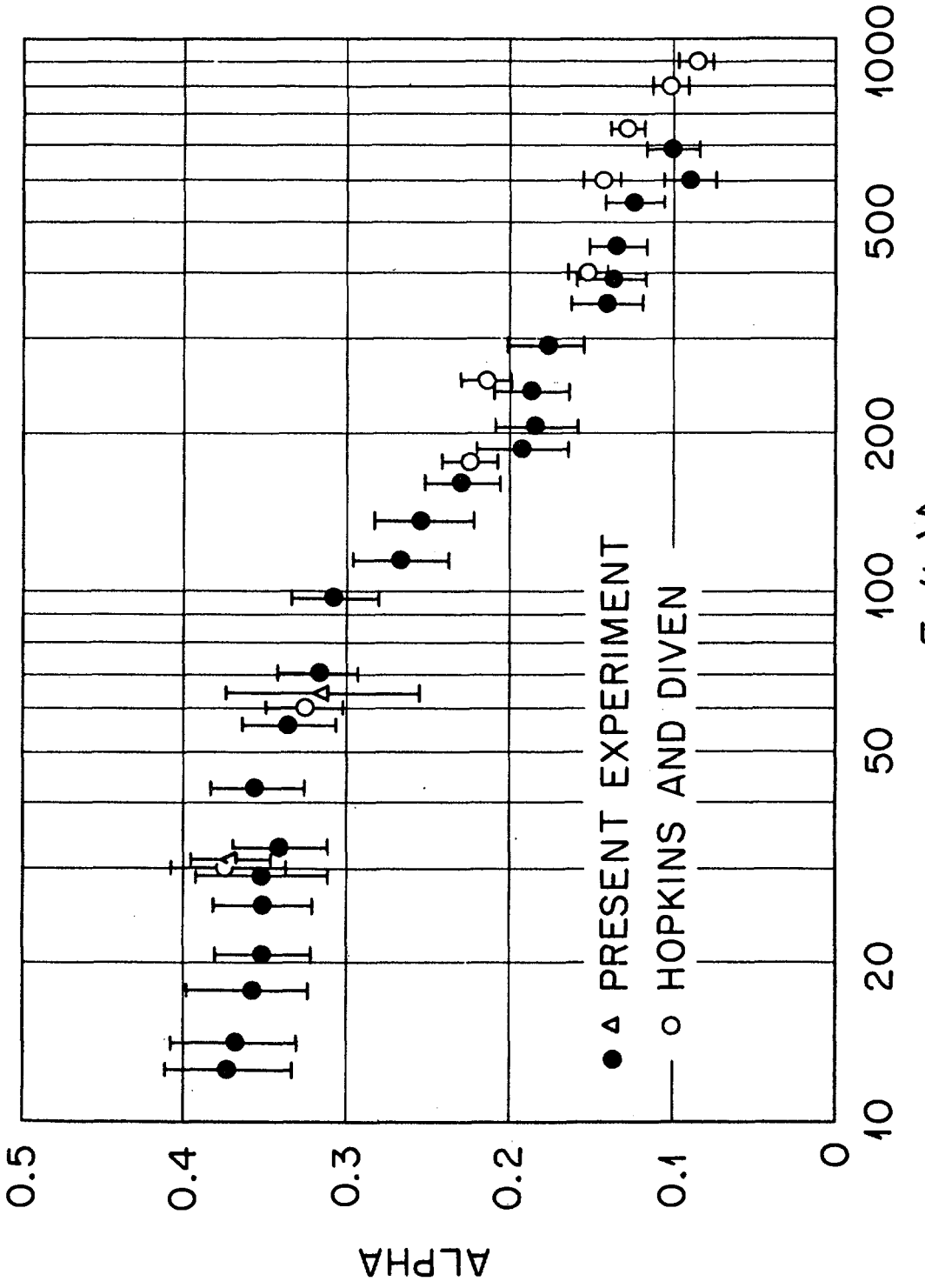

Fig. 5. Ratio of Capture to Fission in U^{235}.

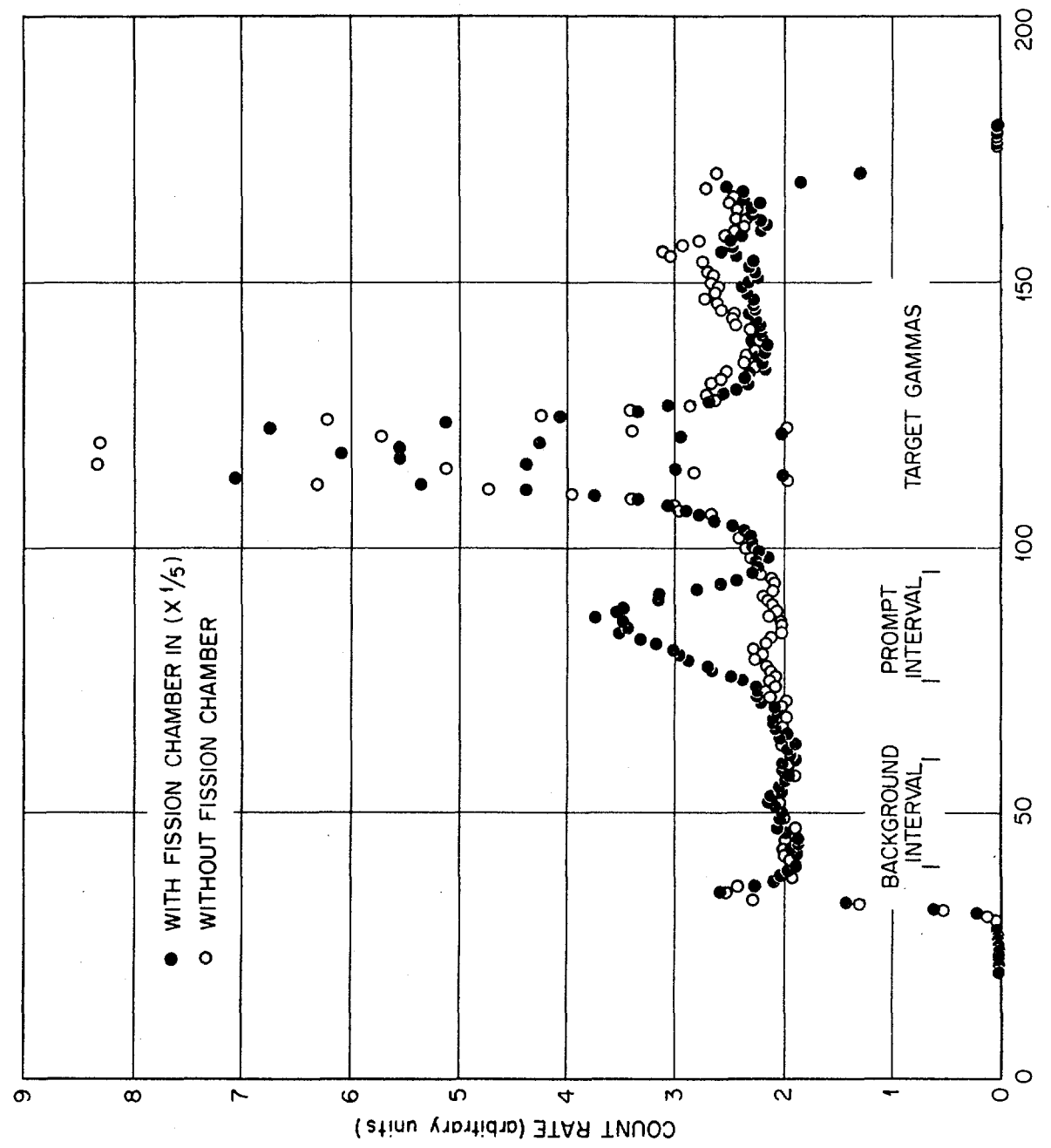

Fig. 6. Time Spectrum of Events With and Without Fission Chamber Inside Liquid Scintillator Tank.

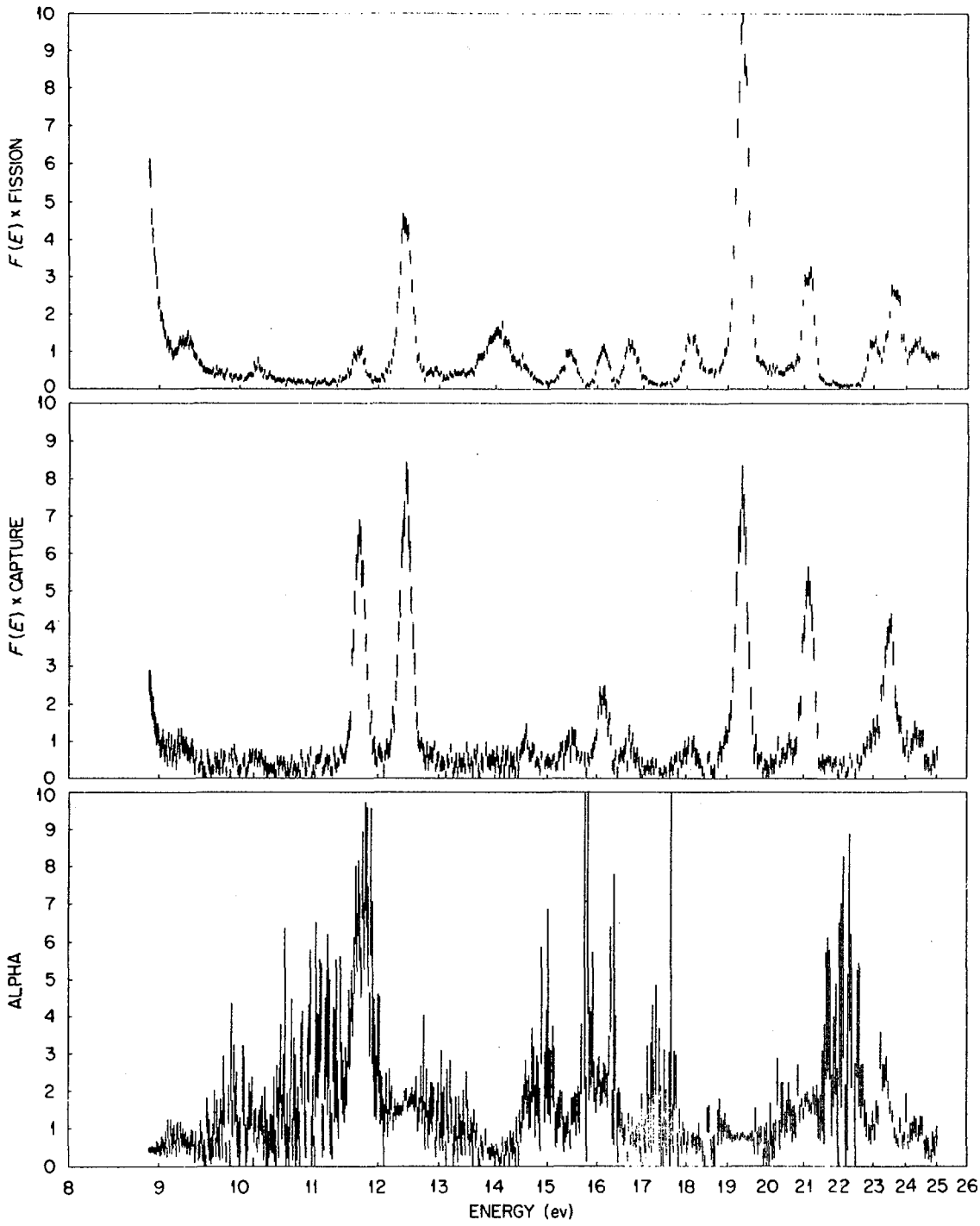

Fig. 7. Fission Events and Capture Events (Uncorrected for Flux) in U^{235} and Their Ratio, α.

The fission chamber efficiency was determined from the pulse-height spectra by using the assumption that no capture gamma ray pulses should exceed 10 MeV (see Fig.4). The relative efficiency of the scintillator to detect the two types of events above the bias was determined in the same manner as described in the previous section.

Table II shows the results of this experiment and a comparison with data by Hopkins and Diven.[10] The agreement between the two experiments is excellent.

Table II. Values of α for U^{235} at 30 and 64 keV

	α(30 ± 8 keV)	α(64 ± 20 keV)	$\frac{\alpha(30\ keV)}{\alpha(64\ keV)}$
This experiment	0.372 ± 0.026	0.315 ± 0.060	1.181 ± 0.260
Hopkins and Diven[10]	0.376 ± 0.036	0.327 ± 0.024	1.115 ± 0.135

This experiment illustrated the applicability of this method of measuring α over a wide neutron energy range below 30 keV with an electron linear accelerator. A co-operative experiment between ORNL and Rensselaer Polytechnic Institute has been initiated with the co-operation of J.E. Russell and R.V.Hockenbury of RPI. Figure 7 illustrates part of the preliminary data.

REFERENCES

1. E. G. Bilpuch, L.W. Weston, and H.W. Newson, Ann. Phys. 10, 455 (1960).
2. J.H. Gibbons, R.L. Macklin, P.D. Miller, and J.H. Neiler, Phys. Rev. 122, 182 (1961).
3. E. Fairstein, ORNL Instrument and Controls Division Annual Progress Report 1957 (unpublished).
4. R.W. Peelle and T.A. Love, ORNL-2389, p. 245 (1957), (unpublished).
5. L. Dresner, Nuclear Instruments and Methods 16, 176 (1962).

6. R.L. Macklin, private communication (to be published).
7. H.W. Schmitt, ORNL-2883 (1960), (unpublished).
8. D.J. Hughes and R.B. Schwartz, BNL-325 (2nd ed.) (1958).
9. R.L. Macklin, N.H. Lazar, and J.S. Lyon, Phys. Rev. 107, 504 (1957).
10. J.C. Hopkins and B.C. Diven, Nuclear Sci. and Eng. 12, 169 (1962).
11. B.C. Diven, J. Terrell, and A. Hemmendinger, Phys. Rev. 109, 144 (1958).
12. R.L. Macklin, J.H. Gibbons, and T. Inada, Phys. Rev. 129, 2695 (1963).

g) THE Mn SO_4 BATH METHOD FOR NEUTRON FLUX MEASUREMENTS IN THE INTERMEDIATE ENERGY REGION

W. Pönitz and G. Brudermüller
Institut für Angewandte Kernphysik,
Kernforschungzentrum Karlsruhe, F.R. of Germany

Abstract:

The neutron flux from the Li^7 (p,n) Be^7 reaction near the threshold has been absolutely determined using a Mn SO_4 bath. Details of the experimental procedure are discussed. A preliminary measurement of the capture cross section of gold yielding 670 mb at 30 keV has been performed.

1. INTRODUCTION

The Mn SO_4 method has been frequently used for the determination of radioactive neutron source strengths (1 - 4) and for the measurement of neutron yields in fission (5). In these experiments, the neutron source is placed in the centre of a big tank containing an aqueous Mn SO_4 solution. A high (and well-known) percentage of the slowed-down neutrons is captured by Mn^{55} leading to the 2.59 h - activity of Mn^{56}. After the irradiation, integration is performed by stirring the solution and the activity of a well-defined quantity of the solution is absolutely counted. In this way, an absolute accuracy of about 2 per cent in the source strength determination can be achieved.

It seems worthwhile to apply the same method to the absolute measurement of neutron fluxes on collimated neutron beams, in particular in the energy region 1 - 100 keV where good standard cross sections for absolute measurements are rare. Therefore, the investigations described in this paper were started.

2. EXPERIMENTAL ARRANGEMENT

The Mn SO_4 solution was contained in a glass sphere with a volume of about 50 litres. Neutrons entered the sphere through an entrance channel made of quartz (see Fig. 1). In order to avoid collimators, the kinematic collimation of neutrons into the

forward cone close to the threshold of the Li^7 (p,n) Be^7 reaction was employed. The proton energy of the van de Graaff accelerator was controlled in such a way that the half angle of the forward cone did not exceed 10°*) so that no neutrons could hit the walls of the entrance channel before they had reached the centre of the tank. The neutrons thus formed a narrow energy group around 30 keV as can be seen in Fig. 2 where the calculated neutron spectrum from a thick Li target for several cone opening angles is shown.

3. THE DETERMINATION OF THE Mn^{56}- ACTIVITY

After each irradiation and after stirring the solution, 4,000 cm^3 of the solution were filled into a perspex container. The intensity of the 845 keV γ peak was counted using two 3" x 3" NaI(Tl) crystals, see Fig. 3.

This counter system had previously been calibrated in the following way: $Mn\,SO_4 \cdot H_2O$ powder was activated by thermal neutrons and was carefully mixed after the irradiation. From this material, pellets as shown in Fig. 4 were prepared. The activity of these pellets was determined absolutely by the $4\pi\beta$ - γ - coincidence method. The specific activity (decays per gramm and per sec) is given by (6)

$$a_{Mn^{56}} = \frac{N_\beta \cdot N_\gamma}{N_c} \cdot \frac{1}{G} \cdot f(d) \quad . \qquad (1)$$

Here, N_β, N_γ and N_c are the counting rates in the β-, γ- and coincidence channel, respectively. G is the weight of the $Mn\,SO_4 \cdot H_2O$ in the pellet and f(d) a correction factor depending on the sample thickness d. For $d \to 0$, $f(d) \to 1$; therefore, by extrapolation of $\frac{N_\beta N_\gamma}{N_c G}$ to $G \to 0$, the true specific activity is obtained. Fig. 4 shows this extrapolation which should give a very precise value of the specific activity.

*) The respective setting of the van de Graaff energy control was found in a preceeding run in which BF_3 counters were placed at various angles.

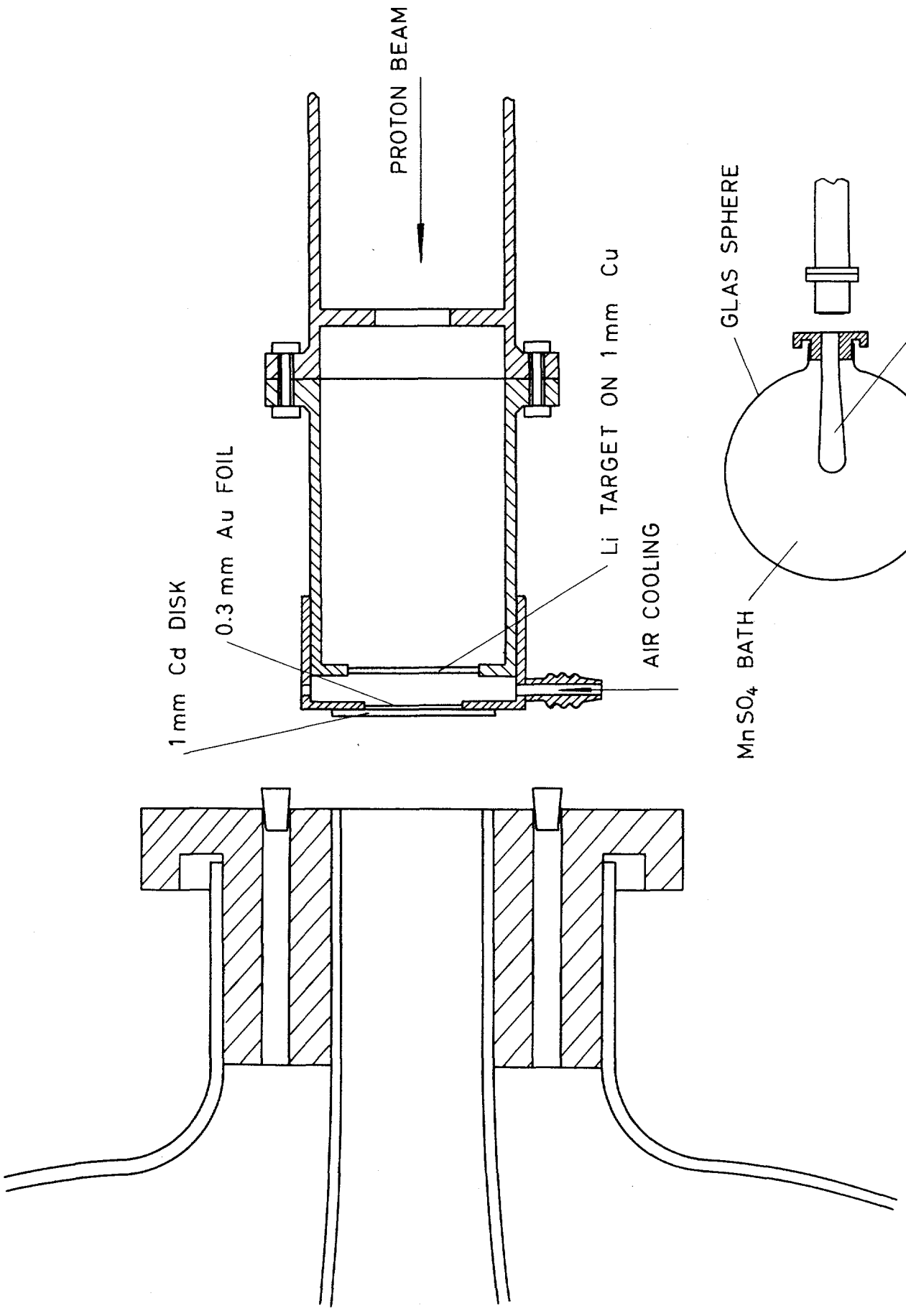

FIG. 1 EXPERIMENTAL SETUP

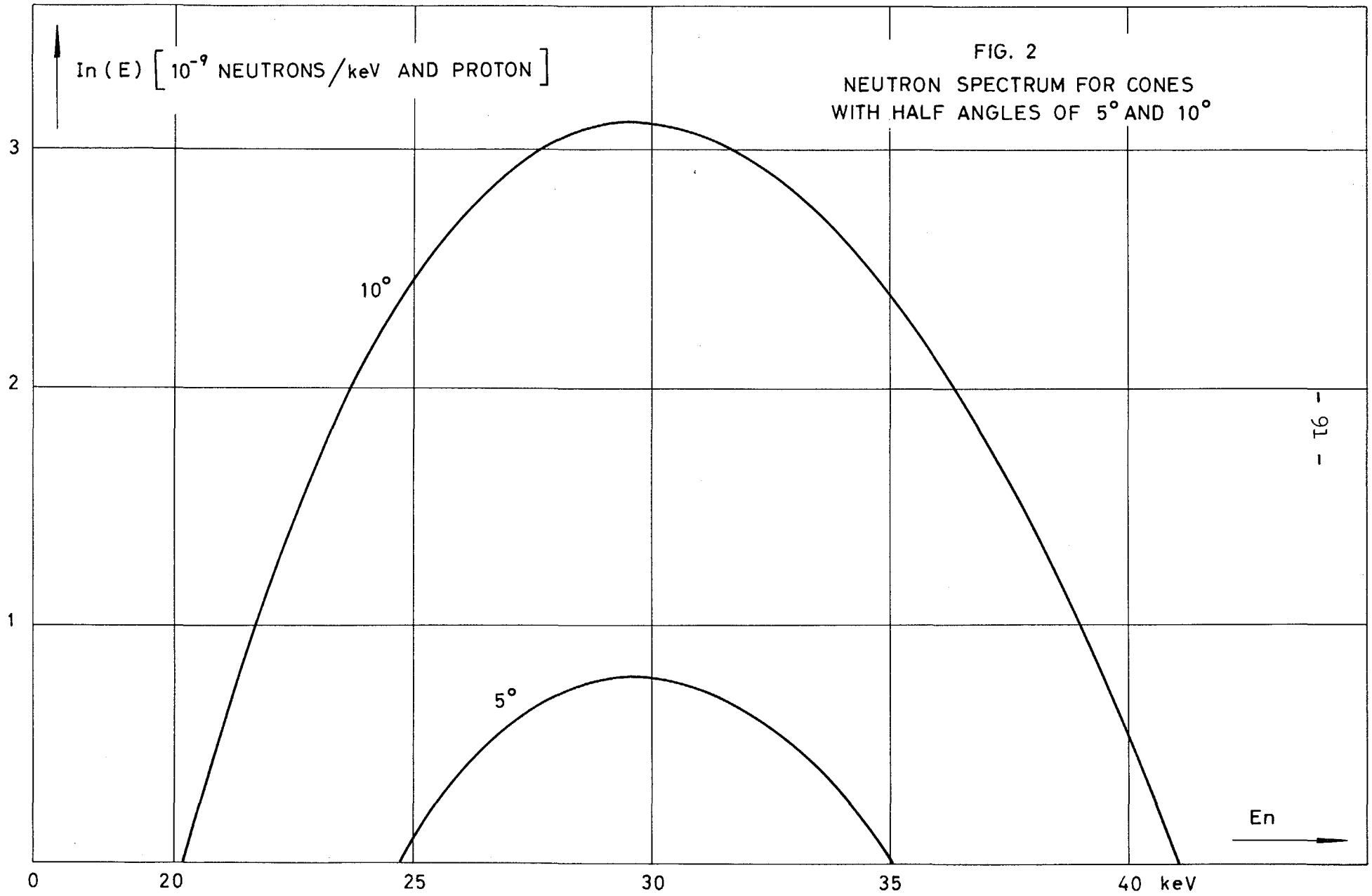
In (E) [10⁻⁹ NEUTRONS / keV AND PROTON]
FIG. 2
NEUTRON SPECTRUM FOR CONES
WITH HALF ANGLES OF 5° AND 10°
3
2
1
10°
5°
En
0
20
25
30
35
40 keV

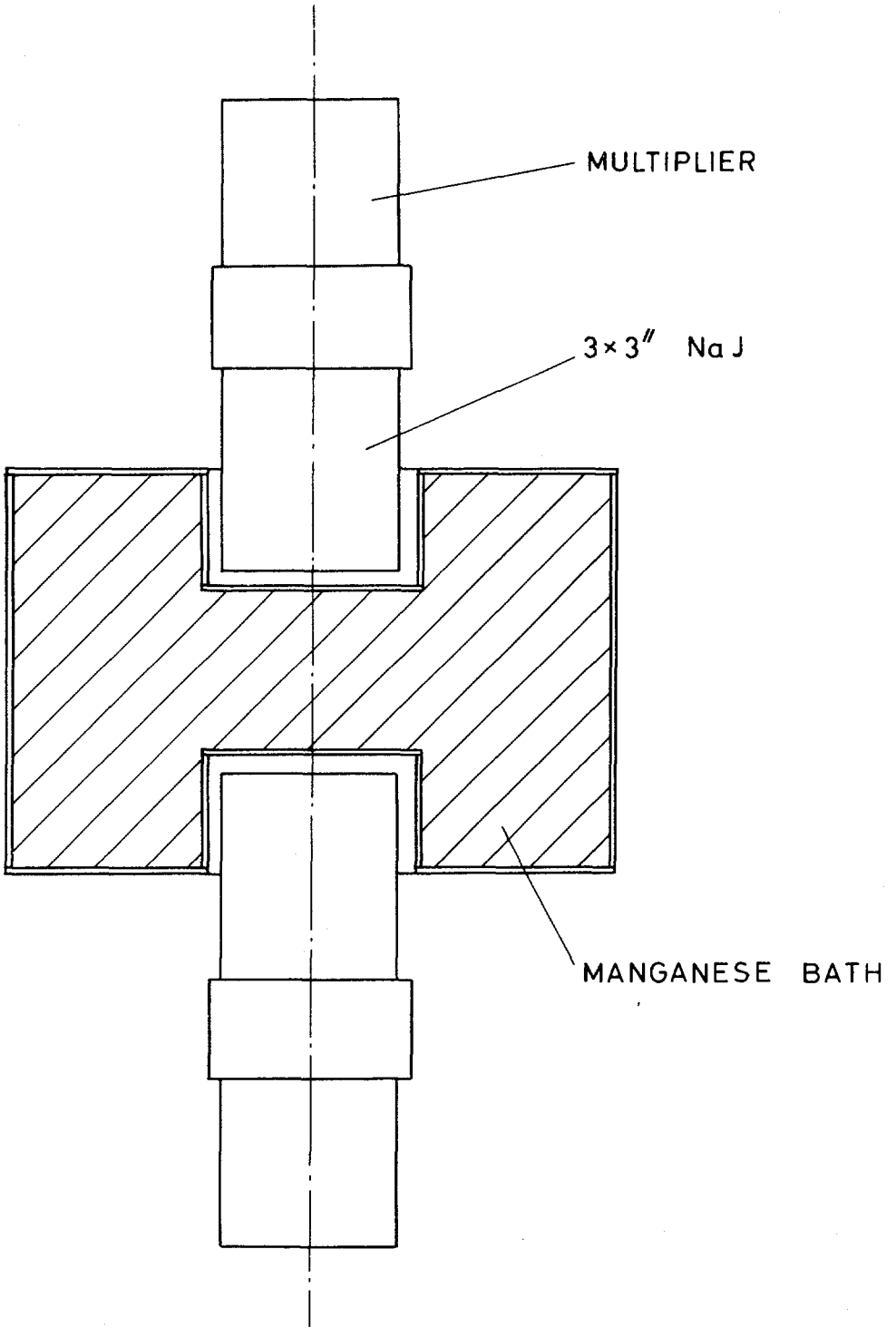

FIG. 3

MANGANESE-BATH COUNTER

From the calibrated $MnSO_4 \cdot H_2O$ powder, solutions of various concentrations were prepared and filled into the counter system. The efficiency

$$\eta_\gamma = \frac{\text{number of counts in the NaI(Tl) detectors}}{\text{number of } Mn^{56} \text{ decays}}$$ was derived

from the counting rate and the amount of $MnSO_4$ present. At a solution density 1.28 g/cm^3 which was normally used in the experiments,

$$\eta^{\circ}_\gamma = (18.95 \pm 0.19) \cdot 10^{-3}$$

was found. For other concentrations, $\eta_\gamma = \frac{\eta^{\circ}_\gamma}{A(\xi)}$ where the experimentally observed $A(\xi)$ is shown in Fig. 5.

Between several runs in these calibration measurements times up to one half life of Mn^{56} elapsed. Therefore, a careful remeasurement of the half life of Mn^{56} was made, yielding

$$T_{1/2} = 2.587 \pm 0.003 \text{ h.}$$

4. CORRECTIONS

From the measurement of the Mn^{56} activity, the number Q_{Mn} of Mn^{56} nuclei formed during the neutron irradiation can be derived. If all neutrons entering the $MnSO_4$ bath would be captured by Mn^{56}, Q_{Mn} would be equal to the neutron source strength Q. Actually, there are competing effects and the relation

$$Q_{Mn} = p\,Q \cdot \frac{N^{Mn}\,\sigma_a^{Mn}}{N^{Mn}\,\sigma_a^{Mn} + N^H\,\sigma_a^M + N^S\,\sigma_a^S} \qquad (2)$$

holds. Here, p is a nonleakage probability*); N^{Mn}, N^H and N^S are the numbers, Mn, H and S atoms per cm^3 and σ_a^{Mn} etc., the respective thermal capture cross sections. p can be calculated using two-group theory; for E = 30 keV and the dimensions of our tank,

---

*) In addition, equ.2 should contain a correction for epithermal capture which is negligibly small due to the low source energy.

$p = 0.994$ was found. In this calculation, neutrons leakage through the entrance channel was neglected, this is indeed extremely small. There should also be some losses by neutrons which enter through the channel, suffer their first collision at the quartz and are scattered backwards so that they leave again the tank. A simple geometrical consideration shows that these losses are smaller than $1.5 \cdot 10^{-3}$.

Introducing $\sigma_a^H = 0.327$ b; $\sigma_a^S = 0.52$ b and $\sigma_a^{Mn} = 13.2$ b into equ. 2, we obtain

$$Q = \frac{1}{p}\left(1.039 + 0.02477 \frac{N_H}{N_{Mn}}\right) Q_{Mn}$$

$$= \left(1.045 + 0.02490 \frac{N_H}{N_{Mn}}\right) Q_{Mn} \qquad (3)$$

which permits the determination of the source strength from the measured Mn^{56} activity. Uncertainties in the cross sections and the calculation of the nonleakage probability give rise to about 1.5 per cent error in Q/Q_{Mn}.

5. A PRELIMINARY MEASUREMENT OF THE Au^{197} (n,γ) Au^{198} CROSS SECTION

A thin gold foil was placed close to the target (see Fig. 1) in such a manner that all neutrons entering the Mn SO_4 bath had to cross it. After the irradiation, its activity was counted with two 3" x 3" NaI(Tl) crystals. The efficiency of this counting system was determined using a thermally activated gold foil which had been calibrated by the 4π β-γ coincidence method. Relating the gold activity to the Mn SO_4 activity,

$$\sigma_a = 670 \text{ mb}$$

was found for the activation cross section of gold at 30 keV. This value is considered as a preliminary one since, unfortunately, the proton energy control during this particular run was not very stable. Thus, the half angle of the cone may have widened exceeding 10° in which case the sensitivity of the Mn SO_4 bath decreases. It is hoped that this difficulty can be overcome in future measurements and that good accuracies (~5 per cent) in the cross section measurement can be achieved.

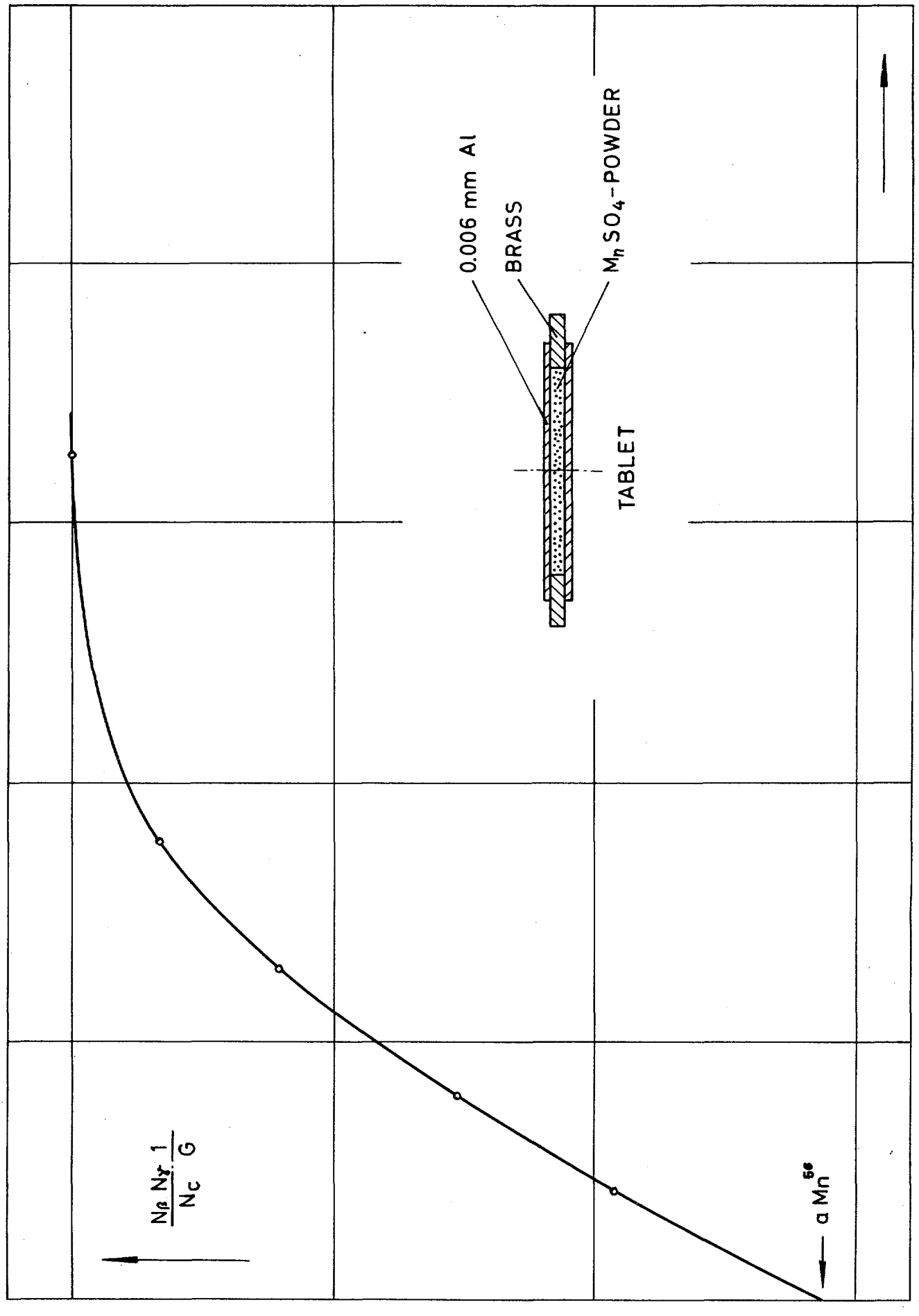

FIG. 4 EXTRAPOLATION OF $\frac{N_a N_r}{N_c} \frac{1}{G}$ AND TABLET

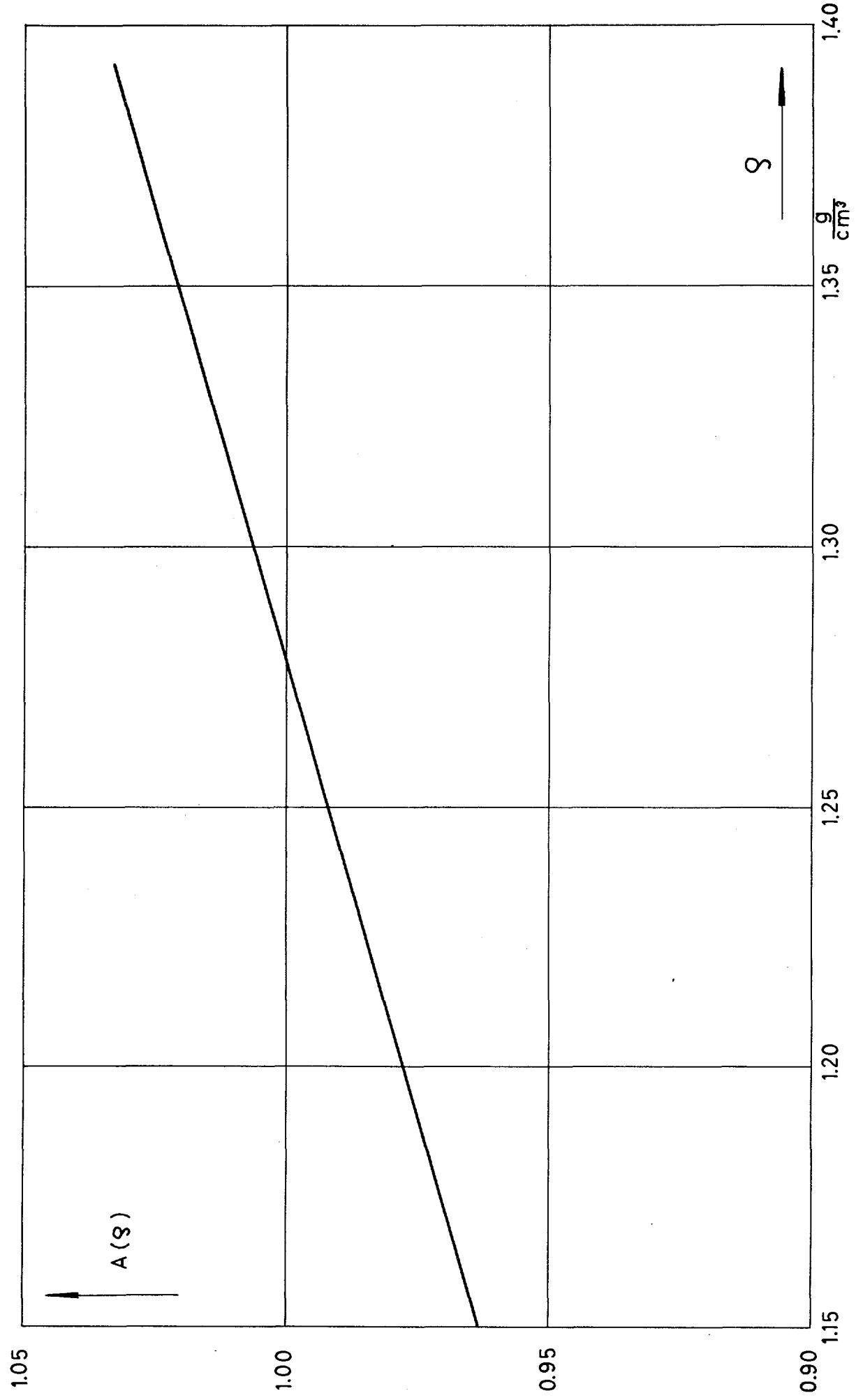

FIG. 5 ABSORPTION FUNCTION FOR 845 keV γ-ABSORPTION

We thank Dr. K.H. Beckurts for the suggestion and his interest in this work. Moreover, we are grateful to Prof. K. Zimmer for the possibility to use the van de Graaff generator of his institute.

References:

(1) R.D. O'Neal and G. Scharff-Goldhaber, Phys. Rev. 69, 368 (1946)
(2) F. Alder and P. Huber, Helv. Phys. Acta 22, 368 (1949)
(3) J. de Juren and J. Chin, J. Res. Nat. Bur. Stand. 55, 311 (1955)
(4) P. Wunderer, Z.f. angewandte Physik 10, 537 (1958)
(5) R.L. Macklin et al. Nucl. Sci. Eng. 8, 210 (1960)
(6) W. Pönitz, Diplomarbeit Karlsruhe (1962)

h) # A GREY NEUTRON DETECTOR FOR FLUX MEASUREMENTS IN THE INTERMEDIATE ENERGY RANGE

W. Pönitz and E. Wattecamps+)

Institut für Angewandte Kernphysik
Kernforschungzentrum Karlsruhe, F.R. of Germany

Abstract:

A quasi prompt neutron detector based on thermalisation of neutrons in a Mn SO_4 - H_2O mixture and subsequent radiative capture of the thermal neutrons in Mn^{55} is described. The neutron detection efficiency is calculated and the detector is calibrated at thermal energy. This calibration and the smooth variation of the detector efficiency curve enables one to perform neutron flux measurements in the energy range from thermal to 1 MeV.

1. INTRODUCTION

Accurate neutron flux measurements in the energy range 1 to 100 keV are difficult to perform. The methods applied in the lower and higher energy range are based on accurately known cross-sections. These methods cannot be extended to the energy range of interest due to the poor accuracy of the directly measured cross-sections (e.g. measured by the spherical shell transmission method). Since more accurate experiments have to be performed in the energy range 1 - 100 keV we developed a transportable, quasi prompt, neutron detector with a calculated neutron detection efficiency which is constant within 1.5 per cent for neutron energies between thermal and 1 MeV.

The smooth curve enables one to calibrate accurately the detector at energies where accurate neutron flux measurements can be performed and to bridge the energy interval of interest. Consequently it is possible to make absolute neutron flux measurements in the energy range from thermal energy to 1 MeV. Unfortunately, the maximum obtainable efficiency, approximately 10^{-2}, is low.

+) delegated from EURATOM

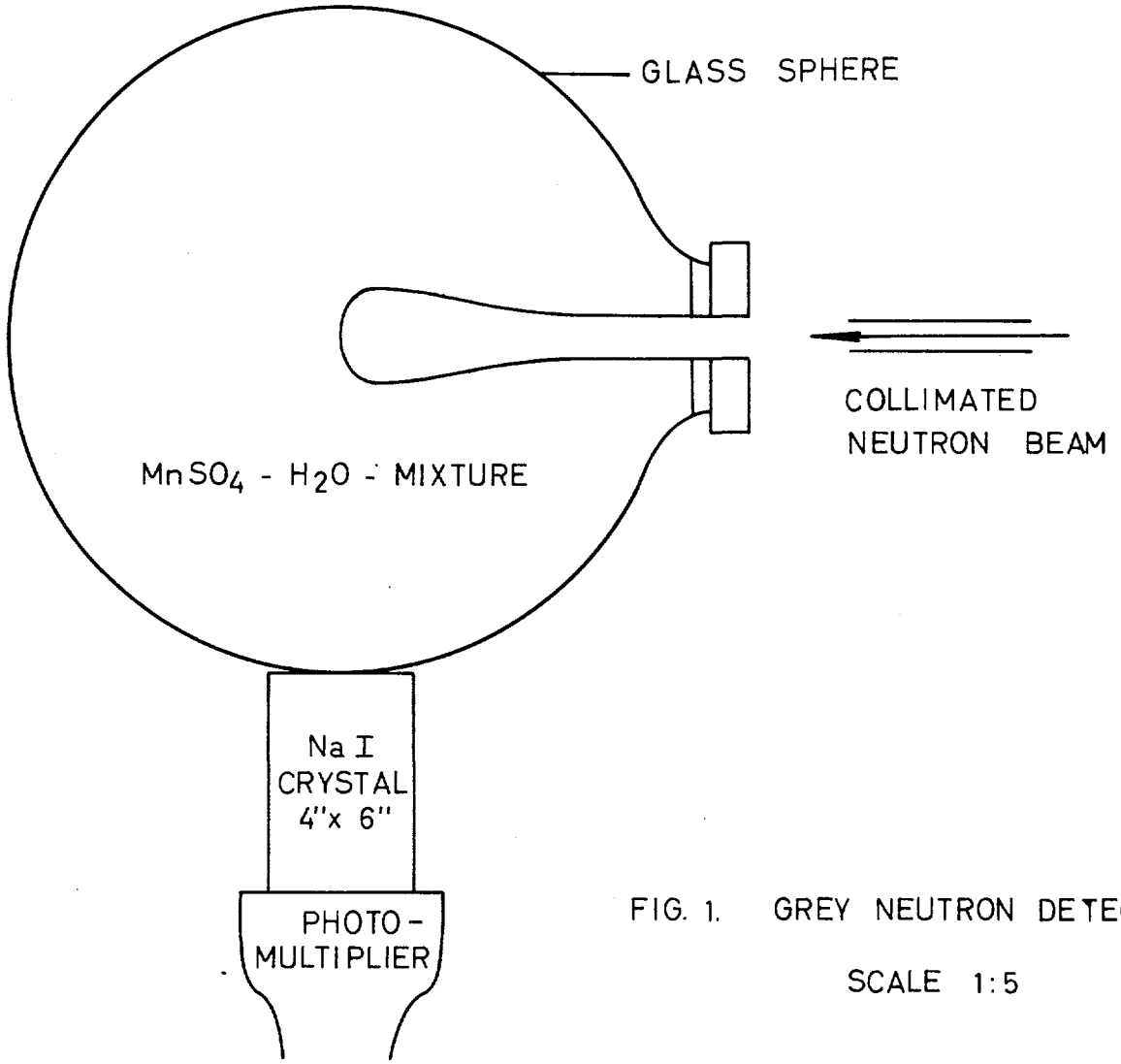

FIG. 1. GREY NEUTRON DETECTOR

SCALE 1:5

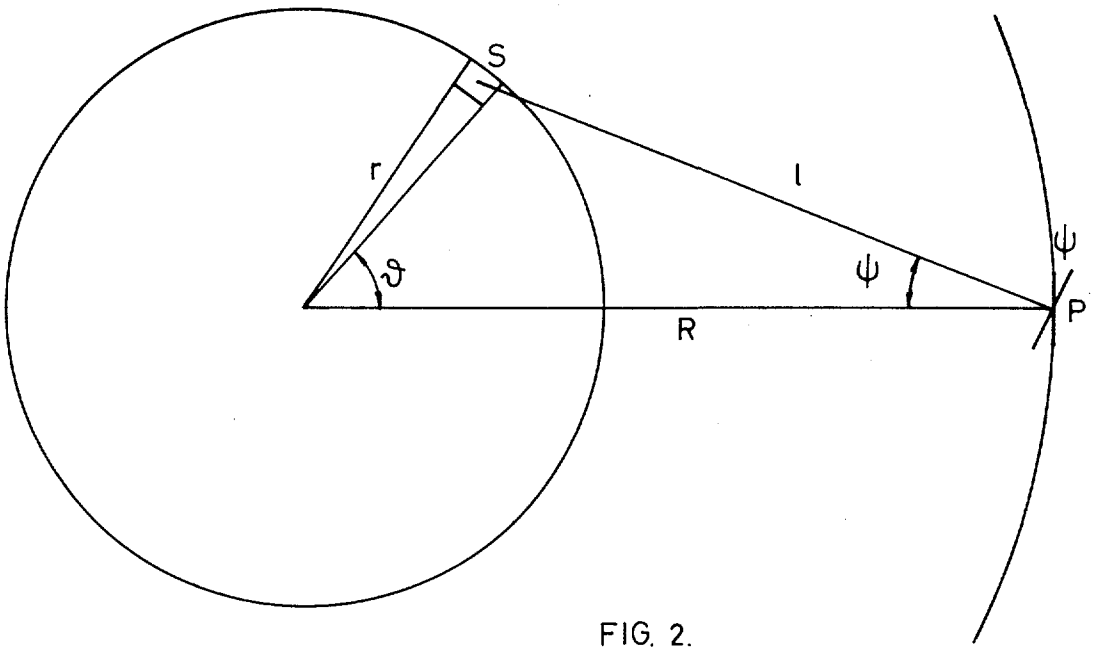

FIG. 2.

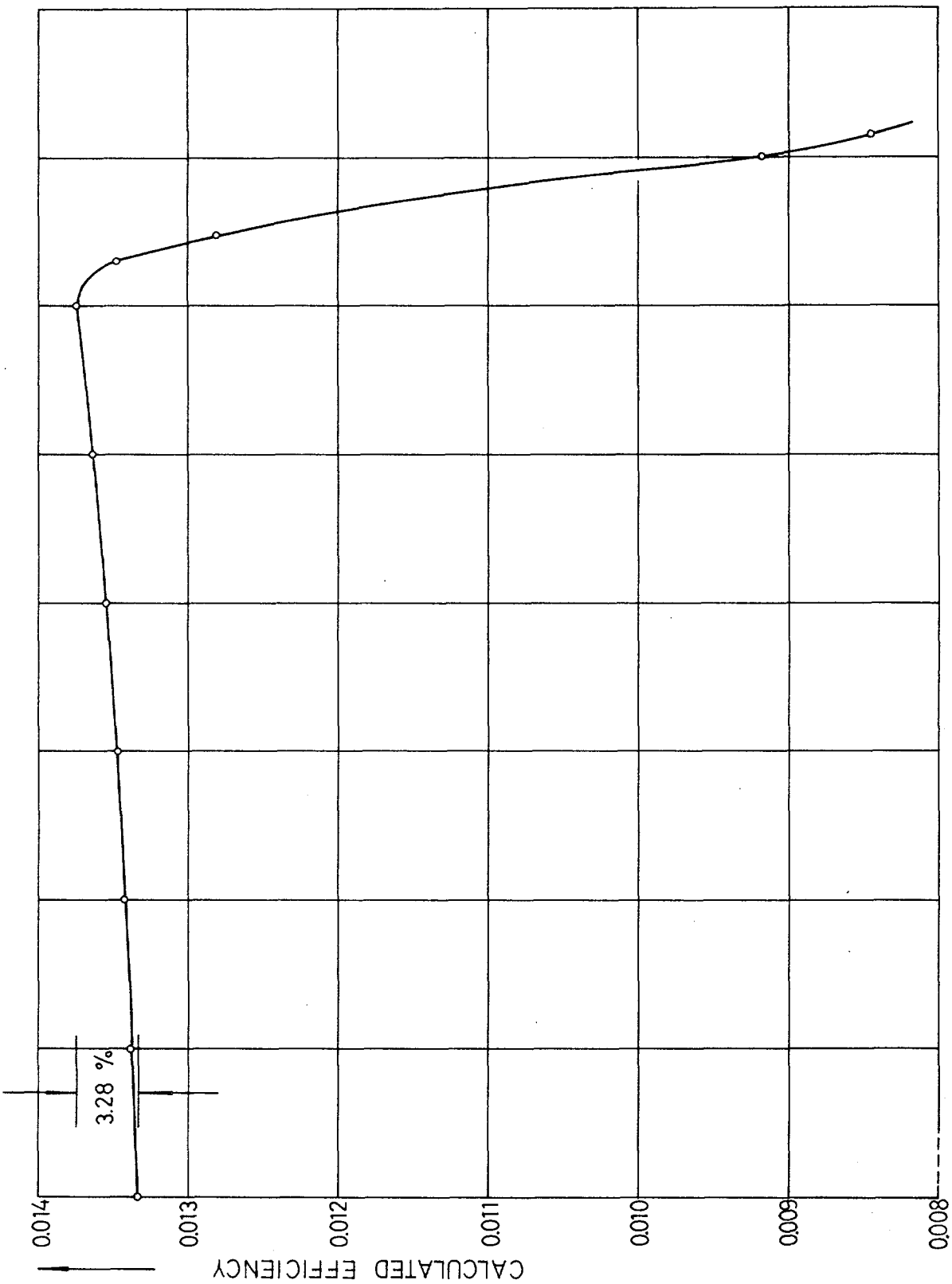

FIG. 3. CALCULATED NEUTRON DETECTION EFFICIENCY AS A FUNCTION OF PRIMARY NEUTRON ENERGY

2. THE NEUTRON DETECTOR

2.1 The Principle of Operation of the Detection System

The detector is illustrated in Fig. 1. A glass sphere, with radius R = 23 cm, is filled with a mixture containing 69.2 per cent H_2O and 30.8 per cent $MnSO_4 \cdot H_2O$ by weight. A radial channel, with minimum diameter 3 cm and length R, is fixed at the surface of the sphere. A collimated neutron beam entering the sphere through this channel is scattered first in the middle of the sphere. The neutrons originated at r = 0 (spherical co-ordinates, see Fig. 2) are slowed down by the moderator and due to their small diffusion length the thermal neutrons are captured by radiative capture, Mn^{55} (n, γ) Mn^{56}, in the very close vicinity of the last collision that made them thermal.

A NaI(Tl)-crystal is placed right on the surface of the sphere and by suitable pulse-height discrimination only those neutron-capture gamma rays with energies between 6 and 7.3 MeV are counted. This energy interval contains 34.5 per cent of the total amount of gamma rays emitted per radiative capture in Mn^{55} (ref. 1).

2.2 The Calculation of the Detection Efficiency

The thermal neutron flux produced by a point source in an infinite moderator as a function of the radius r and the initial neutron energy E_o, deduced by a two group diffusion theory (ref. 2), is given by:

$$\phi_{th}(r, E_o) = \frac{Q}{4\pi\Sigma_a} \frac{1}{L^2 - \tau} \frac{1}{r} \left(e^{-\frac{r}{L}} - e^{-\frac{r}{\sqrt{\tau}}}\right) \qquad (1)$$

where L is the diffusion length for thermal neutrons, Q is the neutron source strength and Σ_a is the macroscopic absorption cross-section. $\tau = \tau_{1.44}(E_o) + \Delta\tau$ is the Fermi-age of thermal neutrons. $\tau_{1.44}(E_o)$ was calculated by H. GOLDSTEIN et al. (ref. 3) as a function of energy E_o. $\Delta\tau = 1$ cm^2 (ref. 2). With this value of τ the calculated $\phi_{th}(r, E_o)$ fits very closely a thermal neutron flux distribution measurement of a Sb-Be neutron source in a large water tank (with E_o = 24 keV).

The spatial intensity distribution of the capture gamma rays equals the thermal neutron distribution. Hence, we calculate the probability for a 7 MeV gamma ray emitted at S, with coordinates r, ϑ, φ; to reach the surface of the sphere with radius R. Fig. 2 illustrates the geometry to be considered. The number of neutrons absorbed in Mn^{55} per sec and per elementary volume dV, giving rise to gamma rays with energy > 6 MeV is

$$0.345 \cdot \Sigma_a^{Mn} \, \phi_{th}(r, E_o) \sin\vartheta \, d\vartheta \, d\varphi \, dr. \qquad (2)$$

From this gamma ray source at S the number of gamma rays reaching an elementary surface at P is

$$0.345 \cdot \Sigma_a^{Mn} \, \phi_{th}(r, E_o) \frac{e^{-\mu l}}{4\pi l^2} \cos\varphi \, d \cos\vartheta \, d\varphi \, r^2 \, dr. \qquad (3$$

(l and φ see Fig. 2)

Since we are only interested in gamma rays with energy larger than 6 MeV, a gamma ray that is scattered once will be considered as absorbed; thus, μ is the total linear attenuation coefficient of the mixture.

From (3) one deduces the contribution of the total distributed gamma ray source to the gamma ray intensity at P

$$I_\gamma(E_o) = 0.345 \, \Sigma_a^{Mn} \frac{Q}{4\pi \Sigma_a} \frac{1}{L^2 - \tau} \cdot$$

$$\int_{r=0}^{R} \int_{\vartheta=0}^{\pi} \int_{\varphi=0}^{2\pi} r\left(e^{-\frac{r}{L}} - e^{-\frac{r}{\sqrt{\pi}}}\right) \frac{e^{-\mu\sqrt{R^2 + r^2 - 2Rr\cos\vartheta}}}{(4\pi R^2 + r^2 - 2Rr\cos\vartheta)^{3/2}} (R - r\cos\vartheta) \, d\vartheta \, d\varphi \, dr. \qquad (4)$$

The integration was performed and subsequently the detection efficiency for a neutron of initial energy E_o can be derived

$$\eta_n(E)_o = \frac{\text{number of counts}}{\text{number of neutrons}} = \frac{Z_\gamma}{Q} \qquad (5)$$

with

$$Z_\gamma = k \cdot F_{eff} \cdot \eta_\gamma \cdot P \cdot I_\gamma(E_o) \qquad (6)$$

k is the number of NaI-crystals with the effective surface area F_{eff}. η_γ is the γ-ray detection efficiency at 7 MeV and P the photo fraction for the same energy.

The function $\eta_n(E_o)$ is plotted in Fig. 3 for $\frac{k \cdot F_{eff}}{4\pi R^2} = 1$ and $\eta_\gamma P = 0.35 \ . \ 0.45$.

3. CALIBRATION OF THE DETECTOR

3.1 The Method

To calibrate the detector at thermal energy, a thermal neutron beam is measured by the grey detector and simultaneously by a gold foil activation. From the latter, the neutron flux is deduced and by comparison with the counting rate of the grey detector $\eta_n\ (E_{th})$ is deduced.

A second calibration based on a different technique is planned at energy > 100 keV by comparison of the grey detector and an absolute recoil particle method. Once the two measurements are performed, the calculated efficiency curve will be shifted parallel to the energy axis in order to fit as closely as possible the two calibration points. Subsequently, it is possible to make absolute neutron flux measurements in the energy range from thermal energy to 1 MeV.

3.2 The Calibration at 0.025 eV

At the thermal column of the FR II reactor a thin gold foil was placed in a collimated neutron beam which is then catched by the grey detector. The number of activated Au-atoms per sec is:

$$C = Q\ (1 - e^{-N \cdot \sigma_a \cdot d}) \qquad (7)$$

with:

Q = beam strength [neutrons/sec]
N = number of Au-atoms/cm³
σ_a = absorption cross-section
d = foil thickness.

Since $N\ \sigma_a\ d$ is small, the exponential function can be approximated very closely by $1 - N\ \sigma_a\ d + \frac{1}{2}\ (N\ \sigma_a\ d)^2$. The energy distribution of the neutron beam is assumed to be a Maxwell spectrum.

Thus we obtain:

$$C = Q \cdot \frac{\sqrt{\pi}}{2} \cdot \Sigma_a \cdot d \cdot g \left[1 - \frac{1}{\sqrt{\pi}} \cdot \Sigma_a \cdot \underline{d}\right] \quad (8)$$

(with g = Westcott-factor (see ref. 4)).

As Z_γ is the number of simultaneously observed gamma ray pulses, the neutron detection efficiency is:

$$\eta_h \text{ (thermal)} = \frac{Z_\gamma}{C} \cdot \frac{\sqrt{\pi}}{2} \cdot \Sigma_a \cdot d \cdot g \left[1 - \frac{1}{\sqrt{\pi}} \cdot \Sigma_a \cdot \underline{d}\right] \frac{1}{e^{-\Sigma_t \cdot d}} \quad (9)$$

The last factor in eq. 9 corrects for the attenuation of the neutron beam by the gold foil.

The value of C is measured by absolute counting of the foil with a 4π β-γ coincidence method (ref. 5).

A typical gamma-ray spectrum from the grey detector is shown in Fig. 4. From the integrated counting rate between 6 and 7.5 MeV and the gold activation measurement the neutron detection efficiency at thermal energy with one NaI-crystal was found to be 3.06×10^{-4} counts per thermal neutron.

The authors acknowledge the considerable contribution made by Dr. K.H. Beckurts in the conception of this system and in its subsequent development.

FIG. 4. OBSERVED GAMMA-RAY SPECTRUM WITH A COLLIMATED THERMAL NEUTRON BEAM

References:

(1) R.A. Charpie and J.V. Dunworth: Atlas of Gamma-Ray Spectra from Radiative Capture of Thermal Neutrons.

(2) K.H. Beckurts and K. Wirtz: Neutron Physics (in press)

(3) H. Goldstein et al.: ORNL-2639 -34 phys. p. 9

(4) C.H. Westcott: EANDC (Can) - 4 (1960)

(5) W. Pönitz, Determination of Absolute Thermal Neutron Flux by Gold Foils (to be published in Nukleonik).

1) NEUTRON FLUX AND CAPTURE MEASUREMENTS USING A LARGE LIQUID SCINTILLATOR*

E. Haddad, R. B. Walton, S. J. Friesenhahn and W. M. Lopez
Genegal Atomic Division of General Dynamics, United States

1. INTRODUCTION

The major emphasis of the neutron capture cross-section program at General Atomic has been to obtain the parameters of individual resonances in the neutron energy range from thermal to 1 keV. For the energy range from 1 to 30 keV preliminary capture cross section, measurements averaged over many resonances, have been obtained for Ag, In, Er, and Au.

To make these measurements a large liquid scintillator was used with a 50 MeV L-band linear accelerator. Neutron bombarding energies were obtained by conventional pulsed beam time-of-flight techniques.

2. NEUTRON CAPTURE GAMMA-RAY DETECTOR

The liquid scintillator used is of modular construction and was designed so that a single 8-MeV gamma-ray originating at the center of the detector would have a probability of 80 per cent of interacting at least once before escaping from the detector. For binding energies of 5.0 MeV and greater the cascade schemes, resulting from neutron capture, are sufficiently complex to ensure a detection efficiency in excess of 90 per cent.

The detector configuration (see Fig. 1) consists of a 2-foot diameter central follow lucite cylinder surrounded by a cylindrical array of 9 in. diameter follow lucite cylinders (logs). All cylinders (units) contain a liquid scintillator solution. Samples for capture measurements are placed inside an evacuated 6.0 in. diameter aluminum liner that is positioned inside and concentric to a 6.5 in. diameter hole that extends through the

---

* Work supported in part by the United States Atomic Energy Commission.

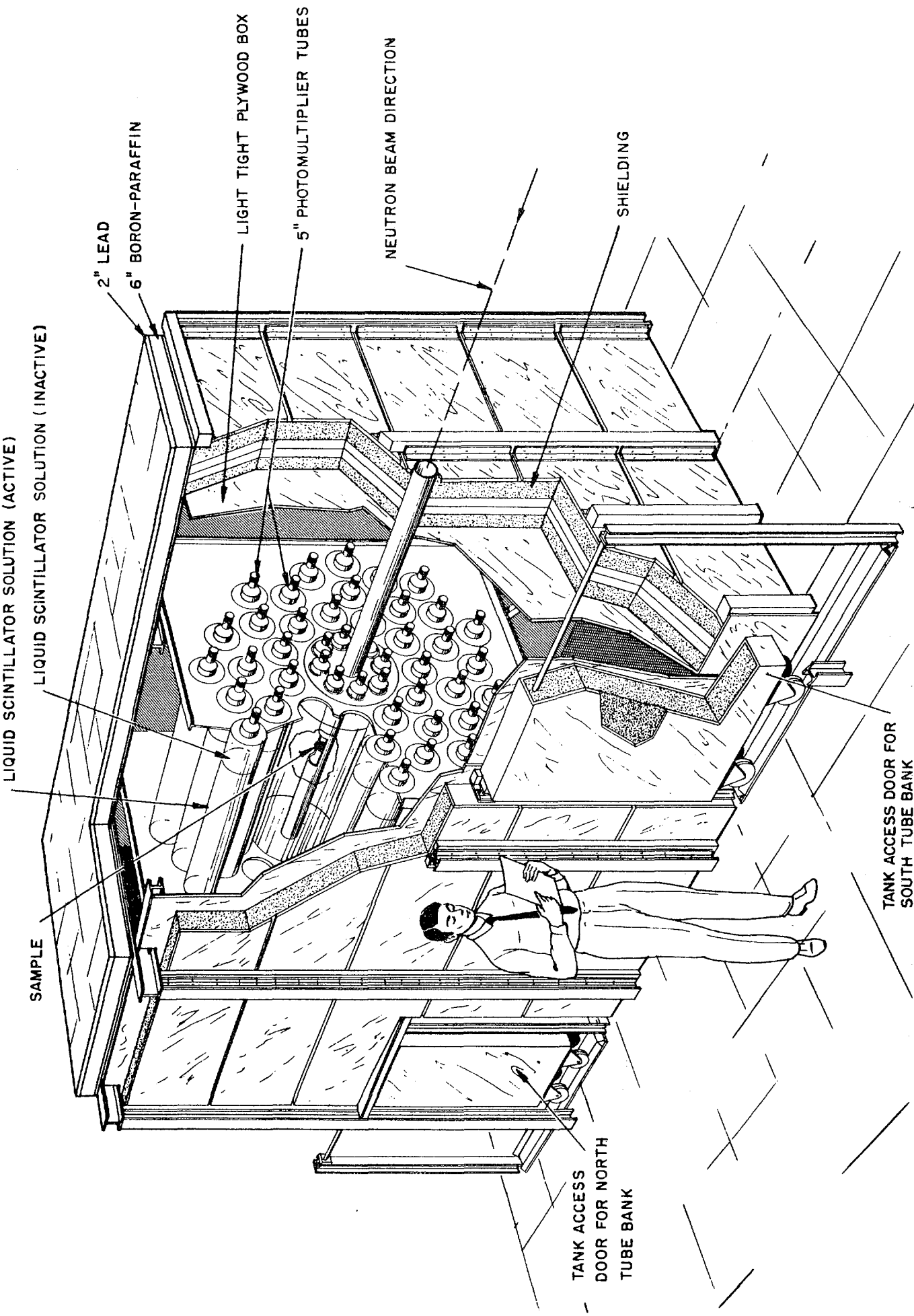

Fig. 1--Drawing of the 4000-liter liquid scintillator

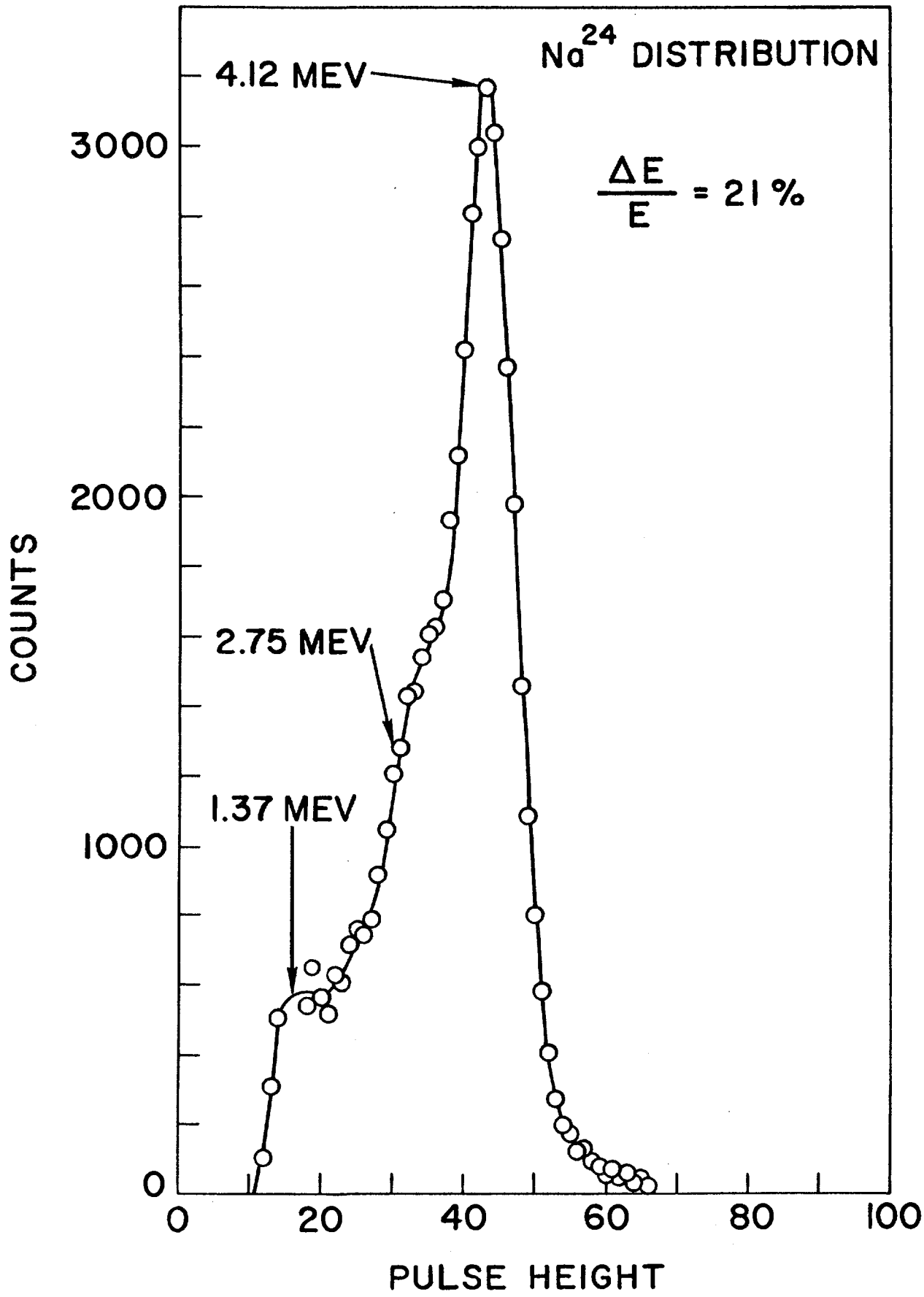

Fig. 2 --Pulse height distribution of Na^{24} source.

2-foot diameter cylinder. The collimated neutron beam enters the detector through a 0.020 in. aluminum window, passes along the evacuated liner, and then bombards the sample positioned at the center of the detector.

Each log, as well as the 2-foot diameter cylinder, is partitioned into three compartments: a center region 60 in. in length filled with scintillator solution and two end sections; each 9 in. in length, filled with unactivated solution. Each end of an individual log is viewed by a 5-in. CBS-7819 photomultiplier tube. Each end of the central cylinder is viewed by eight 5-in. CBS-7819 photomultiplier tubes. The total number of tubes used in the tank is 104. The purpose of the dead space at each end of a module is to increase the resolution of the detector by reducing geometrical effects caused by gamma rays interacting near the photocathode surface. All units are individually wrapped with aluminum foil which is not in optical contact with the lucite. Pulse height distributions taken with a collimated Cs^{137} source as a function of position along the axis of each unit varied by less than 5 per cent over the 60-in. length of active solution.

Pulse height distributions taken with the detector are given for Na^{24} (Fig. 2), for neutron capture gamma rays associated with the 4.91 eV resonances in Au^{197} with the central cylinder loaded with 10 per cent by volume of methyl borate (Fig. 3), and for an Au^{197} distribution without the central cylinder loaded with methyl borate (Fig. 4). The pulse height distribution of Na^{24} shows the excellent summing properties of the detector. The small peaks at 2.76 MeV and 1.37 MeV, which are shown in the figure for Na^{24}, are due to gamma rays which either escape from the hole in the detector or are lost in the 0.25-in. thick lucite walls. Figures 3 and 4 demonstrate the effectiveness of the methyl borate in suppressing the 2.2 MeV gamma rays resulting from in-scattered neutrons being captured by hydrogen.

3. THIN TARGET CROSS-SECTION MEASUREMENTS

3.1 Introduction

The accuracy with which an absolute cross-section measurement can be made, using this detector, is mainly determined by how well one can measure the efficiency of the detector and the absolute neutron flux at the sample position.

3.2 Detector Efficiency

The efficiency of the detector for detecting capture events is the product of the sprectrum fraction (the probability that an output pulse exceeds the bias setting, or in other words the area under the pulse height distribution above the bias divided by the total area) and the "zero bias" detector efficiency. The good summing resolution properties of the total absorption gamma-ray detector make it possible to assign a value of (96 $\pm$ 4) per cent to the zero bias efficiency for binding energies ranging from 6 MeV up. For the Au^{197} data shown in Fig. 6 background consideration required that the detector be biased at 3.0 MeV. At this bias setting the sprectrum fraction was (85 $\pm$ 3) per cent. Thus the efficiency of the detector for detecting gamma-rays associated with neutron capture by the 4.906 eV resonance in Au^{197} is (82 $\pm$ 5) per cent. Many spectrum fractions have been determined with the detector, at different neutron bombarding energies, for Au^{197}, Er^{167}, Ag^{107}, Ag^{109}, and Th^{232}. The results show that the uncertainties in a spectrum fraction measurement, for a given isotope, are essentially independent of the cascade scheme.

3.3 Absolute Flux Determination

The relative neutron flux, for the energy range from 0.01 eV to 30 keV, was determined by using a bank of 1/v BF_3 neutron detectors. The relative flux curve was made absolute by normalizing to an absolute neutron flux measurement at 4.91 eV made with the large scintillator. The absolute flux was determined in the following manner. A 0.020 in. Au^{197} sample was placed in the large scintillator and bombarded with neutrons. The thickness of the sample was chosen to be black to neutrons at 4.91 eV. Then a time distribution run was taken with the detector biased to accept capture events which deposited 3 to 10 MeV of energy in the detector. The number of counts in the time distribution run occurring at the peak of the 4.91 eV resonance is related to the absolute neutron flux by the relationship:

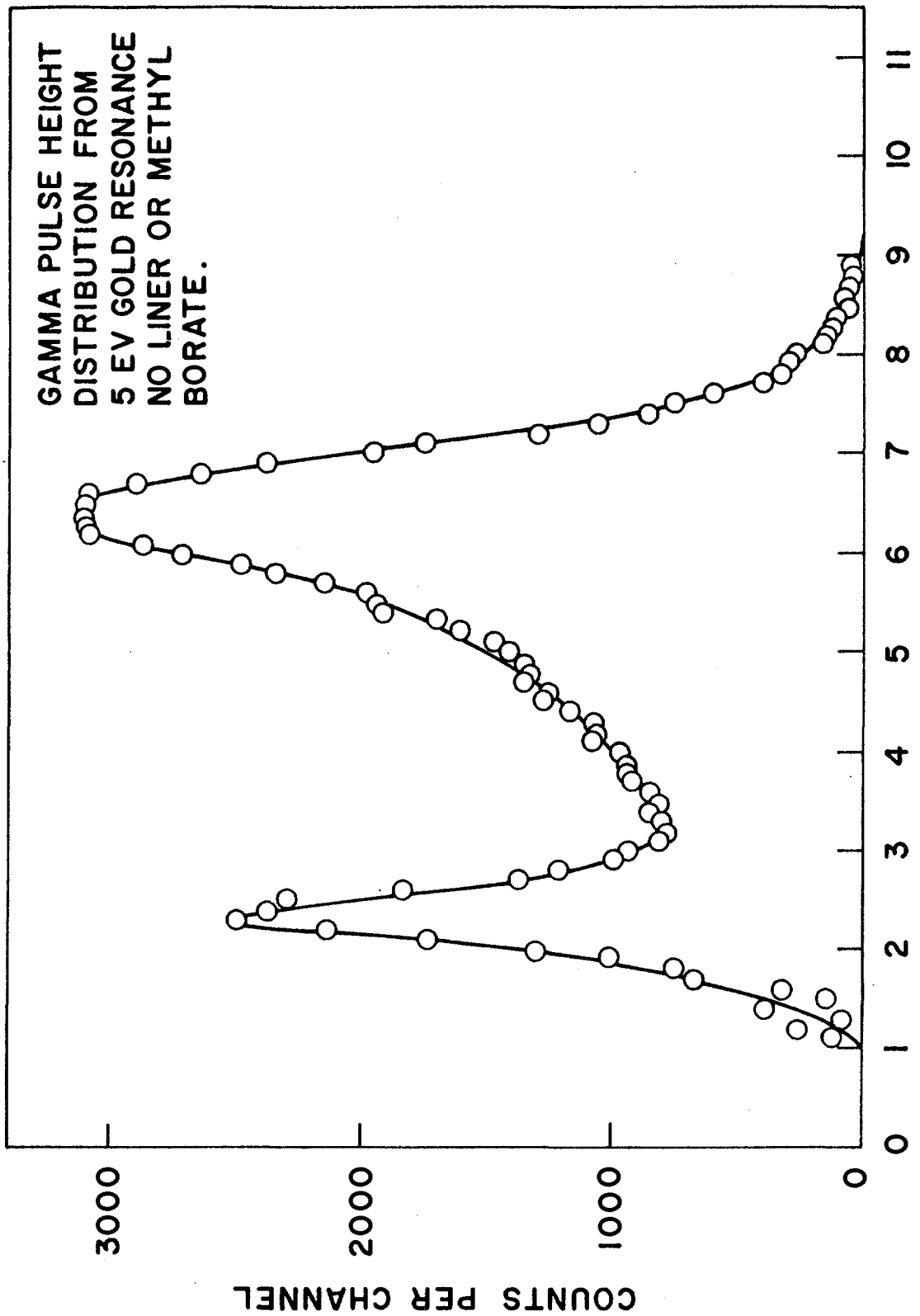

Fig. 3--Observed pulse-height distribution from $Au^{197}(n,\gamma)$ Au^{198} events at 4.91 eV gold resonance and $H(n,\gamma)D$ events from neutrons scattered into 4000-liter liquid scintillator.

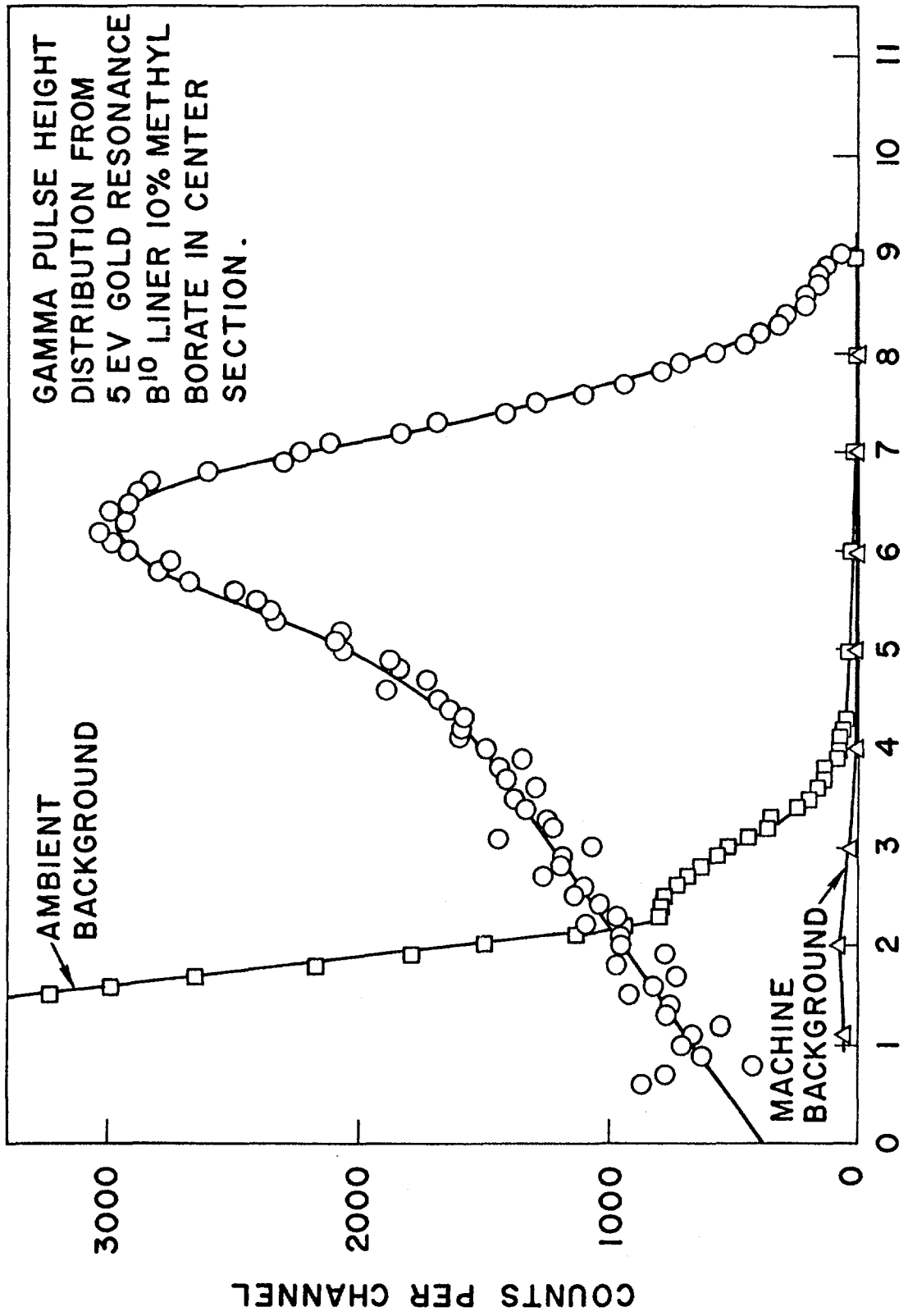

Fig. 4 --Pulse height distribution from the $Au^{197}(n,\gamma)$ Au^{198} events observed with center section of 4000-liter detector loaded with 10% methyl-borate (by volume).

$$F = \left[\frac{C.R.}{A \epsilon \delta}\right]_{E_o = 4.91 \text{ eV}}$$

where: F = neutrons/cm^2 μsec,

A = sample target area,

ϵ = detector efficiency,

δ = backscattering correction,

C.R.= counts/μ sec.

Thus knowing C.R., A and δ and determing the detector efficiency as described above, the value of the absolute neutron flux at 4.91 eV can be evaluated. Thus a flux measurement made in this manner depends only on the detector efficiency and the 1/v dependence of B^{10}. The error in the flux is taken to be the same as the error in the efficiency determination up to 1 keV. Other resonances which proceed primarily by capture can be used to obtain absolute flux values at energies higher than 4.91 eV (one interesting possibility being the 1.2 keV resonance in Fe). The errors in a cross section measurement are considerably reduced when the flux can be determined with the sample under investigation. This results from the fact that the detector efficiency drops out of the cross section determination when the same sample is used both for the flux and cross-section measurements.

3.4 Preliminary Thin Target Cross-Section Data

Figures 5 and 6 show thin target cross-section data for Ag and Au. The uncertainties in the measurements are $\pm$ 15 per cent. These data have not been corrected for doppler broadening nor instrumental resolution. The instrumental resolution that was used in taking these data is shown at various points along the abcissa of the curves. Average cross sections are given in Figures 5 and 6 for data above 400 eV. At 30 keV the Au^{197} result of 525 millibarns is in good agreement with results obtained by other workers using neutron attenuation and prompt gamma cascade detection techniques[1,2].

IV. ISOTOPIC IDENTIFICATION OF RESONANCES

In many cases measurements have been made which yield values for $a\Gamma_n$ where a is the isotopic abundance of the resonance in question and Γ_n is the neutron width of the resonance. Thus being able to make isotopic assignments to resonances makes it possible to obtain neutron widths for many cases reported in BNL-325.

Isotopic identification of resonances can easily be made by making cross-section measurements of samples varying in isotopic abundance. The trouble with this method is that it is often difficult to obtain separated isotopes in sufficient quantities which makes it impractical in most cases. Another approach is to use the difference in neutron binding energy between isotopes[3,4]. This latter technique was used to obtain the data given in Figures 7 and 8.

Figure 7 shows a pulse height distribution, using an unriched sample, of the gamma rays emanating from the 5.2 eV resonance in Ag. This resonance has been previously reported in BNL-325 as an Ag^{109} resonance. The binding energy of Ag^{109} + n is 6.45 MeV. The peak of the pulse height distribution in the figure corresponds to an energy (obtained from an energy calibration curve of the detector) of 6.5 MeV which conforms to the BNL-325 value. Figure 7 also shows a pulse height distribution of a previously reported resonance in BNL-325 at 16.5 eV. The binding energy of Ag^{107} + n is 6.98 MeV. The peak of the pulse height distribution for this resonance as seen in Fig. 7 corresponds to 7 MeV, which confirms the BNL-325 data. Thus these pulse height distributions clearly demonstrate the ability of this technique to make isotopic assignments to resonances, using unenriched samples where binding energies differ by 300 keV or more. This method, for practical reasons, is limited to cases where the amount of the isotope under investigation is sufficient and to where the resonances being studied are resolved.

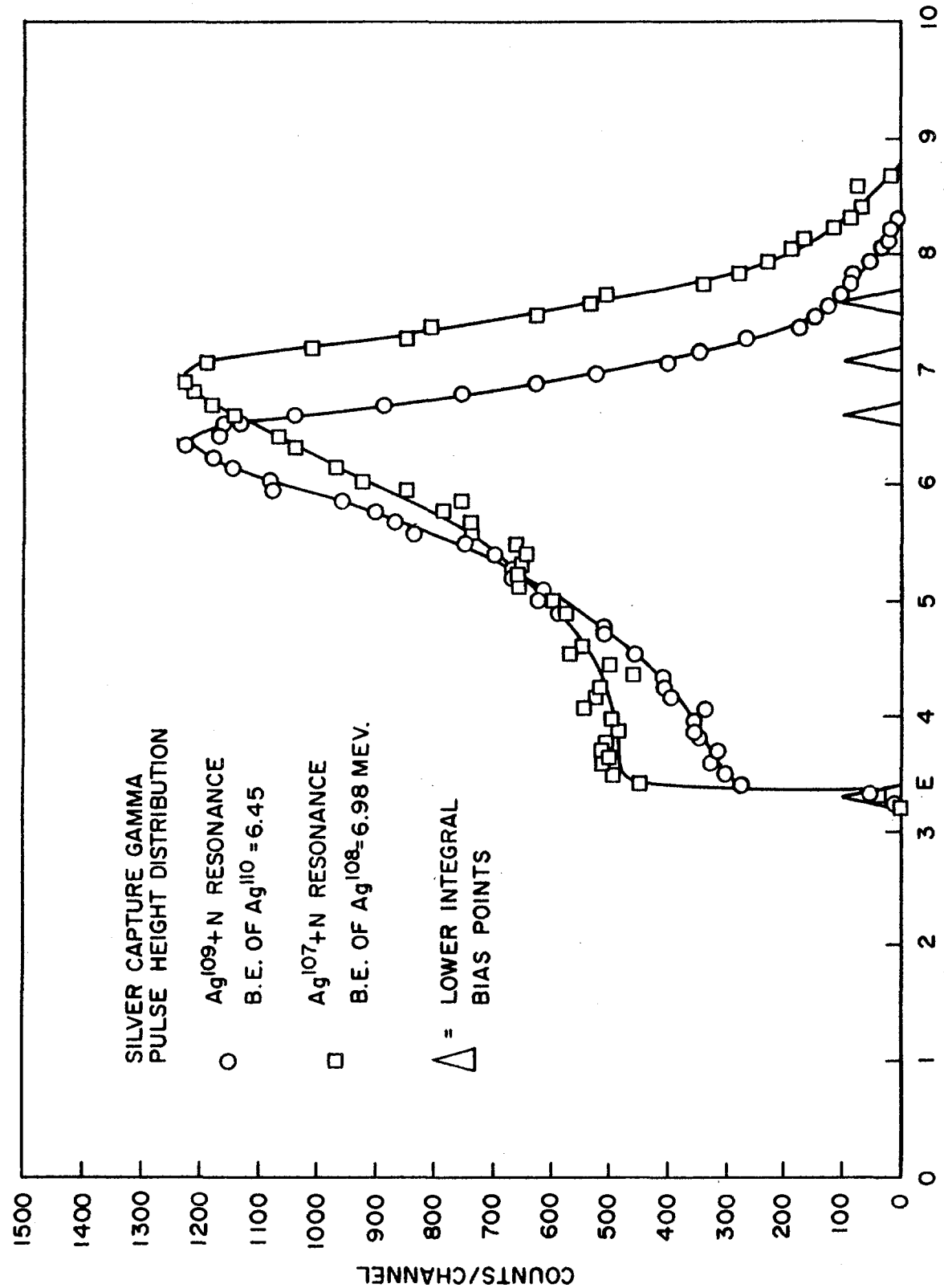

Fig. 5 --Pulse-height distributions of $Ag^{107}(n,\gamma)$ Ag^{108} and $Ag^{109}(n,\gamma)$ Ag^{110} events observed with 4000-liter liquid scintillator.

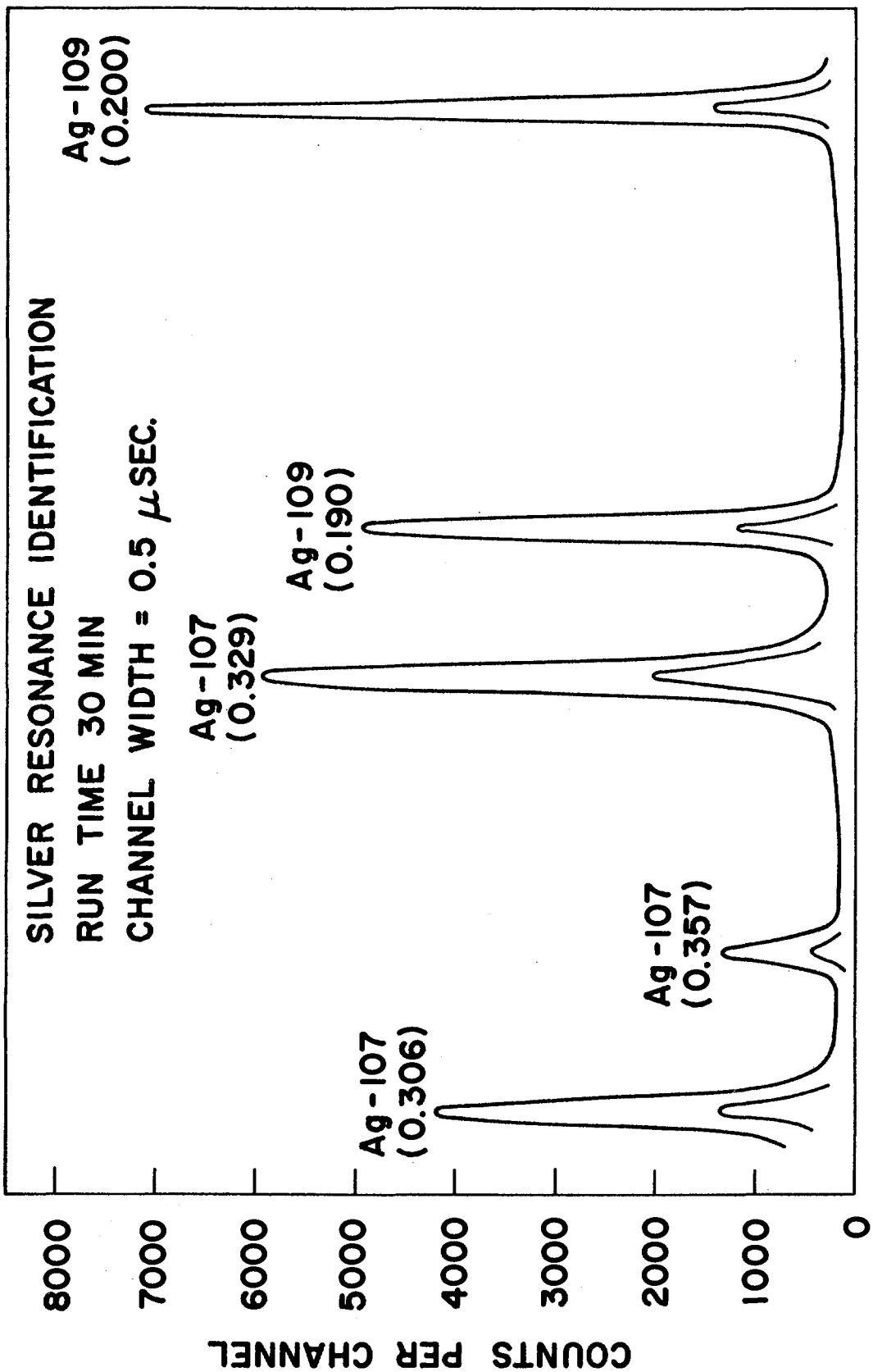

Fig. 6--Time distribution of (n,γ) events taken with normal silver sample at two different pulse-height (or energy) bias settings showing resonances from 41 ev to 71 eV.

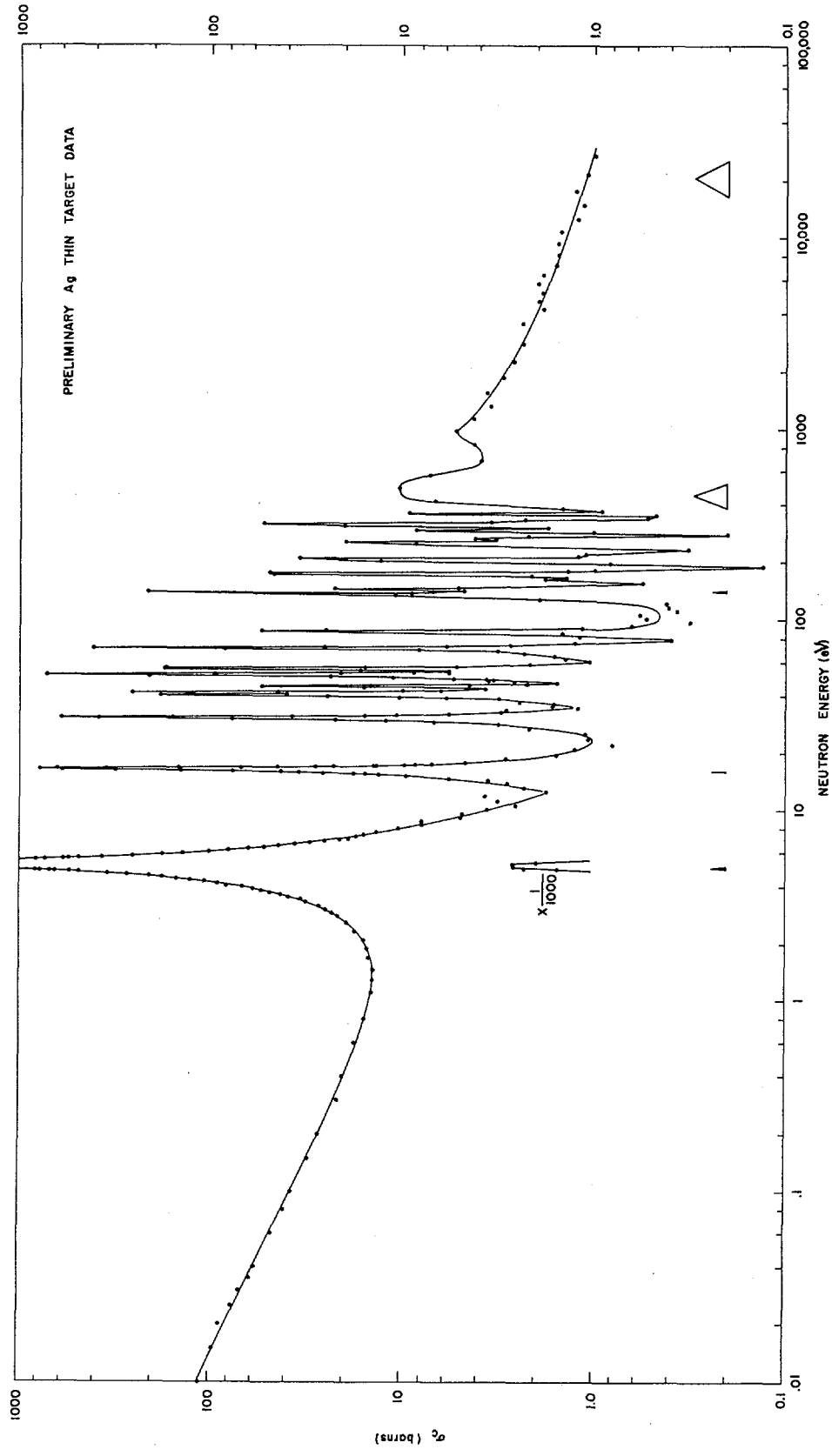

Fig. 7--Preliminary silver capture cross-section data taken with 0.005 inch and 0.010 inch sample thicknesses. Samples used were not thin for cross sections $\geq$ 800 barns.

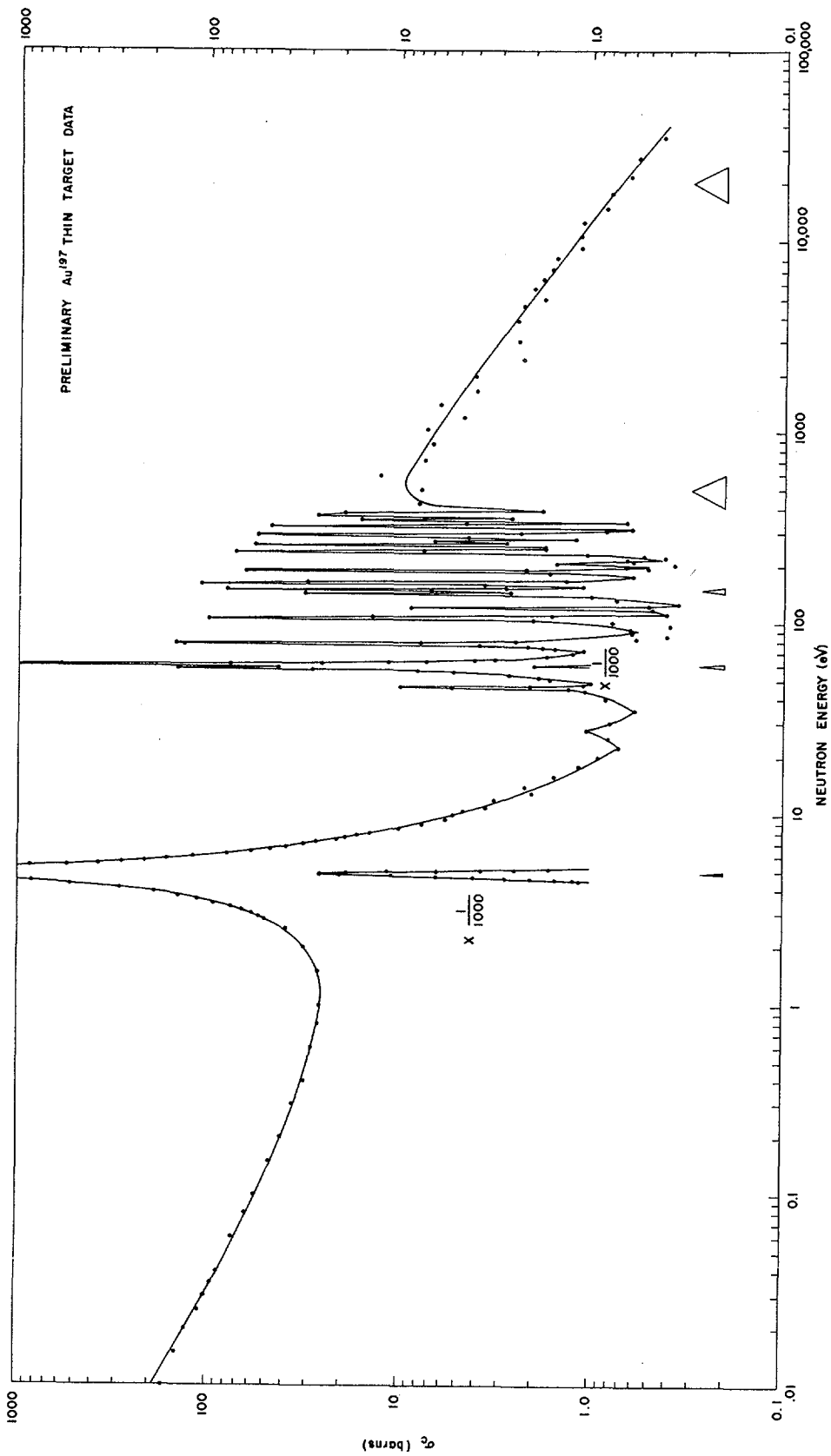

Fig. 8-- Preliminary Au^{197} capture cross-section data taken with 4000-liter liquid scintillator and 0.0005, 0.003, 0.010, 0.020 inch sample thicknesses.

In the above technique isotopic assignments are made by taking pulse height distributions of individual resonances. When there are 50 to 100 resonances to investigate this technique can be quite time consuming.

A method which is fast and which will work for any number of isotopes of a given element, provided their binding energies differ by 300 keV or more, is as follows: a time distribution run is taken over the energy region of interest at a detector bias of 3.0 MeV. The measurement is then repeated at a higher bias setting - in the case of Ag the bias was set at 6.0 MeV. Changing the bias from 3 to 6 MeV drastically changes the efficiency of the detector for accepting pulses from Ag^{107} + n and Ag^{109} + n (see Fig. 7). In fact, the efficiency for the Ag^{109} + n events will be reduced much more than the detector efficiency for the Ag^{107} + n events. Ratios are then taken of the counts at the peaks of the resonances in the 3 MeV run to the counts at the peaks of the resonances in the 6 MeV run. All the Ag^{107} resonances should have one value for their ratios and similarly all the Ag^{109} resonances should have one value for their ratios. The Ag^{109} ratio should be larger than the Ag^{107} ratio, as its binding energy is smaller than the Ag^{107} binding energy. Figure 8 shows isotopic assignments which were made to resonances in Ag over the energy range from 41 to 71 eV. The assignments obtained using these techniques are in complete agreement with work reported in BNL-325.

References:

(1) H. W. Schmitt and C. W. Cook, Nuclear Phys, 20, 202 (1960)

(2) R. L. Macklin, N. H. Lazar and W. S. Lyon, Phys. Rev., 107, 506 (1957)

(3) L. M. Bollinger and R. E. Cote, Neutron Time-of-Flight Methods, EANDC, 199 (1961).

(4) E. Haddad, S. Friesenhahn and W. M. Lopez, "Radiative Capture Cross-Section Measurements", GA-3874, (March 1, 1963).

j) ABSOLUTE MEASUREMENT OF FAST NEUTRON FLUX WITH A LARGE LIQUID SCINTILLATOR

H. Condé, S. Schwarz, and N. Starfelt
Research Institute of National Defence, Stockholm, Sweden

Abstract:

A method of making an absolute measurement of the flux of fast neutrons has been studied. An accurately determined fraction of the neutrons in a collimated beam passing along a channel through a large liquid scintillator is scattered into the scintillator. The detection efficiency of the neutron detector has been measured in an earlier experiment. An absolute measurement of the Li^6 (n, α) T cross section is made by placing a Li^6-glass scintillator in the calibrated neutron beam.

INTRODUCTION

In absolute measurements of cross sections for neutron scattering and for nuclear reactions induced by neutrons knowledge about the flux of the primary neutrons is required. Because of the difficulty in making absolute flux measurements most cross sections have been measured only relatively to other cross sections which have been assumed to be known with sufficient accuracy. It is thus desirable to try to develop accurate and, if possible, simple methods for absolute flux measurements.

The neutron detection efficiency of a large (100 l) liquid scintillator was determined with good accuracy in connection with a measurement of the average number of neutrons, $\bar{\nu}$, emitted per fission in Cf^{252} (1). This determination was made by a coincidence method and does not rely on any other cross section measurement. There are two difficulties involved in the use of the large liquid scintillator in flux measurements: its large sensitivity to γ-rays and the fact that the neutron detection efficiency was determined only for an isotopic source located in the centre of the scintillator tank. In cross section measurements one is usually not interested in the flux integrated

over all angles for a neutron source which does not emit γ-rays. On the contrary the flux of interest is normally concentrated in mall solid angle from a source which emits neutrons of different energies in different directions. In most cases the source also emits γ-rays. With such neutron sources it is not feasible to use the large liquid scintillator directly as a flux meter. A scattering measurement has to be performed where a scatterer mounted at the centre of the scintillator tank acts as a secondary source scattering a known fraction of the neutrons out of a beam collimated along the channel through the scintillator. It is required that this scatterer is a pure scatterer, i.e. all other cross sections have to be negligible compared with the elastic scattering cross section. In the energy region below a few hundred keV lead fulfills this requirement.

It is desirable to use the measurement of neutron flux directly for the determination of a cross section which can serve as a secondary standard. Such a determination should be made without changing the neutron source or the experimental geometry. We selected the Li^6 (n, α)T cross section as such a standard. A Li^6-loaded glass scintillator was then mounted in the center of the liquid scintillator tank and the number of (n, α) reactions in the glass was registered for a certain integrated neutron flux. Time-of-flight techniques had to be used to select the primary neutrons and discriminate against neutrons scattered in the glass and thermalized in the tank. Otherwise these neutrons would spoil the experiment because of the very high cross section for the (n,α)-reaction for thermal neutrons.

Flux Measurement

Neutron Source. Because of the difficulty in using the n-p reaction for flux determination below a few hundred keV the present method is of special interest in this energy region. The pulsed proton beam of a van de Graaff generator was used to produce neutrons through the Li^7 (p,n)Be^7 reaction. In the forward direction this reaction can provide monoenergetic

neutrons down to 110 keV and at backward angles it is possible to get down to about 5 keV. The γ-ray sensitivity of the liquid scintillator made it necessary to use targets of Li-metal, which also proves to be of advantage due to the higher neutron yield as compared to e.g. LiF targets.

Neutron Detector. The experimental arrangement is shown in Fig. 1. The neutrons from the source were collimated by a channel, 40 cm long, through a block of paraffin. The alignment of the collimator with the channel through the scintillator in such a way that the neutron beam is centrally located in this channel has to be made with great care. The liquid scintillator is described in detail in ref. (1). The neutron detection efficiency as a function of neutron energy for a neutron source located in the center of the tank is shown in Fig. 2. To check that the over-all efficiency of the scintillator has not changed, the average number of neutrons per spontaneous fission in Cf^{252} was measured in connection with each measurement with the large liquid scintillator. This was done as described in (1).

To minimize the background counting rate in the scintillator the tank was surrounded by a paraffin shield of a thickness of 30 cm.

As mentioned above the flux in the collimated beam of neutrons was measured by scattering a measurable fraction of the beam by means of a lead scatterer mounted at the center of the tank. Because of the large background from natural radiation sources a scatterer of a diameter larger than the neutron beam was used. In this way the neutron flux integrated over the whole cross section of the beam was measured. By using a scatterer smaller than the beam area it would be possible to measure the flux expressed as neutrons per unit area and time, but then the signal-to-background ratio would be considerably smaller than the value of about 1:10 obtained in the present experiment.

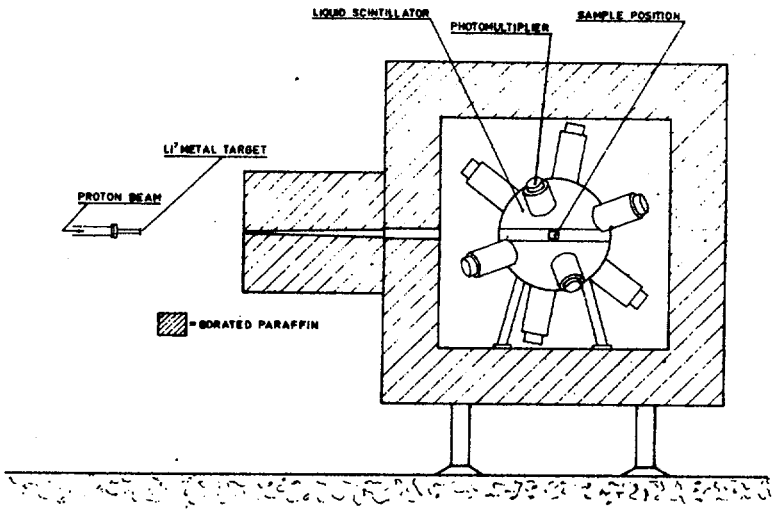

Fig. 1. Experimental arrangement used in the measurement of neutron flux. Sample position is the position where the lead scatterers and the Li^6-glass scintillator are mounted.

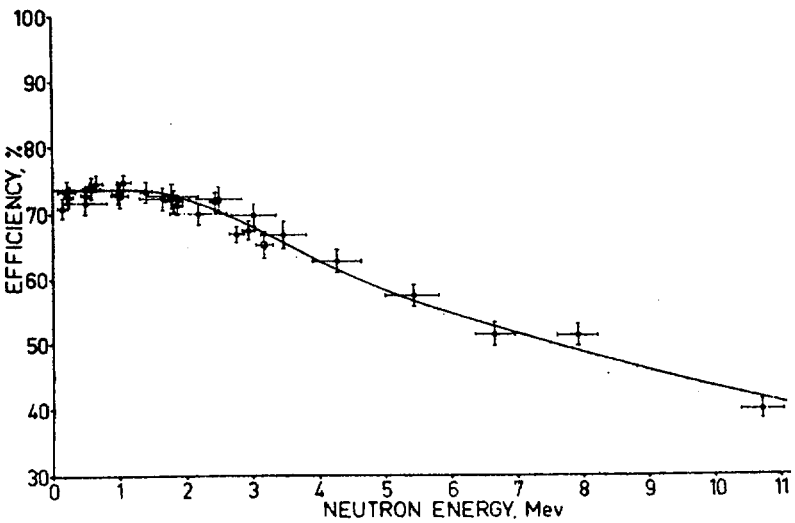

Fig. 2. Neutron detection efficiency of the liquid scintillator for neutrons emitted from the centre of the scintillator tank. Reference (1).

The neutron capture cross section of lead is of the order of 5 mb (2) as compared with a scattering cross section of about 10 barns at 100 keV. The lowest excited state in any of the stable lead isotopes is above 0.5 MeV and the angular distribution for elastic scattering is close to isotopic at 100 keV (3). Thus lead acts as a pure scatterer and no γ-rays are produced. Furthermore, because of the large γ-ray absorption cross section of lead γ-rays from the target are absorbed in the lead scatterer instead of being scattered into the liquid scintillator. To make sure that no scattered γ-rays disturbed the measurements the time spectrum of the pulses obtained from the scintillator with the pulsed neutron source was registered using the circuits shown in Fig. 3. A γ-ray peak due to γ-rays penetrating through the paraffin shield was observed but no difference between runs with the scatterer in position and with the scatterer removed could be detected.

In this measurement the amplification of the start pulse to the time-to-pulse-height converter was adjusted to the same counting rate as that registered by the scaler used in the neutron flux measurement.

The fraction of the neutrons in the beam scattered by the lead scatterer was determined through a measurement in good geometry of the transmission of neutrons through the lead piece. For this purpose a Li^6-loaded glass scintillator was mounted at the far end of the channel through the tank and time-of-flight spectra were record with and without lead scatterer. By making time-of-flight measurements it was possible to discriminate against neutrons scattered in the lead, thermalized in the liquid scintillator, and subsequently absorbed in the glass with high efficiency because of the large cross section for thermal neutrons.

In the actual measurement of neutron flux many alternate runs with and without lead scatterer were made and three different scatterers were used the lengths of which were 2.5, 5, and 10 cm. respectively. Counting rates and transmission coefficients are given in Table 1.

Table 1

Typical primary data

Pb scatterer	Fraction scattered	Liquid count/ sec
0	0	947
2.5	0.595±0.003	1018
5.0	0.816±0.004	1042
10.0	0.970±0.005	1061

Natural background in the tank 575 counts/sec.

The data in column 2 are mean values of several 30 minutes runs. The data in column 3 are mean values of several 3 minutes runs.

Monitors. In a measurement of the present type where the measured quantity is the difference between the number of counts with the scatterer in position and without scatterer and where the signal-to-background ratio is small an accurate monitor for the neutron source is required. The monitor should also serve to connect the neutron flux measurements with the measurement of the $Li^6(n, \alpha)T$ cross section described below. Two types of monitors were used: a current integrator measuring the total charge of the protons bombarding the neutron target and a $Li^6I(Eu)$-scintillator embedded in a sphere of polyethylene (4). This counter was mounted as close as possible to the neutron beam collimator without intercepting the beam passing through the collimator. In this way the monitor did not disturb the neutron flux being measured and the insertion and removal of the lead scatterers and the Li^6-loaded glass scintillator in the channel in the liquid scintillator tank did not influence upon the action of the monitor. The ratio between the source strength as registered by the current integrator and that observed by the Li^6I scintillator was constant to within 2 per cent during the whole experiment.

$Li^6(n,\alpha)T$ Cross Section. The cross section of the $Li^6(n,\alpha)T$ cross section was considered as a suitable standard cross section. Li^6-loaded glass is a good scintillator with good pulse-height resolution. Because of the high Q-value of the reaction it is easy to separate pulses from the (n,α) reaction from background γ-rays by pulse-height discrimination. Fig. 4 shows the pulse distribution obtained from the Li^6-loaded scintillator with 100 keV neutrons. The position of the channel of the single-channel analyzer selecting the proper pulses is also shown. Furthermore, the glass scintillator is fast, making it possible to use time-of-flight techniques to reject pulses caused by neutrons thermalized in the liquid scintillator. A block diagram of the time-of-flight circuitry is shown in Fig. 5. Time-of-flight spectra as registered with the Li^6-loaded glass scintillator are shown in Fig. 6.

From the measurements described above one obtains the neutron flux integrated over the whole cross section area of the beam. To use this information about the neutron flux in the measurement of the Li^6 $(n,\alpha)T$ cross section it is necessary to use a Li^6-loaded scintillator which is large enough to be hit by all the neutrons in the beam. A scintillator of a diameter of 1.5" and a thickness of 3/8" was used. This detector was centered in the channel through the liquid scintillator at about the same position where the lead scatterers were mounted in the earlier part of the experiment. The maximum diameter of the beam at this position was 24 mm.

Corrections and Sources of Error. As this experiment is intended to be an accurate measurement of neutron flux the different possible corrections and sources of error should be examined in some detail.

In the measurement of the transmission of neutrons through the lead scatterers both the scatterer and the Li^6-loaded glass scintillator, used as a neutron detector, were located in the channel through the liquid scintillator. Thus, scattering in the scintillator liquid of neutrons scattered out of the beam

might increase the number of neutrons detected by the Li^6-glass. The use of time-of-flight techniques limits this disturbance to neutrons scattered only a few times and without considerable energy loss. The fairly large distance between scatterer and detector, 32.5 cm., helps in keeping this correction well below 0.5 per cent.

In all applications of the Li-glass multiple scattering in this detector and the resulting increase in detection efficiency has to be considered. This problem was studied in detail by Bollinger et al. (5). An extrapolation from their results shows that the detection efficiency of our glass scintillator at 100 keV is 6 per cent larger than calculated when scattering in the crystal is neglected.

Furthermore, scattering of neutrons by the Li-glass and subsequent scattering in the liquid scintillator may return neutrons to the Li-glass giving rise to an increase in the counting rate. An estimate of this effect gives a correction of 3 per cent. Both these corrections should, however, be investigated more in detail by Monte Carlo methods.

Results and Discussion. The present measurement was made at a neutron energy of 110±5 keV. However, as no analysis of the Li^6 content of the Li-glass has yet been made no cross section result can be given.

It will be of interest to combine the present measurement with a relative measurement of the $Li^6(n, \alpha)T$ cross section recently performed by Schwarz (6). This experiment is based on the assumption that the $Li^7(p,n)Be^7$ cross section is isotopic in the center of mass system at proton energies close to the neutron threshold.

It is concluded that the large liquid scintillator is suitable for absolute measurement of neutron flux with an accuracy of the order of 2 to 3 per cent in the energy region below about 0.5 MeV. At higher energies inelastic scattering and anisotropy in the elastic scattering in lead will cause difficulties. In the direction of low energies the method is limited by the scarcity of monoenergetic neutron sources.

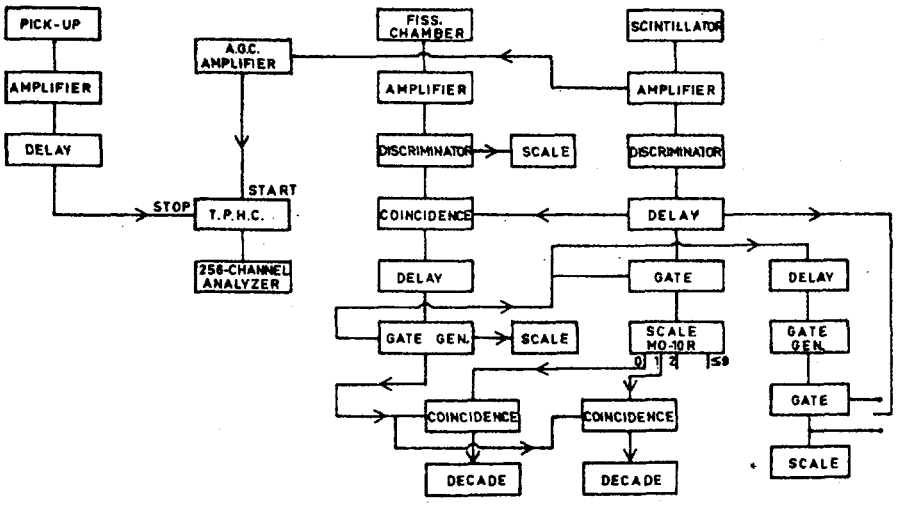

Fig. 3. Block diagram of the electronic circuits used with the liquid scintillator.

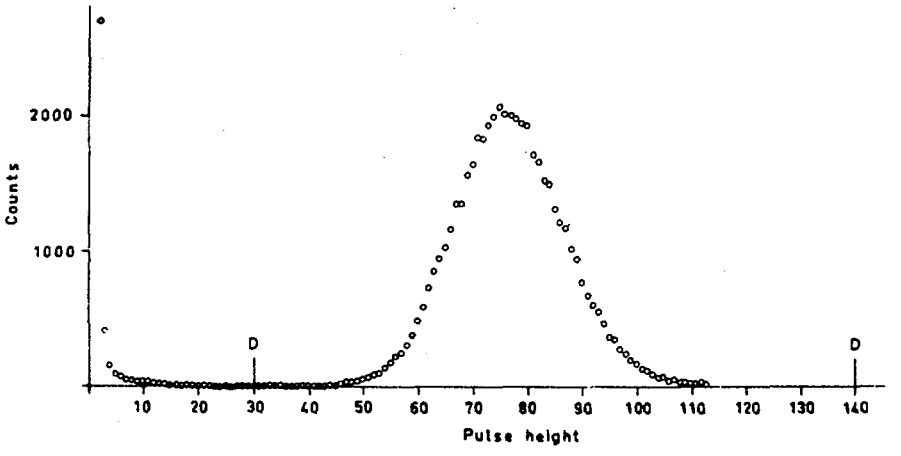

Fig. 4. Pulse spectrum from the Li^6-loaded glass scintillator showing the peak due the $Li^6(n,\alpha)T$ reaction and the background caused by γ-rays below about channel number 10. The setting of the window of the single-channel analyzer selecting (n,α) pulses is marked "D".

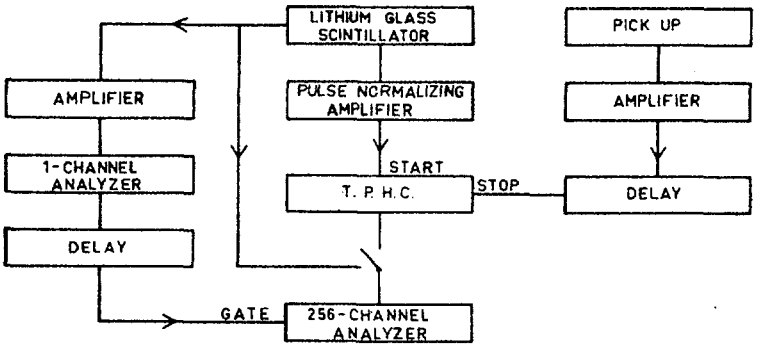

Fig. 5. Block diagram of the electronic circuits used in the time-of-flight measurements with the Li^6-loaded glass scintillator.

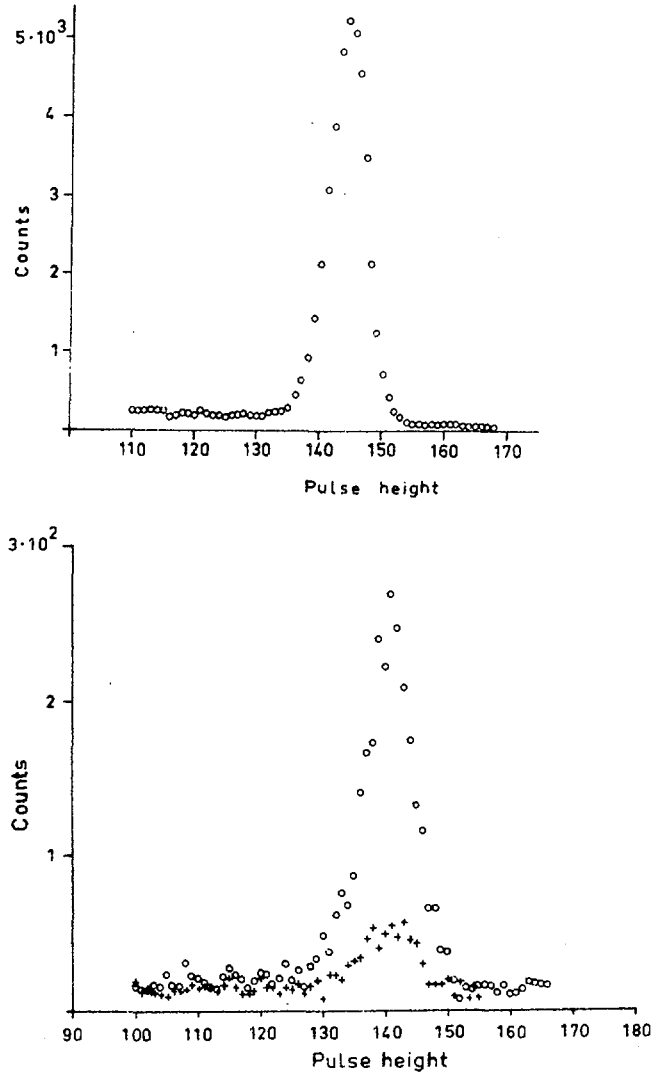

Fig. 6. Time-of-flight spectra as measured with the Li^6-loaded glass scintillator a) with the detector about 15 cm from the neutron target. The tail to the left of the peak is due to scattering in the nearby collimator, b) with the detector in the centre of the scintillator tank with and without a lead scatterer of a length of 5 cm inserted in the beam.

References:

(1) I. Asplund-Nilson, H. Condé and N. Starfelt, Nucl. Sci. Eng. 16, 124 (1963)

(2) B.C. Diven, J. Terrell and A. Hemmendinger, Phys. Rev. 120, 556 (1960)

(3) M.D. Goldberg, V.M. May and J.R. Stehn, "Angular Distributions in Neutron-induced Reactions", BNL-400, (October 1962)

(4) R.L. Bramblett, R.J. Ewing and T.W. Bonner, Nucl. Instr. and Meth. 9, 1 (1960)

(5) L.M. Bollinger, G.E. Thomas and R.J. Ginther, Nucl. Instr. and Meth. 17, 97 (1962)

(6) S. Schwarz, to be published.

k) PROPOSAL FOR THE USE OF THE ASSOCIATED PARTICLE METHOD WITH NEUTRONS OF 100 keV OR LESS

H. Beil, M. Le Rigoleur, J.L. Leroy
Centre d'Etudes Nucléaires de Saclay, France

1. INTRODUCTION

The associated particle method is very attractive for absolute neutron flux measurements, and permits a very high accuracy. It has been used extensively in the field of several MeV neutrons, mainly by means of the T(d,n) He^4 reaction and to a lesser extent of the D (d,n) He^3 reaction.

The T(p,n)He^3 reaction produces large yields of low energy neutrons, as well as an associated He^3 particle. The purpose of this paper is to discuss the feasibility of the detection of this associated particle.

2. PROPERTIES OF THE T(p,n)He^3 REACTION

This reaction, for neutron emission at backward angles, gives a neutron of low energy associated with an He^3 of higher energy emitted at a given forward angle which can in principle be detected. The Fig. 1 gives the neutron energy as a function of the He^3 energy, for different angles of detection. The Fig. 2 and 3 give the energy and emission angle of the neutrons as a function of angle of detection of the He^3 particle, for different proton energy.

It follows from diagram (1) that, provided one can detect a He^3 particle having about 300 keV at an angle of about 10° we can then establish a one to one relationship with 35 keV neutrons.

From diagrams (2) and (3) one can see at once that in order to obtain a good energy resolution for low energy neutrons, one will be forced to use a detector having a very narrow width.

Fig. 1

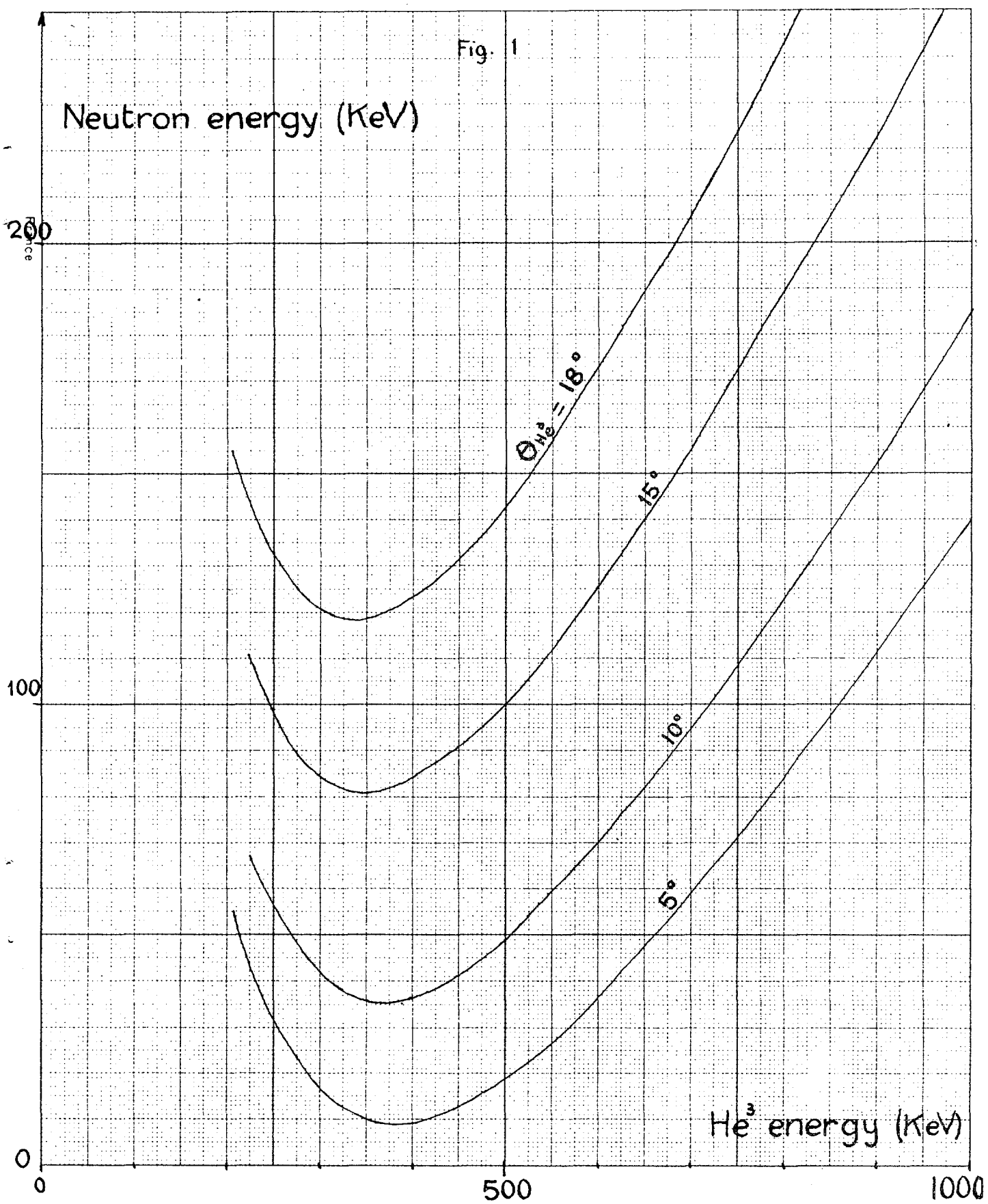
Neutron energy (KeV)
200
100
0
0
500
1000
He^3 energy (KeV)
$\theta_{He^3} = 18°$
15°
10°
5°

Fig. 2

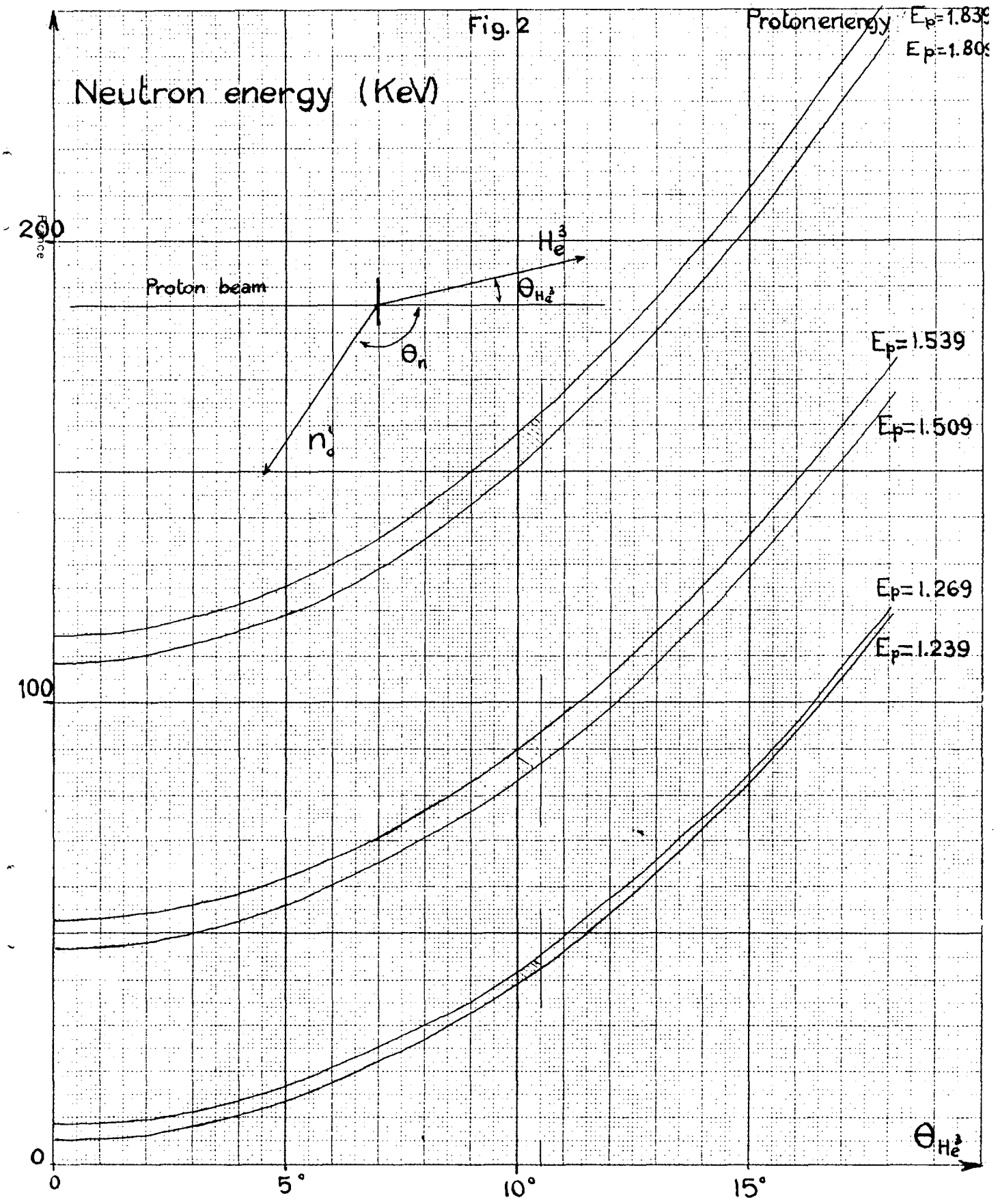
Neutron energy (KeV)
Proton energy
E_p=1.83
E_p=1.80
200
100
0
H_e^3
Proton beam
$\theta_{H_e^3}$
θ_n
n_0^1
E_p=1.539
E_p=1.509
E_p=1.269
E_p=1.239
0
5°
10°
15°
$\theta_{H_e^3}$

Fig. 3

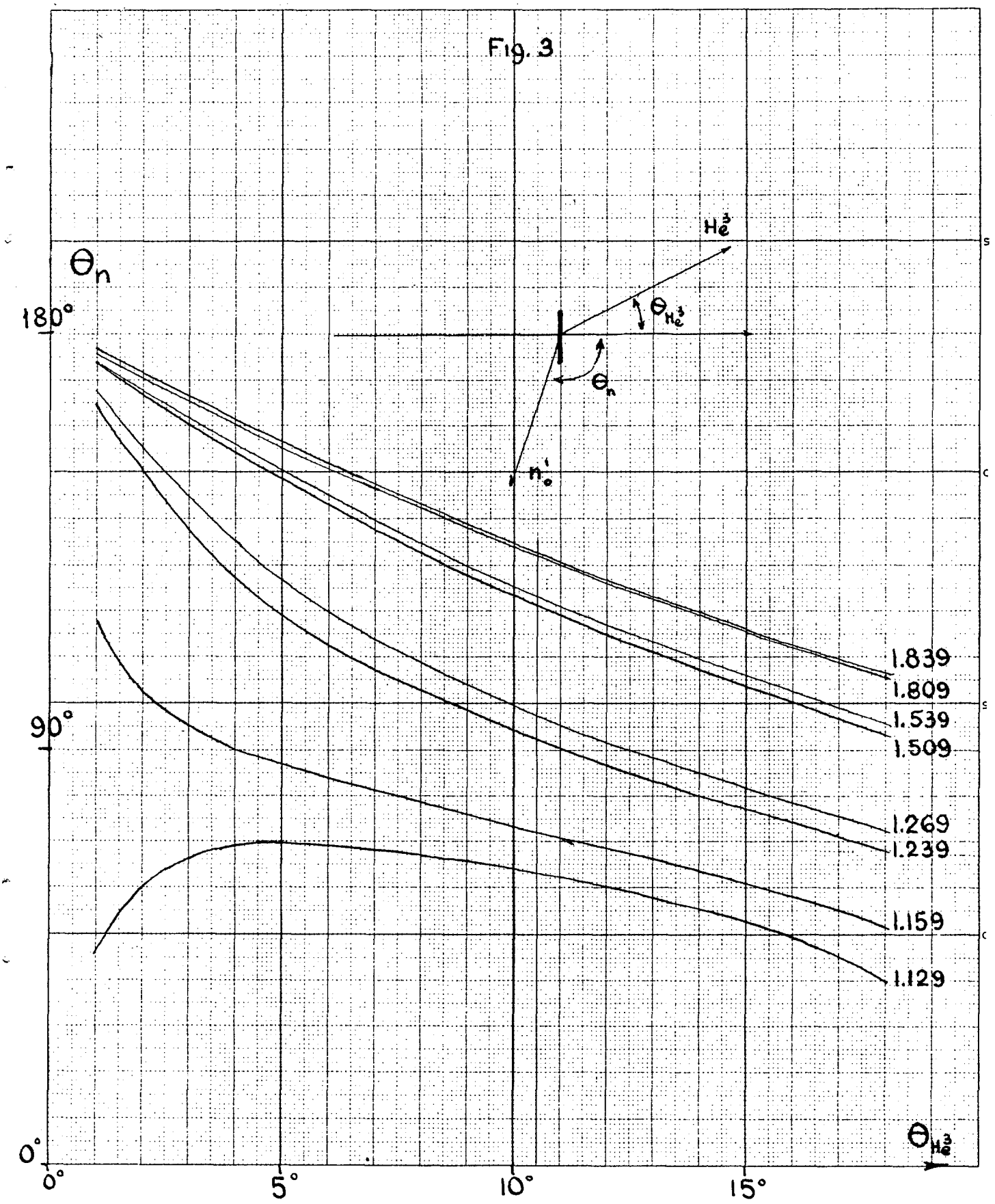
Θ_n
180°
90°
0°
0°
5°
10°
15°
Θ_{He^3}
He^3
Θ_{He^3}
Θ_n
n_o'
1.839
1.809
1.539
1.509
1.269
1.239
1.159
1.129

3. PROPOSED EXPERIMENTAL LAY-OUT (4)

From the above it followes that the He^3 particle can only be usefully detected at relatively small emission angles (say 20° or less).

a) In order to be able to count He^3 particles at such angles one is forced to use thin target backings in transmission position.

b) The detector ought to be able to discriminate between He^3 particles and Coulomb scattered protons.

Such a discrimination can be achieved by means of appropriate deflexion fields, by the use of surface barrier solid state detectors or by a combination of these methods.

The more attractive method is clearly the solid state detector alone.

This method is based on the following facts:

1) The proton range in the detector is much greater than that of the He^3;

2) The "barrier depth" in the detector can be varied by means of an applied polarisation potential in accordance with the formula.

$$B = 0.5 \sqrt{\rho (V_A + V_o)}$$

The resistivity of the silicon chosen is low enough so that B is equal to the range of the He^3 particles for $V_o \approx 0$. In such a case, the energy lost by the scattered protons in the sensitive layer is much smaller than the energy lost there by He^3 particles. The remaining part of the proton energy is spent in a region of the detector where the collection time for the charges is long compared to that in the sensitive layer.

3) The amplifier used is sensitive only to the fast rise time component of the pulse collected at the detector. At the output of this amplifier, the scattered protons appear as a background of numerous

small pulses, and the He^3, as large pulses. In order to avoid a pile up of small proton pulses, one needs an amplifier as fast as possible, associated with a fast discriminator.

4. DISCUSSION OF THE POSSIBILITIES OF THIS METHOD

Trials as to the fabrication of Tritium targets on thin backings made by the Radiochemical Division at Saclay, indicate no serious problems.

Backings of 1 μ of Ni where found to be satisfactory.

Our detectors are surface barrier (Si-n) type and have a small rectangular surface (1 x 5) mm and a resistivity of ρ = 50 ohm.cm. which, for a polarisation of 1 volt gives a barrier depth of about 4 μ .

We have further constructed a fast electronic chain consisting of a fast low noise preamplifier.

This preamp is followed by three C.R.C. distributed amplifiers. This chain gives a total gain of $\approx$ 10,000. An output signal of 1 volt having a width of 15 ns at half height is obtained from this chain for a collected energy of 130 keV. The noise is about 30 keV.

Now the problem is to determine the beam current for which the pile up rate is of the order of 1 per cent of the He^3 counting rate. Calculations, as well as our first experimental results, show that this current is only of the order of 10^{-8}A.

This current is small but is probably sufficient to make an absolute measurement of the efficiency of a Lithium glass scintillator.

This maximum current can be increased very strongly if one uses an electrostatic or electromagnetic separator between the target and the He^3 detector. Time of flight selection of the charged particles may also be very helpful.

1) He^3 NEUTRON SPECTROMETER WITH PULSE RISE-TIME DISCRIMINATION I. ¤

A. Sayres and M. Coppola
Columbia University, New York, United States

Abstract:

A He^3 filled proportional counter can be used as a neutron spectrometer in the range 100 keV to 8 MeV by using the He^3 (n,p)T reaction. The major limitation as a neutron spectrometer is that the He^3 recoil distribution, arising from the elastic scattering of the higher energy neutrons present, masks the He^3 (n,p)T peaks due to lower energy neutron groups. Since a He^3 recoil and a proton of equal energies have different specific ionizations and therefore different ranges in the counter filling, one therefore has a means to distinguish between pulses from the He^3 (n,p)T and He^3 (n,n)He^3 reactions. For appropriate operating conditions the rise-time of the pulses for these two events will be different. By converting this rise time to a pulse height and only accepting pulses with long rise times (which correspond to protons from the He^3 (n,p)T reaction) one now has a neutron spectrometer useful in an energy interval between the maximum neutron energy present and that energy for which the proton range equals the range of the maximum energy He^3 recoil.

¤ Supported by United States Atomic Energy Commission.

He^3 NEUTRON SPECTROMETER WITH PULSE RISE-TIME DISCRIMINATION II.*

M. Coppola and A. Sayres
Columbia University, New York, United States

Spectra of monoenergetic neutrons obtained with a He^3 filled proportional counter and the pulse rise-time discrimination as described in the previous abstract will be presented to illustrate the energy range over which this detector may now be used as a neutron spectrometer. From these spectra one obtains the relative efficiency of the detectors. For these operating conditions, spectra of the following reactions were obtained. $Mg^{24}(d,n)Al^{25}$, $Si^{28}(d,n)P^{29}$, $S^{32}(d,n)Cl^{33}$. The merits of this new neutron spectrometer will be discussed.

* Supported by United States Atomic Energy Commission.

m) NOTES ON SHELL TRANSMISSION THEORY

P.H. White
Atomic Weapons Research Establishment,
Aldermaston, United Kingdom

REFERENCES

Analytical Shell Theory

H.A. Bethe, J.R. Beyster and R.E. Carter
J. Nuclear Energy 3, 207 (1956)
3, 273 (1956)
4, 3 (1957)
4, 147 (1957)

Computer Methods

R.T. Ackroyd and E.D. Pendlebury
A Report DEG 362 (R)

See also

Proceedings of the Eleventh Symposium in Applied Mathematics of the American Mathematical Society Editors G. Birkhoff and E.P. Wigner.

Shell Work relevant to keV region

A.O. Hanson LADC 323 (1952)
V.N. Andreev J. Nuclear Energy 9, 151 (1959)
T.S. Belanova Sov, Phys, JETP 34, 397 (1958)
H.W. Schmitt and C.W. Cook
Nuclear Physics 20, 202 (1960)

References Resonance Absorption

Resonance Absorption in Nuclear Reactors
by L. Dresner
Pergamon Press 1960

ORNL - L. Dresner

A program of research and calculations of resonance absorption

GA2527 - L.W. Nordheim

Sphere Transmission Method

Equation for transmission using multigroup theory

φ_i = source strength u group i

X_i X_i^1 ξ = correction terms finite source size

$$q_i = \varphi_i T_i (1 - X_i^1 + \xi) + P_i^+ \Sigma \frac{C_{ji}}{J_{trj}} \left(\varphi_j (1 - T_j (1 - X_j)) + \frac{1-P_j}{P_j^+} (q_j - \varphi_j T_j (1 - X_j^1 + \xi) \right)$$

$$T = \Sigma q_i S_i$$

Finite source to detector distance

$$P_i^+ = P_i + \frac{1}{2b^2} P_i^* + \frac{3}{8b^4} P_i^{**}$$

Finite source size - detector on x axis

$$\xi = \frac{\langle 3x^2 - y^2 - z^2 \rangle}{b^2}$$

$$X_i = \frac{\sigma_{tri}}{2} \left(\frac{1}{r_1} - \frac{1}{r_2}\right) \frac{2}{3} \langle x^2 + y^2 + z^2 \rangle$$

$$X_i^1 = \frac{\sigma_{tri}}{2} \left(\frac{1}{r_1} - \frac{1}{r_2}\right) \langle y^2 + z^2 \rangle$$

Four group elastic scattering

$$C_{ji} = \downarrow i \begin{vmatrix} 0 & 0 & 0 & 0 \\ \sigma_{et\ 1} & 0 & 0 & 0 \\ 0 & \sigma_{et\ 2} & 0 & 0 \\ 0 & 0 & \sigma_{et\ 3} & \sigma_{et\ 4} \end{vmatrix} \qquad \varphi_i = \begin{vmatrix} 1 \\ 0 \\ 0 \\ 0 \end{vmatrix}$$

$$T = S_1 q_1 + S_2 q_2 + S_3 q_3 + S_4 q_4$$

$$T = T_1 (1 - X_1^1 + \xi) + (1-T_1(1-X_1)) \frac{\sigma_{et\ 1}}{\sigma_{tr\ 1}} \left(P_2 S_2 + (1-P_2) P_3 S_3 \frac{\sigma_{et\ 2}}{\sigma_{tr\ 2}} + \frac{(1-P_2)(1-P_3) P_4 S_4 \frac{\sigma_{et\ 2}}{\sigma_{tr\ 2}} \frac{\sigma_{et\ 3}}{\sigma_{tr\ 3}}}{\left[1 - \frac{\sigma_{et\ 4}}{\sigma_{tr\ 4}} (1-P_4)\right]} \right)$$

Four group elastic scattering geometry

$$C_{ji} = \downarrow i \begin{vmatrix} 0 & \sigma_{et\,1} & 0 & 0 \\ 0 & 0 & \sigma_{et\,2} & 0 \\ 0 & 0 & 0 & \sigma_{et\,3} \\ 0 & 0 & 0 & \sigma_{et\,4} \end{vmatrix} \qquad \varphi_i = \begin{vmatrix} 1 \\ S_2 \\ S_3 \\ S_4 \end{vmatrix}$$

$$T = q_1$$

$$T = T_1 (1-X_1^1+ \xi) + (1-T_2(1-X_2)) \frac{\sigma_{et\,1}}{\sigma_{tr\,2}} S_2 P_1$$

$$+(1-T_3(1-X_3)) \frac{\sigma_{et\,1}}{\sigma_{tr\,2}} \frac{\sigma_{et\,2}}{\sigma_{tr\,3}} S_3(1-P_2) P_1$$

$$+ \frac{(1-T_4(1-X_4)) \frac{\sigma_{et\,1}}{\sigma_{tr\,2}} \frac{\sigma_{et\,2}}{\sigma_{tr\,3}} \frac{\sigma_{et\,3}}{\sigma_{tr\,4}} S_4 (1-P_2)(1-P_3) P_1}{\left[1- \frac{\sigma_{et\,4}}{\sigma_{tr\,4}} (1-P_4)\right]}$$

n)

THE CROSS SECTION OF THE REACTION Au^{197} (n, γ) Au^{198} FOR 30 keV NEUTRONS

W. Pönitz
Kernforschungszentrum Karlsruhe,
F.R. of Germany

Abstract

The Au^{197} (n, γ) Au^{198} cross section is measured at the threshold of the Li^7 (p,n) Be^7 reaction by an activation method. The absolute neutron flux is determined by counting the Be^7 activity. A preliminary value of 598 ± 60 mb is obtained.

1. INTRODUCTION

During the last years, many (n,γ) cross sections in the energy range 1 - 100 keV have been measured. However, values reported by the different authors show discrepancies which sometimes arise to 100%. In many cases, these discrepancies are due to uncertainties in the absolute flux determination. Therefore, more reliable methods for absolute flux measurements have to be found.

A very convenient method which can be used in connection with the Li^7(p,n)Be^7 reaction consists in the absolute determination of the source strength by counting the 53.6 d-activity of the Be^7 nucleus. This method was applied to a measurement of the gold capture cross section at 30 keV.

2. EXPERIMENTAL ARRANGEMENT

Fig. 1 shows the experimental arrangement. The van de Graff-proton energy was controlled in such a way that the upper one of the two BF_3 counters gave signals whilst the lower one did not. In this way the neutrons were confined into a forward cone of less than 10° with an average energy of 30 keV. The proton beam was limited by an aperture in such a way that all neutrons generated in the target had to cross the gold foil. The average proton current was 2 μA and it was defocused in order to keep the target heating low. This is important because evaporation and cathode sputtering

will introduce errors into the source strength determination.

3. COUNTING PROCEDURE

The gold foil was irradiated for a period of 6 hours [1]. The number of Au^{198} nuclei at time t after the irradiation is given by

$$B_{Au} = \frac{Q_n \Sigma_a d}{\lambda_{Au}} \left[1-e^{-\lambda_{Au} T}\right] e^{-\lambda_{Au} t} \qquad (1)$$

Q_n [sec^{-1}] is the source strength, T the irradiation time, λ the decay constant, d the gold foil thickness and Σ_a the activation cross section. The number of Be^7 nuclei present in the target at time t' is

$$B_{Be} = \frac{Q_n}{\lambda_{Be}} \left[1-e^{-\lambda_{Be} T}\right] e^{-\lambda_{Be} t'} \qquad (2)$$

The Au^{198} and Be^7 activities were counted with two 3 in. x 3 in. Na I (Tl) crystals. Only the photopeaks corresponding to the 411 keV line of Au^{198} and the 477 keV line of Be^7 were used. The ratio of the counting rates is given by

$$\frac{Z_{Au}}{Z_{Be}} = \frac{\lambda_{Au} B_{Au}}{\lambda_{Be} B_{Be}} \cdot \frac{(\eta_\gamma P_\gamma)_{Au}}{(a \eta_\gamma P_\gamma)_{Be}}$$

$$= \Sigma_a d \cdot \frac{(1-e^{-\gamma_{Au} T}) e^{-\gamma_{Au} t}}{(1-e^{-\gamma_{Be} T}) e^{-\gamma_{Be} t'}} \cdot \frac{(\eta_\gamma P_\gamma)_{Au}}{(a \eta_\gamma P_\gamma)_{Be}} \qquad (3)$$

a = 0.12 is the fraction of Be^7 decays which yield a 477 keV γ-quantum[1]. η_γ is the probability to register a γ-quantum and P_γ the photopeak-to-total ratio. In our case,

$$\frac{(\eta_\gamma P_\gamma)_{Au}}{(\eta_\gamma P_\gamma)_{Be}} = 1.138 \quad (2)$$

---

1) Actually, it was irradiated six times one hour and after each run, the target was turned in order to get a homogenous irradiation. The respective corrections are straight forward and will be omitted here for simplicity reasons.

4. RESULTS

Evaluating the measured counting rate ratio with equ. 3 yields

$$\tilde{\sigma}_a = 598 \text{ mb}$$

for the activation cross section of gold at 30 keV. Errors resulting from counting statistics and from uncertainties in the $\eta_\gamma P_\gamma$ ratio are very small. The decay scheme of Be^7 introduces a considerable error since a is known to only about 5%. An additional uncertainty is caused by evaporation of some Be^7 nuclei from the target. The total error on $\tilde{\sigma}_a$ is estimated to be $\pm$ 60 mb.

It is believed, however, that the method outlined in this paper can yield much more accurate results. Loss of Be^7 nuclei from the target can be safely avoided by a very thin protective layer on the target. a could be determined with good precision, for instance by the use of a Mn SO_4 bath method for neutron source strength measurement.

I thank Dr. K.H. Beckurts for the suggestion and his interest in this work. Moreover, I am grateful to Prof. K. Zimmer for the possibility to use the van de Graaff generator of his Institute.

References

(1) Landolt-Börnstein, Numerical Data and Functional Relationship in Science and Technology, New Series, I, Volume 1, Springer 1961.

(2) R.L. Heath, IDO 16 408.

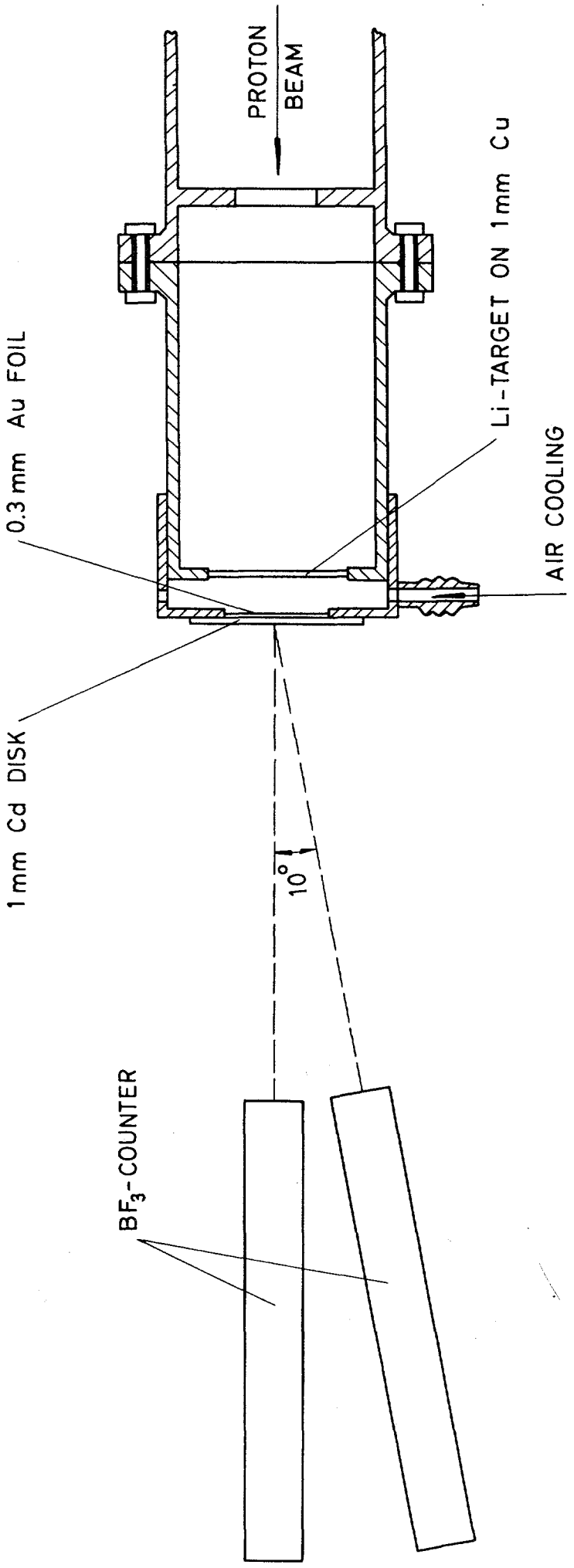

FIG. 1 SETUP FOR DEFINING THE NEUTRON CONE

LIST OF DELEGATES TO THE SYMPOSIUM

Dr. J.F. Barry	Atomic Weapons Research Establishment, Aldermaston, Berkshire, United Kingdom.
Prof. H.H. Barschall	University of Wisconsin, Madison 6, Wisconsin, United States.
Mr. R. Batchelor	Atomic Weapons Research Establishment, Aldermaston, Berkshire, United Kingdom.
Dr. K.H. Beckhurts	Institut für Angewandte Kernphysik, Kernforschungszentrum Karlsruhe, Weberstrasse 5, 75 Karlsruhe, Federal Republic of Germany.
Dr. G. Brudermüller	Institut für Angewandte Kernphysik, Kernforschungszentrum Karlsruhe, Weberstrasse 5, 75 Karlsruhe, Federal Republic of Germany.
Dr. P.J. Campion	National Physical Laboratory, Teddington, Middlesex, United Kingdom.
Dr. R.S. Caswell	National Bureau of Standards, Washington 25, D.C., United States.
Dr. B.C. Diven	Los Alamos Scientific Laboratory, P.O. Box 1663, Los Alamos, New Mexico, United States.
Dr. A.T.G. Ferguson	Atomic Energy Research Establishment, Harwell, Didcot, Berkshire, United Kingdom.
Dr. S.C. Fultz	Lawrence Radiation Laboratory, University of California, Livermore, California, United States.
Dr. E. Haddad	General Atomics, General Dynamics, P.O. Box 608, San Diego 12, California, United States.
Prof. W.W. Havens, Jr.	Columbia University, New York 27, New York, United States.
Dr. G.D. James	Atomic Energy Research Establishment, Harwell, Didcot, Berkshire, United Kingdom.
Dr. R.G. Johnson	Lockheed Missile and Space Company, Palo Alto, California, United States.

Mr. J.L. Leroy	Commissariat à l'Energie Atomique, Centre d'Etudes Nucléaires de Saclay, B.P. No. 2, Gif-sur-Yvette, Seine & Oise, France.
Dr. R.L. Macklin	Oak Ridge National Laboratory, P.O. Box X, Oak Ridge, Tennessee, United States.
Prof. H.W. Newson	Duke University, Durham, North Carolina, United States.
Mr. N. Papadopoulos	Nuclear Research Centre "Democritus", Aghia Paraskevi Attikis, Athens, Greece.
Prof. E.B. Paul	Manchester University, Manchester 13, United Kingdom.
Dr. J.L. Perkin	Atomic Weapons Research Establishment, Aldermaston, Berkshire, United Kingdom.
Mr. W. Pönitz	Institut für Angewandte Reaktorphysik, Kernforschungszentrum Karlsruhe, Weberstrasse 5, 75 Karlsruhe, Federal Republic of Germany.
Dr. M.J. Poole	Atomic Energy Research Establishment, Harwell, Didcot, Berkshire, United Kingdom.
Dr. E.R. Rae	Atomic Energy Research Establishment, Harwell, Didcot, Berkshire, United Kingdom.
Dr. H.W. Schmitt	Oak Ridge National Laboratory, P.O. Box X, Oak Ridge, Tennessee, United States.
Dr. A.B. Smith	Argonne National Laboratory, 9700 South Cass Avenue, Argonne, Illinois, United States.
Dr. J. Spaepen	Bureau Central de Mesures Nucléaires, Communauté Européenne de l'Energie Atomique, Steenweg naar Retie, Geel, Belgium.
Dr. M,G. Sowerby	Atomic Energy Research Establishment, Harwell, Didcot, Berkshire, United Kingdom.
Dr. N. Starfelt	Research Institute of National Defence FOA, Stockholm 80, Sweden.

Mr. J. Thomas	Danish Atomic Energy Commission, Research Establishment Risø, Roskilde, Denmark.
Mr. E. Wattecamps	Institut für Angewandte Reaktorphysik, Kernforschungszentrum Karlsruhe, Weberstrasse 5, 75 Karlsruhe, Federal Republic of Germany.
Dr. J. Weale	Atomic Weapons Research Establishment, Aldermaston, Berkshire, United Kingdom.
Dr. L.W. Weston	Oak Ridge National Laboratory, P.O. Box X, Oak Ridge, Tennessee, United States.
Dr. P.H. White	Atomic Weapons Research Establishment, Aldermaston, Berkshire, United Kingdom.
Dr. T. Wiedling	AB Atomenergi, Studsvik, Nyköping, Sweden.